

НАЦІОНАЛЬНА АКАДЕМІЯ НАУК УКРАЇНИ
ІНСТИТУТ ОРГАНІЧНОЇ ХІМІЇ НАН УКРАЇНИ
НАЦІОНАЛЬНИЙ ФАРМАЦЕВТИЧНИЙ УНІВЕРСИТЕТ

Рік заснування – 1966

ЖУРНАЛ
ОРГАНІЧНОЇ ТА
ФАРМАЦЕВТИЧНОЇ
ХІМІЇ

JOURNAL OF
ORGANIC AND
PHARMACEUTICAL
CHEMISTRY

2024 — том 22, випуск 1 (85)

Харків
НФаУ

Головні редактори І. М. Владимірова (Харків)
М. В. Вовк (Київ)

Заступники головного редактора С. В. Власов (Харків)
Ю. В. Рассукана (Київ)

Відповідальні секретарі Д. О. Лега (Харків)
Т. А. Васільєва (Київ)

Редакційна колегія:

Н. А. Бісько (Київ), М. К. Братенко (Чернівці), В. С. Броварець (Київ),
Ю. В. Буйдін (Київ), Ж. Ф. Буйон (Руан, Франція), А. Варнек (Страсбург, Франція),
З. В. Войтенко (Київ), Д. М. Волочнюк (Київ), В. А. Георгіянець (Харків),
І. С. Гриценко (Харків), З. Гуджинскас (Вільнюс, Литва), М. М. Доля (Київ),
І. О. Журавель (Харків), Л. Запрутко (Познань, Польща),
Л. Іванаускас (Каунас, Литва), М. М. Івашура (Харків), О. А. Коваленко (Миколаїв),
С. І. Коваленко (Запоріжжя), С. М. Коваленко (Харків), С. Козачок (Пулави, Польща),
М. І. Короткіх (Київ), А. Ж. Костич (Белград, Сербія), О. М. Костюк (Київ),
С. М. Крамарьов (Дніпро), Р. Б. Лесик (Львів), В. В. Ліпсон (Харків),
В. Манос (Нікозія, Кіпр), О. О. Михайленко (Харків), М. Д. Обушак (Львів),
П. П. Онисько (Київ), Л. О. Рябовол (Умань), А. В. Семеніхін (Ніжин),
О. Б. Смолій (Київ), М. В. Стасевич (Львів), О. О. Стасик (Київ),
Г. Федорова (Чеські Будейовиці, Чехія), Л. А. Шемчук (Харків)

Редакційна рада:

С. А. Андронаті (Одеса), О. М. Біловол (Харків), А. І. Вовк (Київ),
Б. С. Зіменковський (Львів), В. І. Кальченко (Київ), Г. Л. Камалов (Одеса),
В. А. Чебанов (Харків), В. П. Черних (Харків), Ю. Г. Шермолівич (Київ),
Ю. Л. Ягупольський (Київ)

У журналі розглянуто проблеми синтезу й аналізу органічних та елементо-органічних сполук, аналогів природних сполук і лікарських субстанцій, наведено результати фізико-хімічних досліджень у вищезазначених напрямках. Також з погляду (біо)органічної, фармацевтичної, аналітичної та фізичної хімії проаналізовано питання з різних аспектів рослинництва, ґрунтознавства й дослідження навколишнього середовища.

Для працівників науково-дослідних установ, вищих навчальних закладів та фахівців хімічного, фармацевтичного, біологічного, медичного і сільськогосподарського профілів.

«Журнал органічної та фармацевтичної хімії» внесено до затвердженого МОН України Переліку наукових фахових видань України (категорія «Б») для опублікування результатів дисертаційних робіт за спеціальністю 102 – Хімія та 226 – Фармація, промислова фармація (наказ МОН України від 28.12.2019 р. № 1643); індексовано в наукометричних базах даних: Chemical Abstracts (CAS), Index Copernicus; внесено до каталогів та пошукових систем: Directory of Open Access Journals (DOAJ), Bielefeld Academic Search Engine (BASE), Directory of Open Access scholarly Resources (ROAD), PKP Index, Ulrich's periodicals, Worldcat, НБУ ім. В. І. Вернадського і УРЖ «Джерело».

Затверджено до друку вченою радою Інституту органічної хімії НАН України, протокол № 8 від 27.05.2024 р.

Затверджено до друку вченою радою Національного фармацевтичного університету, протокол № 5 від 30.05.2024 р.

Адреса для листування: 61002, м. Харків, вул. Пушкінська, 53, Національний фармацевтичний університет, редакція «Журналу органічної та фармацевтичної хімії». E-mail: publish@nuph.edu.ua, orgpharm-journal@nuph.edu.ua. Сайт: <http://orphcj.nuph.edu.ua>

Передплатні індекси: для індивідуальних передплатників — 08383, для підприємств — 08384

Свідоцтво про державну реєстрацію серії КВ № 23086-12926ПР від 05.01.2018 р.

Підписано до друку 12.06.2024 р. Формат 60 × 84 1/8.

Папір офсетний. Друк ризо. Умовн. друк. арк. 9,3. Обліков.-вид. арк. 10,76. Тираж 50 прим.

Редактори — О. Ю. Гурко, Л. І. Дубовик. Комп'ютерне верстання — О. М. Білінська

«Журнал органічної та фармацевтичної хімії». Том 22, випуск 1 (85), 2024

ISSN 2308-8303 (Print)

ISSN 2518-1548 (Online)

UDC 519.85:615.252

M. M. Suleiman, A. P. Semenets, N. P. Kobzar, L. O. Perekhoda

National University of Pharmacy of the Ministry of Health of Ukraine,
53 Hryhorii Skovoroda str., 61002 Kharkiv, Ukraine

The Theoretical Substantiation of the Targeted Search for New DPP4 Inhibitors. Computational Studies of Potential Candidates

Abstract

Growing evidence suggests that dipeptidyl peptidase 4 (DPP4) inhibitors, in addition to their role in improving glycemic control, help to reduce endothelial dysfunction and have hypolipidemic, anti-atherosclerotic, antitumor, antiviral, and neurotropic properties. This multi-target property may be one of the reasons for repurposing therapeutic treatment strategies with existing agents and the basis for finding new agents to inhibit this target. Based on the structural prerequisites and the evolutionary path of creating DPP4 inhibitors, an inhibitory (*R*)- β -aminoamide base was used as the basis for constructing potential candidates. It contained a substituted piperazine-2-one derivative and (*S*)-pyrrolidine-2-carbonitrile fragment, as well as phenyl and diphenyl rings, which were additionally saturated with substituents of various electronic structures, in position 4 of the β -aminoamide chain. The construction of the molecules was carried out taking into account the correspondence of chiral centers to combinations of chiral chains at the DPP4 binding site to possibly prevent a decrease in the inhibitory activity. *In silico* assessment of the "drug-likeness" and pharmacokinetic profile of the group of compounds studied showed that it had favorable characteristics and could be recommended for further molecular docking in order to predict the likely inhibition of the catalytic activity of DPP4. According to the results of docking, molecules with a moderate and high affinity were found. A detailed analysis of the resulting complexes showed that only nine compounds had a binding mode similar to classical inhibitors. According to the calculated array of values and analysis of the results of docking among the derivatives tested, a hit compound was found as a promising DPP4 inhibitor.

Keywords: gliptins; dipeptidyl peptidase-4 (DPP4); virtual screening; ADMET; molecular docking

М. М. Сулейман, А. П. Семенець, Н. П. Кобзар, Л. О. Перехода

Національний фармацевтичний університет Міністерства охорони здоров'я України,
вул. Григорія Сковороди, 53, м. Харків, 61002, Україна

Теоретичне обґрунтування цілеспрямованого пошуку нових інгібіторів DPP4. Обчислювальні дослідження потенційних кандидатів

Анотація

Дедалі більша кількість доказів свідчить про те, що інгібітори дипептидилпептидази 4 (DPP4), окрім їхньої ролі в покращенні глікемічного контролю, допомагають полегшити ендотеліальну дисфункцію, володіють гіполіпідемічною, антиатеросклеротичною, протипухлинною, противірусною та нейротропною властивостями. Така мультитаргетна властивість може бути однією з підстав перепрофілювати терапевтичні стратегії лікування наявними засобами та приводом для пошуку нових агентів для інгібування цієї мішені. З огляду на структурні передумови та еволюційний шлях створення інгібіторів DPP4 для конструювання потенційних кандидатів було використано (*R*)- β -аміноамідну молекулярну платформу. Вона містила заміщене похідне піперазин-2-ону і (*S*)-піролідін-2-карбонітрильний фрагмент, а також фенільні й дифенільні кільця в положенні 4 β -аміноамідного ланцюга, які додатково було насичено замісниками різної електронної будови. Побудову молекул проведено з урахуванням відповідності хіральних центрів до комбінацій хіральних ланцюгів у сайті зв'язування DPP4 для можливого запобігання зниженню інгібіторної активності. *In silico* оцінювання «лікоподібності» і фармакокінетичного профілю досліджуваної групи сполук засвідчило, що вона має сприятливі характеристики і може бути рекомендована для подальшого молекулярного докінгу, за результатами якого виявлено молекули, які мали помірний і високий афінитет, проте лише дев'ять сполук мали тип зв'язування, подібний до класичних інгібіторів. За обчисленим масивом значень та аналізом результатів докінгу було визначено сполуку-хіт як перспективний інгібітор.

Ключові слова: гліптени; дипептидилпептидаза-4 (DPP4); віртуальний скринінг; ADMET; молекулярний докінг

Citation: Suleiman, M. M.; Semenets, A. P.; Kobzar, N. P.; Perekhoda, L. O. The Theoretical Substantiation of the Targeted Search for New DPP4 Inhibitors. Computational Studies of Potential Candidates. *Journal of Organic and Pharmaceutical Chemistry* 2024, 22 (1), 3–12.

<https://doi.org/10.24959/ophcj.24.302677>

Received: 5 March 2024; **Revised:** 27 March 2024; **Accepted:** 29 March 2024

Copyright © 2024, M. M. Suleiman, A. P. Semenets, N. P. Kobzar, L. O. Perekhoda. This is an open access article under the CC BY license (<http://creativecommons.org/licenses/by/4.0>).

Funding: The authors received no specific funding for this work.

Conflict of interests: The authors have no conflict of interests to declare.

■ Introduction

The search for new drugs among small molecules does not lose its relevance, and an effective tool for achieving this goal is certainly to identify a target that would be involved in a large number of biochemical and physiological processes. Based on this strategy, the therapeutic effectiveness of existing drugs used for other diseases can be repurposed for the treatment of seemingly unrelated pathologies. In our opinion, one of these targets is dipeptidyl peptidase-4 (DPP4), a widely expressed transmembrane glycoprotein with peptidase activity in the extracellular domain, which regulates numerous biological processes. DPP4 is a serine protease that can cleave substrates with proline or alanine fragments in the penultimate position [1]. Native substrates of the enzyme are glucagon-like peptide-1, neuropeptide Y, secretin, pituitary adenylate cyclase activating polypeptide, endorphins, endomorphins, brain natriuretic peptide, beta-melanocyte stimulating hormone, amyloid peptides. DPP4 degrades and regulates numerous chemokines and cytokines and acts as a cell surface receptor, binds to adenosine deaminase, interacts with the extracellular matrix, and controls cell migration and differentiation [2, 3]. Today, there is a group of substances (gliptins) that inhibit this protease [4, 5]. In addition to their role in improving glycemic control, they can relieve endothelial dysfunction in patients with Type 2 diabetes [6]. The anti-inflammatory effect of DPP4 inhibitors, which has been reported in clinical and preclinical studies of endothelial dysfunction and diabetic ulcers, indicates the additional usefulness of this class of drugs [7]. It is known that chronic vascular complications associated with diabetes are associated with atherosclerosis. DPP4 inhibitors are involved in controlling risk factors by regulating blood lipids and lowering blood pressure. The atherosclerotic effect is also associated with improved endothelial cell dysfunction by increasing the level of circulating endothelial progenitor cells, regulating mononuclear macrophages, and suppressing inflammation and oxidative stress [7, 8]. A large number of studies

demonstrate that this protease also plays an important role in the immune system, and is especially expressed in immune cells, such as T cells, B cells, NK cells, dendritic cells, and macrophages [9]. In this regard, research is underway on known inhibitors for the treatment of immune-mediated diseases. Currently, there are studies on the possibility of using gliptins against COVID-19. Recent studies have shown that the binding domain of the spike protein receptor can interact with human DPP4 to facilitate viral entry, in addition to the usual pathway of binding to angiotensin-converting enzyme 2 (ACE2) [10, 11]. Interfering with such an interaction is a potential strategy for effectively preventing viral replication, but long-term clinical data have not yet been obtained. Growing evidence suggests that endogenous peptides, such as glucagon-like peptide-1 (GLP-1) and stromal cell-derived factor-1 α (SDF-1 α) provide neuroprotection in a number of experimental models of Alzheimer's disease. Thus, maintaining the functional activity of SDF-1 α and GLP-1 by inhibiting DPP4 will enhance the involvement of resident and non-resident circulating brain stem cells, which is a non-invasive approach for stimulating neurogenesis [12, 14].

DPP4 inhibitors are considered viable agents for the treatment of neurodegenerative diseases, such as Parkinson's disease, which neuroprotective and therapeutic potential is provided by leveling dopaminergic degeneration, promoting neuronal regeneration [13, 14]. **Figure 1** shows the scheme of pharmacologically determined and potential therapeutic use of DPP4 inhibitors.

It should be noted that the use of existing DPP4 inhibitors for these pathologies has a softening effect. This effect is explained by the fact that the known inhibitors can affect peripheral DPP4 since they cannot pass through the intact blood-brain barrier [14]. In this regard, the search for the "ideal" DPP4 inhibitor is continuing so far.

■ Materials and methods

The design of potential inhibitors of dipeptidyl peptidase-4 for virtual screening was carried out using the Marvin Sketch 20.5 program.

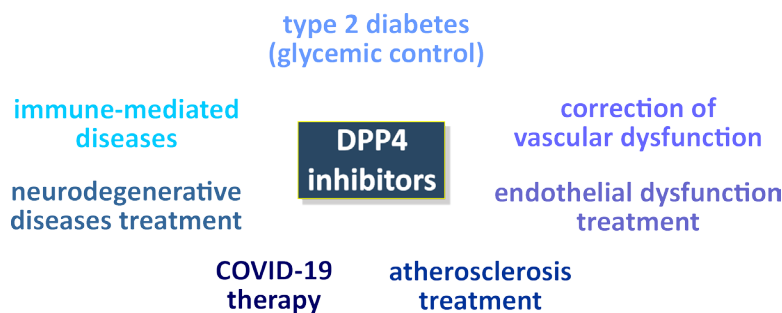


Figure 1. Pharmacologically determined and potential therapeutic use of DPP4 inhibitors

ADMET parameters were calculated using *in silico* tool – pkCSM [15]. Toxicity was assessed using the ProTox 3.0 online program [16]. For calculations, 2D structures of molecules were converted to the SMILES format using the SMILES Translator online tool. The Autodock 4.2 software package was used for the receptor-oriented flexible docking. Ligands were prepared using the MGL Tools 1.5.6 program. The Ligand optimization was performed using the Avogadro program. To perform calculations in the Autodock 4.2 program, the output formats of the receptor and ligand data were converted to a special PDBQT format. In our previous studies, a similar software package was used [17, 18]. The active macromolecule center of the dipeptidyl peptidase-4 (dpp4) (PDB ID: 5Y7J) from the Protein Data Bank (PDB) was used as a biological target for docking. The receptor maps were made in MGL Tools and AutoGrid programs. Water molecules, ions, and the ligand were removed from the PDB file. Visualization of the resulting complexes of the molecules studied in the active sites of the receptors was carried out using the Discovery Studio Visualizer program. The following docking parameters were set: the translational step was 2 Å; the torsional freedom coefficient was 0.2983; the cluster tolerance was 2 Å; the external lattice energy – 1000; the maximum initial energy – 0; the maximum number of attempts – 10,000; the number of structures in the population – 150; the maximum number of stages of energy estimation – 2,500,000; the maximum number of generations – 27,000; the number of structures passing to the next generation – 1; the level of gene mutation – 0.02; the level of the crossover – 0.8; the method of the crossover – arithmetic. The α -Gaussian distribution parameter was equal to 0, and the β -parameter of the Gaussian distribution was 1.

■ Results and discussions

Many DPP4 inhibitors have appeared in the pharmaceutical market. They are used as

a relatively new class of hypoglycemic drugs called “gliptins” [19]. There are warnings that these compounds may have an increased risk of toxic effects on the pancreas, namely due to the occurrence of pancreatitis and pancreatic cancer during their long-term use. Large independent studies conducted by the Food and Drug Administration have not shown evidence of pancreatic toxicity and are not consistent with available scientific data [20]. Therefore, the search for new structural analogs of this group is undoubtedly relevant and justified. It should be noted that each of DPP4 inhibitors introduced into clinical practice has its own structural differences and binding mechanisms. At the first stage of the targeted search for new gliptins, empirical experience and logical-structural analysis were used to theoretically substantiate the choice of basic structures. **Figure 2** shows the Structure/Activity Relationships of the known DPP4 inhibitors.

Based on the structural prerequisites and the evolutionary path of creating gliptins, an inhibitory (*R*)- β -aminoamide platform was taken as a basis for constructing potential inhibitors (**Table 1**). It contained either a substituted piperazine-2-one core or (*S*)-pyrrolidine-2-carbonitrile fragment, as well as phenyl rings in position 4 of the β -aminoamide chain, which were additionally saturated with substituents of various electronic structures. The configuration of the molecule is crucial for ligand-enzyme interactions, so that the construction of the molecules was carried out taking into account the correspondence of the chiral centers to combinations of chiral chains at the DPP4 binding site to possibly prevent a decrease in the inhibitory activity.

For the constructed molecules, the parameters of “drug-likeness” were calculated for compliance with the Lipinsky’s rule (**Table 1**). The Lipinski’s rule of five requires that a compound has a molecular weight of no more than 500, should not form more than five hydrogen bonds, and should not accept more than ten hydrogen bonds, while the $\log P$ coefficient should be less than 5 [23].

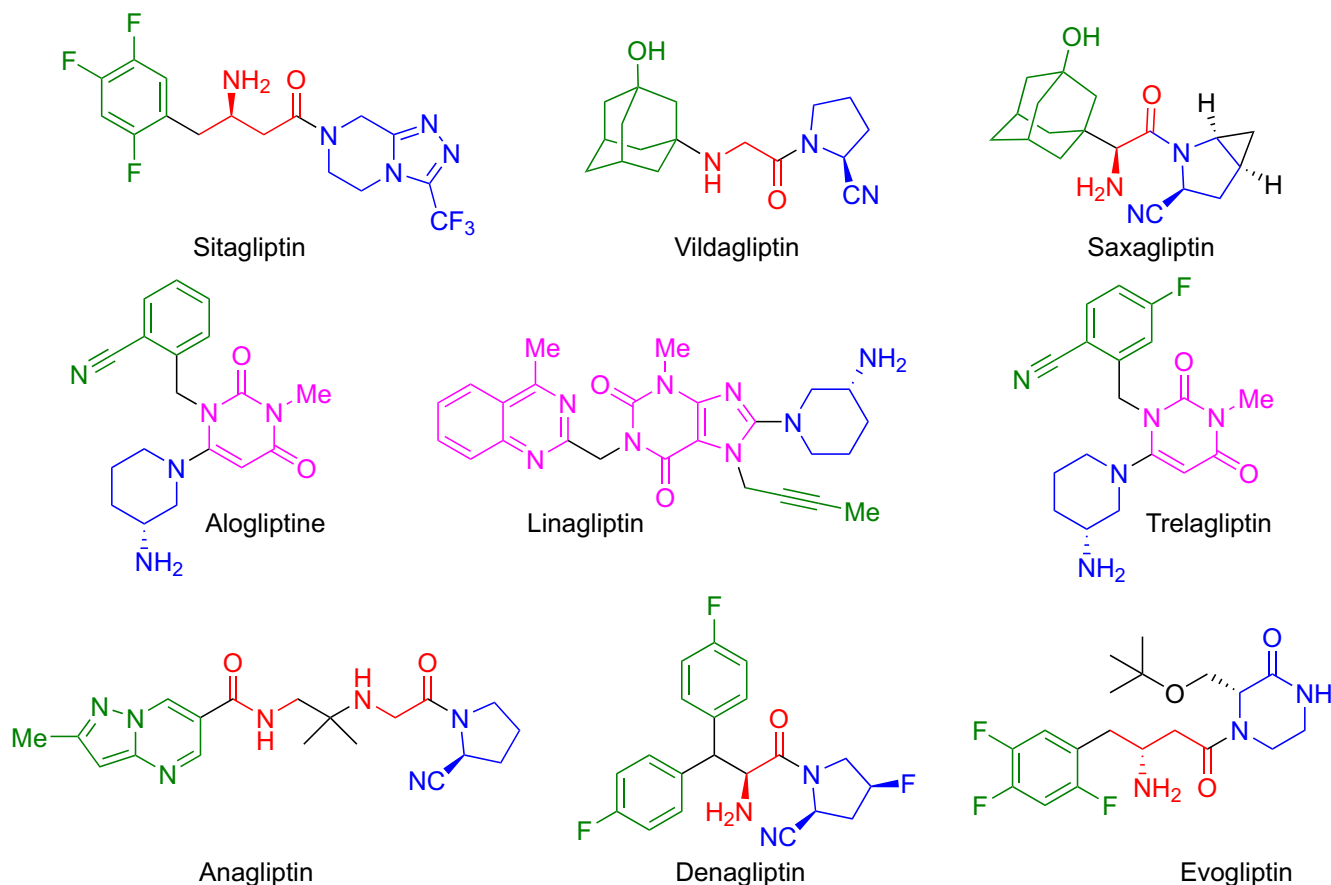


Figure 2. Structure/Activity Relationships within the group of known DPP4 inhibitors. Mandatory fragments responsible for the inhibitory activity of the enzyme are highlighted in red, blue, and green (occupy subsites S1, S2 and S2ext respectively); additional fragments highlighted in purple are located in subsites S1' and S2', which contribute to the increase of inhibitory activity [21, 22]

Based on the calculations, only compound **2** had a molecular weight not significantly higher than the established criteria, so we subjected all the compounds studied to the predictive ADMET analysis.

Absorption plays a significant role in the drug activity, i.e. poorly water-soluble drugs show a lower rate of absorption when taken orally, which may affect the revision of the dosage level. The calculated parameters for solubility and absorption determined that the molecules tested had moderate solubility and a high level of absorption in the intestine (**Table 2**).

P-glycoprotein is known to function as a biological barrier displacing toxins and xenobiotics from cells. According to the calculated data, compounds **1**, **2**, **10** and **11** are likely to have appropriate pharmacokinetic effects that can be used to obtain certain therapeutic benefits or lead to contraindications.

However, the calculated volumes of distribution of these compounds had optimal values comparable to other molecules studied. The level of the predicted fraction that will be unbound in plasma, the parameters of a possible penetration through the BBB and CNS indicate that all molecules have the moderate penetration and distribution

indicators to a greater extent. Clinical trials have shown that the induction of isoenzymes, such as CYP2C9 and CYP3A4 is associated with diabetes; therefore, the interference with metabolism can lead to a decrease in the drug activity [23].

According to the values obtained, none of the compounds was a substrate for CYP2C9, and only compounds **1**, **2**, **10**, and **11** showed a possible inhibition of CYP3A4. As for the substrate activity to OCT2, only compound **1** might have a potential drug interaction, all other compounds did not show this possibility (**Table 2**).

In the next step, we assessed the toxic effects of the molecules tested using the pkCSM and ProTox tools and determined the class for each compound (**Table 3**). The lethal drug is classified as Class I, and the least toxic or beneficial compound as Class VI. Based on these properties, we have found that compounds **1–5** belong to Class V, and all others belong to Class IV [24]. The next step in computer assessment, which would allow selection of the most promising compounds for further experimental studies, is the computational molecular analysis method to describe the binding efficiency and affinity (molecular docking).

Table 1. The calculated parameters of “drug-likeness” for potential DPP4 inhibitors

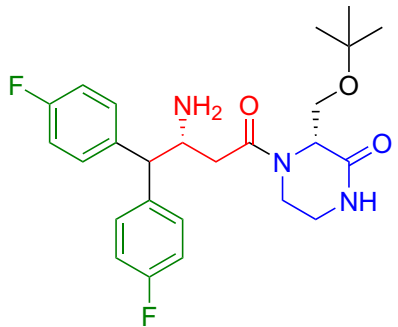
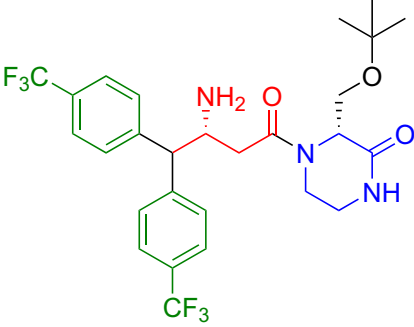
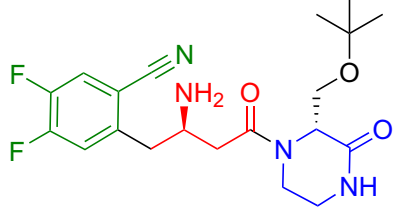
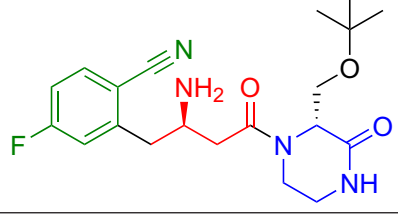
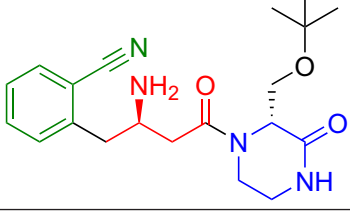
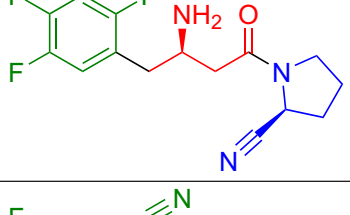
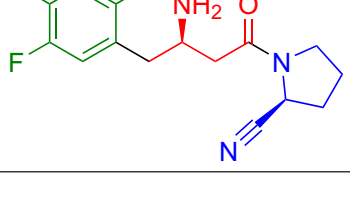
Compound	Structural formulas	LogP	Molecular Weight	H bond Donors	H bond Acceptors
1	2	3	4	5	6
1		2.9	459	2	4
2		4.7	559	2	4
3		1.2	408	2	5
4		1.1	390	2	5
5		0.9	372	2	5
6		1.8	311	1	3
7		1.6	318	1	4

Table 1 (continued)

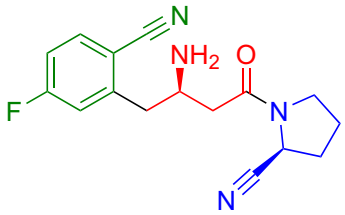
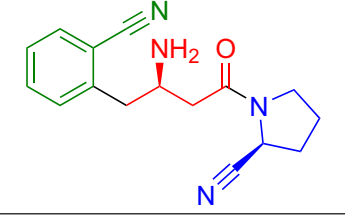
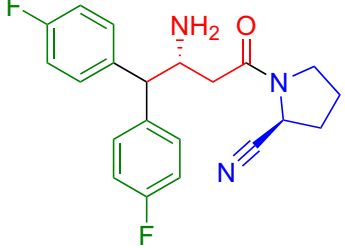
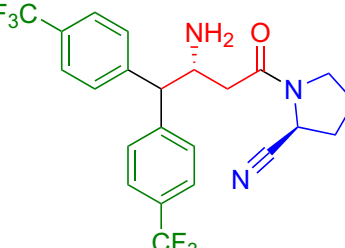
1	2	3	4	5	6
8		1.4	300	1	4
9		1.3	282	1	4
10		3.3	369	1	3
11		5.1	469	1	3

Table 2. The calculated ADME parameters for potential DPP4 inhibitors

Compound	Water solubility ¹	Caco-2 permeability ²	Intestinal absorption (human) ³	P-glycoprotein substrate / inhibitor I / II	VD _{ss} Human ⁴	Fraction unbound ⁵	BBB permeability ⁶	CNS permeability ⁷	CYP3A4 substrate / inhibitor	CYP2C9 inhibitor	Total clearance ⁸	Renal OCT2 substrate
1	-4.759	1.017	96.476	Yes / Yes / Yes	0.79	0.102	-0.962	-2.615	Yes/ Yes	No	0.543	Yes
2	-4.766	0.99	90.996	Yes / Yes / Yes	0.671	0.061	-1.134	-2.175	Yes/ Yes	No	0.279	No
3	-3.297	0.209	73.656	Yes / No / No	0.104	0.312	-0.996	-2.974	No / No	No	0.726	No
4	-3.335	0.201	75.419	Yes / No / No	0.174	0.338	-0.793	-2.936	No / No	No	0.764	No
5	-3.301	0.186	72.034	Yes / No / No	0.275	0.389	-0.574	-2.876	No / No	No	0.831	No
6	-3.289	1.215	92.497	No / No / No	0.254	0.383	-0.622	-2.98	No / No	No	0.679	No
7	-3.269	0.146	80.607	No / No / No	0.227	0.357	-0.585	-3.002	No / No	No	0.708	No
8	-2.833	0.134	82.355	No / No / No	0.401	0.367	-0.38	-2.617	No / No	No	0.747	No
9	-2.211	0.12	78.938	No / No / No	0.588	0.379	-0.095	-2.561	Yes / No	No	0.831	No
10	-4.611	1.072	93.365	Yes / Yes / Yes	0.766	0.11	-0.187	-2.325	Yes / Yes	No	0.567	No
11	-5.741	0.55	87.878	Yes / Yes / Yes	0.997	0	-0.557	-1.874	Yes / Yes	No	0.309	No

Note: units of measurement ¹(logS in mol L⁻¹), ²(logP_{app} in 10⁻⁶ cm sec⁻¹), ³(%absorbed), ⁴(log in L kg⁻¹), ⁵(Fu), ⁶(log BB), ⁷(log PS), ⁸log in mL min⁻¹ kg⁻¹)

Table 3. Basic toxicity parameters calculated using the pkCSM and ProTox tools

Compound	pkCSM tool		ProTox tool	
	Oral Rat Chronic Toxicity (LOAEL) log in mol kg ⁻¹	Oral Rat Acute Toxicity (LD50) mol kg ⁻¹	LD50 in mg kg ⁻¹	toxicity class
1	1.193	3.338	2973	V ¹
2	0.909	3.251	2973	V
3	2.506	2.925	2973	V
4	1.428	2.745	2973	V
5	1.372	2.588	2973	V
6	2.070	2.600	1160	IV ²
7	2.068	2.461	1160	IV
8	1.521	2.398	1160	IV
9	1.439	2.604	630	IV
10	1.412	2.606	1850	IV
11	0.932	3.016	326	IV

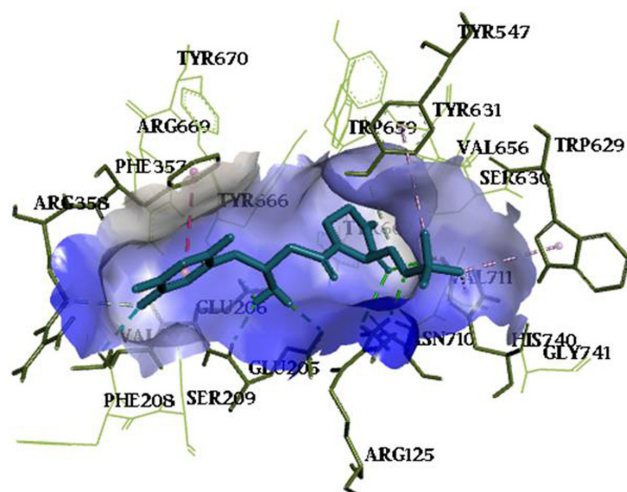
Note: ¹Class V: may be harmful if swallowed (2000 < LD50 ≤ 5000);

²Class IV: harmful if swallowed (300 < LD50 ≤ 2000)

Molecular docking of compounds was performed relative to the selected crystallographic model (PDB ID: 5Y7J) at the well-controlled binding site of DPP4 inhibitors. Evogliptin was chosen as a reference drug since it was co-crystallized relative to the selected target, and the redocking results obtained (scoring function, free energy, and binding constant) were used as standard ones.

As a result of Evogliptin redocking, key interactions with DPP4, which were in good agreement with the results of crystallographic studies, were identified [25] (**Figure 3**).

According to the estimated values (**Table 4**), the molecules studied had the best energy positions

**Figure 3.** Visualization of Evogliptin redocking relative to DPP4

with moderate values of the scoring function, except for molecules **2** and **11**, which had absolute affinity values higher than those of Evogliptin. In turn, compound **11** had a better result in terms of free energy and binding constant values compared to the reference indicators.

To assess the binding modes of new molecules relative to the DPP4 binding site, a detailed analysis of the geometric location of energy advantageous positions was performed, and all the resulting complexes with the target under study were analyzed.

As expected, almost all of the compounds tested (**3–9**) had the same binding mode to Evogliptin (**Figure 4, A**), namely the substituted phenyl rings occupied the hydrophobic pocket S1 and interacted with *Ser630*, *Val656*, *Trp659*, *Tyr662*, *Tyr666*, *Val711*, and *Asn710* amino acid residues; piperazin-2-one and pyrrolidine parts were located against the *Phe357* side chain, thus occupying the extended S2 and S2ext subsites where the S2 pocket referred to the pocket formed by *Arg125*, *Arg669*, *Glu205*, *Glu206*, *Phe357*, and *Arg358*, and the S2ext subsite referred to the subsite formed by *Phe357*, *Arg358*, *Ser209*, and *Val207*. The (*R*)- β -amino part of the butanoyl group formed hydrogen bonds with *Tyr662*, *Glu206*, and *Glu205* residues. In some complexes, hydrogen bonds with the *His740* amino acid residue – a part of the catalytic triad of the enzyme (*Ser630*, *His740*, *Asp708*) – were observed. It should be noted that molecules **10** and **11**, which substituted diphenyl rings in the (*R*)- β -amino group, contributed to the immersion of molecules in both the hydrophobic pocket S1 and site S2 forming broad interactions with the corresponding amino acid chains (**Figure 4, B**).

Table 4. The estimated values of docking of the compounds studied in the DPP4 site

Compound	Affinity DG ¹ , kcal mol ⁻¹	EDoc ² , kcal mol ⁻¹	Ki ³ , μ M
1	-8.5	-5.62	75.64
2	-9.0	-4.87	270.34
3	-8.4	-5.66	70.60
4	-8.0	-5.37	115.18
5	-8.0	-6.22	27.62
6	-7.6	-5.90	47.31
7	-7.7	-6.54	16.08
8	-8.1	-6.25	26.41
9	-8.1	-6.40	20.25
10	-8.4	-6.72	11.81
11	-9.7	-7.32	4.34
Evogliptin	-8.5	-5.53	88.17

Note: ¹scoring function; ²binding free energy; ³binding constant

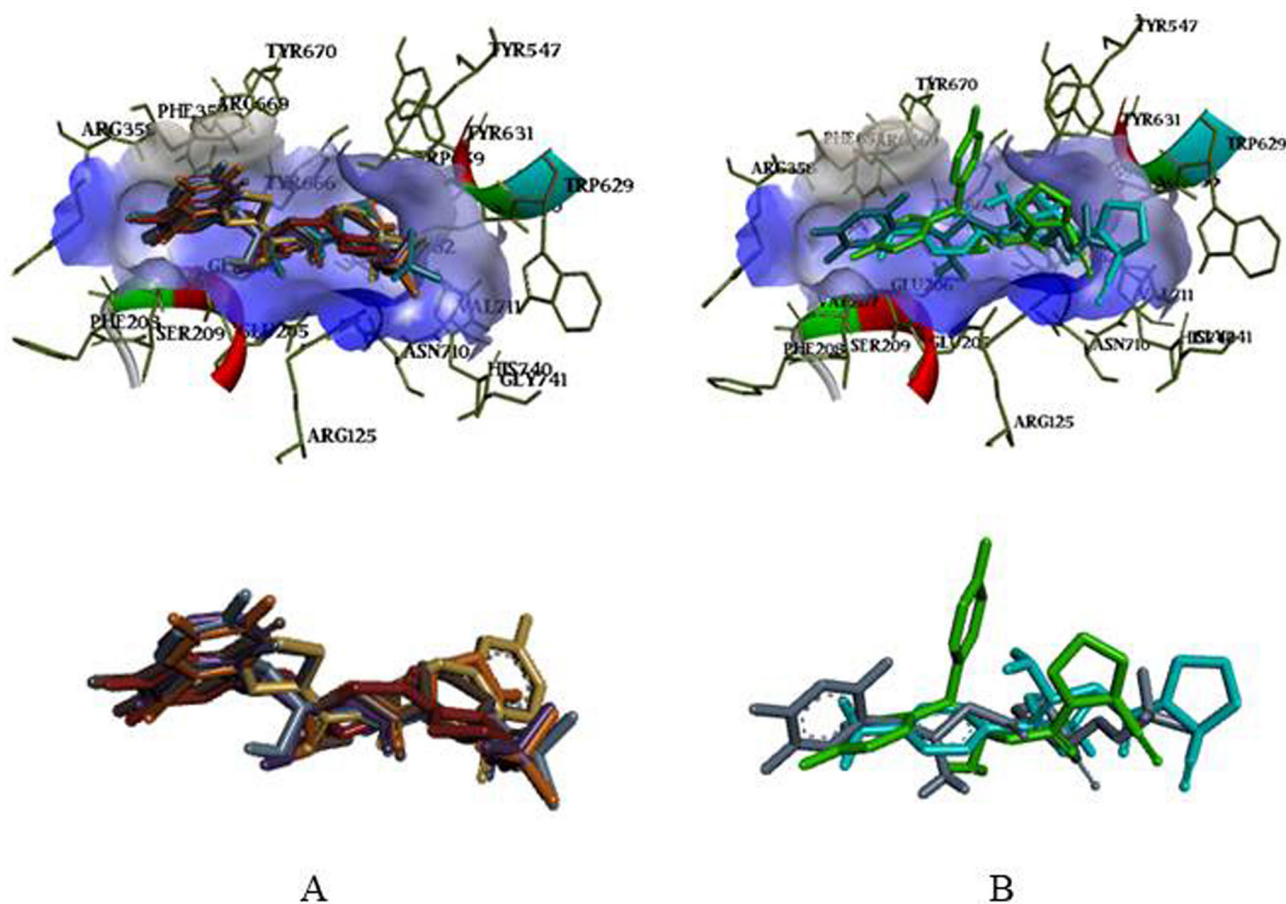


Figure 4. Superpositions of molecules 3–9 (A), and 10–11 (B) at the DPP4 binding site compared to Evogliptin (compound 3 – orange, compound 4 – gray, compound 5 – purple, compound 6 – red, compound 7 – brown, compound 8 – yellow, compound 9 – lilac, compound 10 – green, compound 11 – blue, Evogliptin – blue)

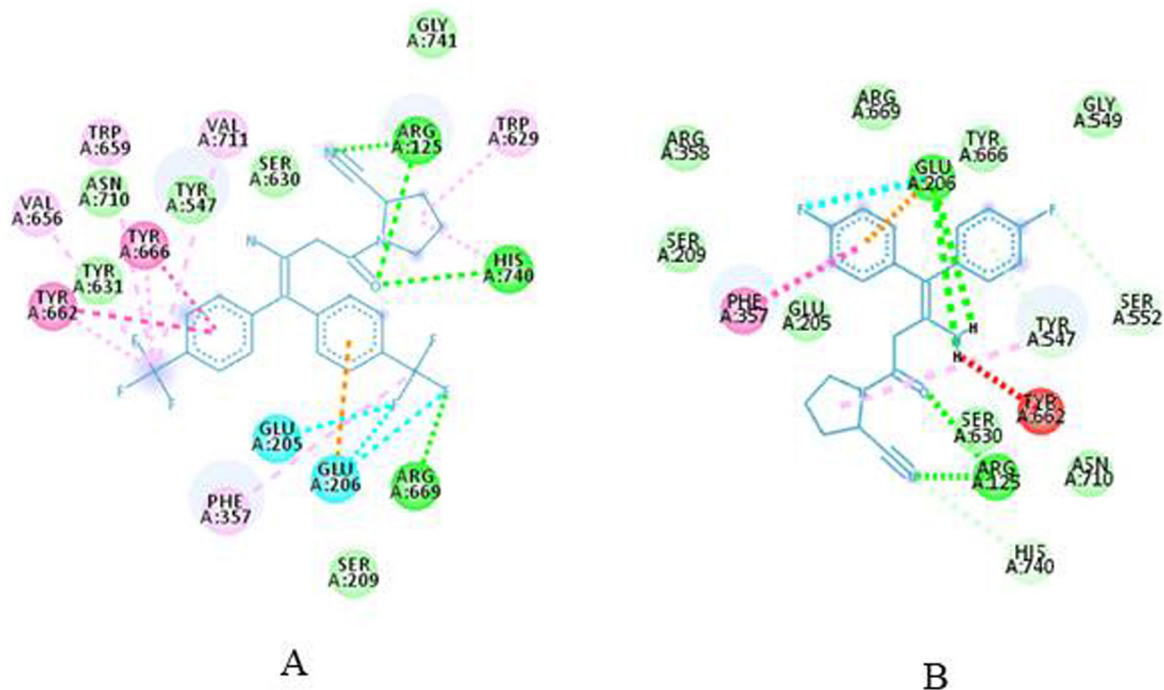


Figure 5. Diagrams of intermolecular interactions of hit compound 11 (A) and compound 10 (B). Visualization of bonds is shown by dashed lines of the corresponding color: Vander Waals forces – light green, hydrogen bonds – green, light gray; halogen – blue; π -anion interaction – orange; donor–donor bond – red; π - π interaction – purple, π -Alk and Alk interaction – pink

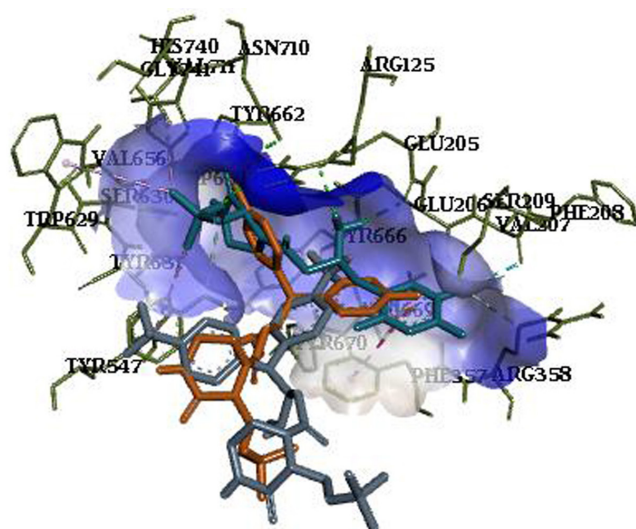


Figure 6. Superpositions of compound **1** (orange) and compound **2** (gray) relative to DPP4 compared to Evogliptin (blue)

Among the molecules studied, a hit compound **11** (affinity $DG = -9.7$ kcal mol⁻¹, $E_{Doc} = -7.32$ kcal mol⁻¹, $K_i = 4.34$ μm) was found. It formed a number of favorable interactions with the amino acid chains of the DPP4 site (**Figure 5, A**). However, among the compounds that had an inherent binding mode for enzyme inhibitors, compound **10** was found with moderate calculated docking values (affinity $DG = -8.4$ kcal mol⁻¹, $E_{Doc} = -6.72$ kcal mol⁻¹, $K_i = 11.81$ μm). It formed an unfavorable donor–donor interaction with the *Tyr662* residue with the participation of the (*R*)-β-amino part of the butanoyl group (**Figure 5, B**). This type of interaction can lead to non-binding efficacy. Therefore, compound **10** is not recommended for further research.

References

- Klemann, C.; Wagner, L.; Stephan, M.; von Hörsten, S. Cut to the chase: a review of CD26/dipeptidyl peptidase-4's (DPP4) entanglement in the immune system. *Clin. Exp. Immunol.* **2016**, *185*, 1–21. <https://doi.org/10.1111/cei.12781>.
- Gilbert, M. P.; Pratley, R. E. GLP-1 Analogs and DPP-4 Inhibitors in Type 2 Diabetes Therapy: Review of Head-to-Head Clinical Trials. *Frontiers in Endocrinology* **2020**, *11*, 178. <https://doi.org/10.3389/fendo.2020.00178>.
- Vincenzo, F.; Manfredi, T.; Carmine, C.; Mario, R. CD26: a multi-purpose pharmacological target. *Curr. Clin. Pharmacol.* **2014**, *9* (2), 157–164. <https://doi.org/10.2174/1574884708666131111201654>.
- An update on the 'gliptins'. *Drug and Therapeutics Bulletin* **2016**, *54*(12), 138–141. <https://doi.org/10.1136/dtb.2016.12.0442>.
- Ahmad, E.; Lim, S.; Lamptey, R.; Webb, D. R.; Davies, M. J. Type 2 diabetes. *Lancet* **2022**, *400* (10365), 1803–1820. [https://doi.org/10.1016/S0140-6736\(22\)01655-5](https://doi.org/10.1016/S0140-6736(22)01655-5).
- Brunton, S. Pathophysiology of Type 2 Diabetes: The Evolution of Our Understanding. *The Journal of Family Practice* **2016**, *65* (4 Suppl).
- Yazbeck, R.; Jaenisch, S. E.; Abbott, C. A. Dipeptidyl peptidase 4 inhibitors: Applications in innate immunity? *Biochem. Pharmacol.* **2021**, *188*, 114517. <https://doi.org/10.1016/j.bcp.2021.114517>.
- Liu, H.; Guo, L.; Xing, J.; Li, P.; Sang, H.; Hu, X.; Du, Y.; Zhao, L.; Song, R.; Gu, H. The protective role of DPP4 inhibitors in atherosclerosis. *Eur. J. Pharmacol.* **2020**, *875*, 173037. <https://doi.org/10.1016/j.ejphar.2020.173037>.
- Hu, X.; Wang, X.; Xue, X. Therapeutic Perspectives of CD26 Inhibitors in Immune-Mediated Diseases. *Molecules* **2022**, *27* (14), 4498. <https://doi.org/10.3390/molecules27144498>.
- Mani, S.; Kaur, A.; Jakhar, K.; Kumari, G.; Sonar, S.; Kumar, A.; Das, S.; Kumar, S.; Kumar, V.; Kundu, R.; Pandey, A. K.; Singh, U. P.; Majumdar, T. Targeting DPP4-RBD interactions by sitagliptin and linagliptin delivers a potential host-directed therapy against pan-SARS-CoV-2 infections. *Int. J. Biol. Macromol.* **2023**, *245*, 125444. <https://doi.org/10.1016/j.ijbiomac.2023.125444>.
- Posadas-Sánchez, R.; Sánchez-Muñoz, F.; Guzmán-Martín, C. A.; Hernández-Díaz Couder, A.; Rojas-Velasco, G.; Fragoso, J. M.; Vargas-Alarcón, G. Dipeptidylpeptidase-4 levels and DPP4 gene polymorphisms in patients with COVID-19. Association with disease and with severity. *Life Sci.* **2021**, *276*, 119410. <https://doi.org/10.1016/j.lfs.2021.119410>.

Among the compounds studied, molecules **1** and **2** had a binding mode that was not characteristic for DPP4 inhibitors. According to a detailed analysis of the location of these molecules, it has been found that the interaction with the site occurs due to the substituted diphenyl rings that interact with the corresponding amino acid chains of sites S1 and S2, and the inhibitory (*R*)-β-amino group and the substituted piperazine-2-one part do not have a characteristic binding to amino acids in well-documented sites. This indicates that these compounds probably will not be able to inhibit the catalytic activity of DPP4, despite the fairly good calculated docking values (**Table 3**). Therefore, they are not recommended for further research. **Figure 6** shows superpositions of compounds **1** and **2** relative to the target under study compared to Evogliptin.

Conclusions

In silico assessment of the “drug-likeness” and pharmacokinetic profile of the group of compounds studied has shown that it has favorable characteristics and can be recommended for further molecular docking in order to predict the likely inhibition of the catalytic activity of DPP4. According to the results of docking, molecules with a moderate and high affinity have been found. A detailed analysis of the resulting complexes has demonstrated that only 9 compounds have a binding mode similar to classical inhibitors. According to the calculated array of values and analysis of the results of docking hit compound **11** has been found as a promising inhibitor.

12. Chalichem, N. S. S.; Gonugunta, C.; Krishnamurthy, P. T.; Duraiswamy, B. DPP4 Inhibitors Can Be a Drug of Choice for Type 3 Diabetes: A Mini Review. *American Journal of Alzheimer's Disease & Other Dementias* **2017**, *32* (7), 444–451. <https://doi.org/10.1177/1533317517722005>.
13. Maanvi; Kumari, S.; Deshmukh, R. Dipeptidyl peptidase 4(DPP4) inhibitors stride up the management of Parkinson's disease. *Eur. J. Pharmacol.* **2023**, *939*, 175426. <https://doi.org/10.1016/j.ejphar.2022.175426>.
14. Bernstein, H. G.; Keilhoff, G.; Dobrowolny, H.; Steiner, J. The many facets of CD26/dipeptidyl peptidase 4 and its inhibitors in disorders of the CNS – a critical overview. *Rev. Neurosci.* **2022**, *34* (1), 1–24. <https://doi.org/10.1515/revneuro-2022-0026>.
15. Pires, D. E.; Blundell, T. L.; Ascher, D. B. pkCSM: Predicting Small-Molecule Pharmacokinetic and Toxicity Properties Using Graph-Based Signatures. *J. Med. Chem.* **2015**, *58* (9), 4066–4072. <https://doi.org/10.1021/acs.jmedchem.5b00104>.
16. Banerjee, P.; Eckert, A. O.; Schrey, A. K.; Preissner, R. ProTox-II: a webserver for the prediction of toxicity of chemicals. *Nucleic Acids Res.* **2018**, *46* (W1), W257–W263. <https://doi.org/10.1093/nar/gky318>.
17. Semenets, A. P.; Suleiman, M. M.; Fedosov, A. I.; Shtrygol, S. Y.; Havrylov, I. O.; Mishchenko, M. V.; Kovalenko, S. M.; Georgiyants, V. A.; Perekhoda, L. O. Synthesis, docking, and biological evaluation of novel 1-benzyl-4-(4-(R)-5-sulfonylidene-4,5-dihydro-1H-1,2,4-triazol-3-yl)pyrrolidin-2-ones as potential nootropic agents. *Eur. J. Med. Chem.* **2022**, *244*, 114823. <https://doi.org/10.1016/j.ejmech.2022.114823>.
18. Semenets, A.; Suleiman, M.; Georgiyants, V.; Kovalenko, S.; Kobzar, N.; Grinevich, L.; Pokrovskii, M.; Korokin, M.; Soldatov, V.; Bunyatyan, V.; Perekhoda, L. Theoretical justification of a purposeful search of potential neurotropic drugs. *ScienceRise: Pharmaceutical Science* **2020**, *4*, 4–17. <https://doi.org/10.15587/2519-4852.2020.210042>.
19. Dowarah. J.; Singh, V. P. Anti-diabetic drugs recent approaches and advancements. *Bioorg. Med. Chem.* **2020**, *28* (5), 115263. <https://doi.org/10.1016/j.bmc.2019.115263>.
20. Egan, A. G.; Blind, E.; Dunder, K.; Graeff, P. A. d.; Hummer, B. T.; Bourcier, T.; Rosebraugh, C. Pancreatic Safety of Incretin-Based Drugs – FDA and EMA Assessment. *N. Engl. J. Med.* **2014**, *370* (9), 794–797. <https://doi.org/10.1056/NEJMp1314078>.
21. Feng, J.; Zhang, Z.; Wallace, M. B.; Stafford, J. A.; Kaldor, S. W.; Kassel, D. B.; Gwaltney, S. L. Discovery of Alogliptin: A Potent, Selective, Bioavailable, and Efficacious Inhibitor of Dipeptidyl Peptidase IV. *J. Med. Chem.* **2007**, *50*(10), 2297–2300. <https://doi.org/10.1021/jm0701041>.
22. Mathur, V.; Alam, O.; Siddiqui, N.; Jha, M.; Manaihiya, A.; Bawa, S.; Sharma, N.; Alshehri, S.; Alam, P.; Shakeel F. Insight into Structure Activity Relationship of DPP-4 Inhibitors for Development of Antidiabetic Agents. *Molecules* **2023**, *28*(15), 5860. <https://doi.org/10.3390/molecules28155860>.
23. Sneha, P.; Doss, C. G. P. Gliptins in managing diabetes – Reviewing computational strategy. *Life Sci.* **2016**, *166*, 108–120. <https://doi.org/10.1016/j.lfs.2016.10.009>.
24. Drwal, M. N.; Banerjee, P.; Dunkel, M.; Wettig, M. R.; Preissner, R. ProTox: a web server for the in silico prediction of rodent oral toxicity. *Nucleic Acids Res.* **2014**, *42* (W1), W53–W58. <https://doi.org/10.1093/nar/gku401>.
25. Lee, H. K.; Kim, M.-K.; Kim, H. D.; Kim, H. J.; Kim, J. W.; Lee, J.-O.; Kim, C.-W.; Kim, E. E. Unique binding mode of Evogliptin with human dipeptidyl peptidase IV. *Biochem. Biophys. Res. Commun.* **2017**, *494* (3), 452–459. <https://doi.org/10.1016/j.bbrc.2017.10.101>.

Information about the authors:

Marharyta M. Suleiman (corresponding author), Ph.D. in Pharmacy, Associate Professor of the Medicinal Chemistry Department, National University of Pharmacy of the Ministry of Health of Ukraine; <https://orcid.org/0000-0001-6388-5342>; e-mail for correspondence: suleiman.nfau@outlook.com.

Anton P. Semenets, Ph.D. in Pharmacy, Bayer Ukraine; <https://orcid.org/0000-0002-7156-3375>; e-mail for correspondence: semenetsanton1996@gmail.com.

Nataliia P. Kobzar, Ph.D. in Pharmacy, Associate Professor of the Medicinal Chemistry Department, National University of Pharmacy of the Ministry of Health of Ukraine; <https://orcid.org/0000-0002-2062-2769>.

Lina O. Perekhoda, Dr.Sci. in Pharmacy, Professor, Head of the Medicinal Chemistry Department, National University of Pharmacy of the Ministry of Health of Ukraine; <https://orcid.org/0000-0002-8498-331X>.

UDC 615.032:616-00.03.06.08

O. F. Piminov, R. V. Sahaidak-Nikitiuk, A. I. Kvitchata, S. M. Rolik-Attia

Institute for Advanced Training of Pharmacy Specialists of the National University of Pharmacy
of the Ministry of Health of Ukraine, 17 Zakhysnykiv Ukrainy sq., 61001 Kharkiv, Ukraine

Immunotherapy of Diseases and Nanotechnology: Current State and Prospects

Abstract

Nanotechnology can be used to treat a number of diseases, which are currently the main cause of death in the world, and allow to achieve the desired therapeutic effect for the patient. This mini-review focuses on the analysis of scientific literary sources dealing with the application of nanotechnology in the immunotherapy of diseases and covers the period from 2016 to 2022. In particular, it provides an overview of recently discovered nanotechnologies (including immunomodulatory nanosystems) used for the prevention and treatment of various diseases, including cancer, infectious, inflammatory, and autoimmune diseases. The review also discusses the role of nanosystems in cancer immunotherapy. Additional attention is paid to nanomaterials with new structures, properties, and functions, which are used in the modern practice of treating viral and bacterial infections. A part of the paper is devoted to nanoparticles that enhance the effect of immunosuppressive cells in the treatment of inflammatory and autoimmune diseases. The analysis performed clearly demonstrates the relevance of nanotechnologies for the use in the immunotherapy of diseases. We hope it will allow researchers to identify new areas for using nanoparticles in the treatment of diseases of various etiologies.

Keywords: nanosystem; nanotechnology; nanoparticle; nanomaterials; autoimmune disease; disease treatment

О. Ф. Пімінов, Р. В. Сагайдак-Нікітюк, А. І. Квітчата, С. М. Ролік-Аттія

*Інститут підвищення кваліфікації спеціалістів фармації Національного фармацевтичного
університету Міністерства охорони здоров'я України,
майдан Захисників України, 17, Харків, 61001, Україна*

Імунотерапія захворювань та нанотехнології: сучасний стан та перспективи

Анотація

Нанотехнології можна використовувати для лікування певних захворювань, що сьогодні є основною причиною смертності у світі, бо це дозволяє досягти необхідного терапевтичного ефекту для пацієнта. Цей мініогляд, що охоплює період з 2016 до 2022 рр., зосереджено на аналізі наукових літературних джерел, у яких висвітлено застосування нанотехнологій в імунотерапії захворювань. Йдеться, зокрема, про нещодавно відкриті нанотехнології (разом з імуномодулювальними наносистемами), що їх застосовують для профілактики і лікування раку, інфекційних, запальних та аутоімунних захворювань. Розглянуто особливості використання в сучасній практиці лікування вірусних і бактеріальних інфекцій наноматеріалів з новими структурами, властивостями та функціями. Схарактеризовано наночастинки, які посилюють дію імуносупресивних клітин у лікуванні запальних та аутоімунних захворювань. Проведений аналіз наочно демонструє актуальність нанотехнологій для імунотерапії захворювань і, сподіваємось, дозволить дослідникам визначити нові напрями використання наночастинок у лікуванні захворювань різної етіології.

Ключові слова: наносистема; нанотехнологія; наночастинка; наноматеріали; аутоімунні захворювання; лікування захворювань

Citation: Piminov, O. F.; Sahaidak-Nikitiuk, R. V.; Kvitchata, A. I.; Rolik-Attia, S. M. Immunotherapy of Diseases and Nanotechnology: Current State and Prospects. *Journal of Organic and Pharmaceutical Chemistry* **2024**, *22* (1), 13–21.

<https://doi.org/10.24959/ophcj.24.304776>

Received: 27 March 2024; **Revised:** 13 April 2024; **Accepted:** 17 April 2024

Copyright © 2024, O. F. Piminov, R. V. Sahaidak-Nikitiuk, A. I. Kvitchata, S. M. Rolik-Attia. This is an open access article under the CC BY license (<http://creativecommons.org/licenses/by/4.0>).

Funding: The authors received no specific funding for this work.

Conflict of interests: The authors have no conflict of interests to declare.

■ Introduction

Today, immunotherapy has evolved into an effective strategy for the prevention and treatment of various diseases, including cancer, infectious, inflammatory, and autoimmune diseases. Immunomodulatory nanosystems can easily improve therapeutic effects while simultaneously overcoming many barriers to treatment, such as inadequate immune stimulation, side effects, and the loss of bioactivity of immune agents during circulation. In recent years, researchers have been constantly developing nanomaterials with new structures, properties and functions.

In cancer immunotherapy, nanosystems play an important role in activating immune cells and modulating the tumor microenvironment, as well as in combination with other antitumor approaches.

Regarding infectious diseases, there are many promising results of using vaccines made of nanomaterials against viral and bacterial infections. In addition, nanoparticles also enhance the effect of immunosuppressive immune cells in the treatment of inflammatory and autoimmune diseases.

A human immune system is able to protect them from many diseases based on a process called “immune surveillance”. In theory, viruses, bacteria and cancer cells can be quickly identified as foreign antigens and eliminated by immune cells. However, pathogens have developed a number of effective mechanisms to evade immune clearance by inhibiting phagocytosis, blocking antigen presentation, or directly killing immune cells. Cancer cells can shift the tumor microenvironment (TME) into a highly immunosuppressive state by recruiting immunosuppressive immune cells and expressing a series of inhibitory cytokines, enzymes, and checkpoint molecules, thereby promoting tumor immune evasion. These barriers certainly reduce the efficiency and intensity of immune responses. Conversely, aberrant activation of immune cells can cause uncontrolled inflammatory, autoimmune or allergic diseases. Abnormal inflammation can also lead to the transplant rejection and hinder the regeneration of tissues and organs, so therapeutic interventions are necessary to maintain the homeostasis and function of the immune system [1].

■ Results and discussion

Nanotechnology can solve the existing problems and thus achieve the desired therapeutic effect. Studies have shown that nanoplatforms

exhibit many useful properties, including co-delivery of antigens and adjuvants to the same antigen-presenting cells (APC) or intracellular compartments [2]; increased half-life of bioactive cargo molecules due to prevention of decomposition by enzymes during blood circulation; increased accumulation in tumor tissues due to the size-dependent effect of the enhanced permeability and retention (EPR) [3]; surface modification to certain target tissues or cells [4]; the stimulus-sensitive behavior for safe circulation and intelligent drug release [5, 6]; more tolerable doses due to less accumulation in non-target organs and tissues [7]; the surface binding of both antigens and costimulatory molecules to create of artificial APC (aAPC) for powerful T-cell activation [8]; various routes of drug delivery, such as intranasal administration or subcutaneous delivery using a patch with microneedles [2, 9]; internal immunomodulatory functions of created nanoparticles [10].

Researchers have synthesized nanoparticles with different structures and biological functions for drug delivery. Some of the most commonly used nanosystems are polymer nanoparticles [11, 12], liposomes [13, 14], micelles [15, 16], nanogels [4, 17, 18], gold nanoparticles [19, 20] and carbon nanomaterials [21]. These nanoplatforms have demonstrated phenomenal capabilities in facilitating the immunostimulatory or immunosuppressive regulation through targeted delivery and controlled release of antigens, adjuvants and immunoregulatory agents in response to a stimulus. One of the strategies to improve the localization of encapsulated cargoes in tissues or target cells is the chemical modification of nanoparticles with target fragments. For example, nanomaterials decorated with a DEC-205 antibody (Ab), CD40 Ab, CD11c Ab or mannose can be internalized predominantly by dendritic cells (DC) *via* the receptor-mediated endocytosis [22, 23]. Similarly, folic acid, lectins, and CD44 are used to recognition by the corresponding receptors overexpressed on macrophages [24]. The surface binding of CD3 Ab or tLyp1 peptide showed an increased uptake by T-cells and regulatory T-cells (Treg), respectively [25, 26]. In addition, nanoplatforms consisting of dextran or dextran sulfate have intrinsic properties of targeting macrophages [27].

Researchers have devoted considerable attention to the specific functionalization of nanoparticles in the treatment of a wide range of diseases where nanoparticles act as the main component rather than delivery vehicles. In particular, in

tumor immunotherapy, stimuli-sensitive nanomaterials are being developed to maintain the structural integrity in the serum and promote the release of a specific payload in TME [28, 29]. Internal and external stimulus – responsive strategies (pH [6, 30, 31], reduction [5, 32], enzymes [14, 33] light [34], heat and reactive oxygen species (ROS) [35]) are involved in creation of nanoparticles and achieved an improved antitumor effect. In addition, other antitumor molecules and agents can be added to these nanoplatforams for the synergistic combination therapy.

It should be noted that in the last few decades, immunotherapy has become a rapidly growing method of cancer treatment [36, 37]. Unlike chemotherapy, radiation therapy and surgery, it aims to activate immune cells to identify and destroy tumor cells. In this way, side effects on normal organs and tissues can be significantly reduced. Moreover, the immunotherapeutic strategy also provides long-term protection against tumor recurrence due to the induction of the immunological memory [38].

Recently, much attention has been paid to the immune checkpoint blockade therapy targeting cytotoxic T-lymphocyte antigen 4 (CTLA-4), programmed cell death 1 (PD-1) or ligand, cell death 1 (PD-L1), negative regulation of T-lymphocytes [39]. Adoptive cell transfer (ACT), especially chimeric antigen receptor (CAR)-T therapy using *ex vivo* expanded and genetically engineered T-cells for antigen-specific tumor therapy, has also recently been approved by the United States Food and Drug Administration (FDA) for B-cells and therapy of non-Hodgkin's lymphoma [40]. Based on the results obtained, the effectiveness of cancer immunotherapy can be further improved with the help of nanotechnology. However, immunotherapeutic treatments for solid tumors are limited due to the strong immunosuppressive TME, as well as the abnormal extracellular matrix. More seriously, the "off-target" effects of immunomodulatory agents can cause damage to normal tissues and cells.

Today, nanotechnology has been proven to improve the therapeutic efficacy of cancer immunotherapy mainly due to three aspects:

- protection of antigens and adjuvants, especially in the case of nucleic acid;
- effective delivery to APC and initiation of a powerful tumor antigen-specific immune response;
- reprogramming of the TME to restore immune surveillance.

Recently, a large number of nanoparticle-based delivery systems aimed at modulating immune cells have been developed for cancer treatment [41, 42] and some of them have undergone various stages of clinical trials [43], confirming their great therapeutic potential as anticancer agents. For example, during *Phase III* clinical trials, non-small cell lung cancer (NSCLC) patients vaccinated with tecemotide (L-BLP25) containing the immunoadjuvant monophosphoryl lipid A and synthetic mucin 1 lipopeptide (MUC1) showed an increased three-year survival rate of 49% compared to 27% of patients receiving only maintenance therapy. In addition, it should be noted that another 12 new liposomal drugs for the treatment of cancer patients developed by various manufacturers (Merck, Oncothyreon Canada Inc., Biontech RNA Pharmaceutical, GlaxoSmithKline, Lipotec Pty Ltd.) are completing clinical trials. GlaxoSmithKline also developed a liposomal drug for the treatment of malaria; Crucell Berna Biotech LTD – liposomes for the treatment of hepatitis A; Statens Serum Inst. – a liposomal drug for the treatment of tuberculosis; Biotherapeutics Inc., Crucell Bema Biotech Ltd., CSL Biotherapies are studying virosomal drugs against influenza. To achieve accurate and controlled drug delivery, smart nanoparticles with more complex structure and special drug release properties are also produced according to the distinctive features of TME, such as slightly acidic pH (6.5–6.8), high levels of glutathione and hydrogen peroxide (H₂O₂), disruption of the production of proteinases, such as matrix metalloproteinase-2 (MMP-2) [33, 44].

Recently, advances in the field of nanotechnology have stimulated the study of a large number of nanomaterials for the activation and maturation of APC. Liposomes are the most favorable material of immunotherapeutic nanosystems for clinical use due to the lack of toxicity and immunogenicity, Lipo-MERIT, iscomatrix, Lipovaxin MM, etc. It has been proven that, in addition to liposomes, some other nanomaterials are safe for the human. For example, Oncoquest-L, an anti-cancer vaccine undergoing phase I clinical trials, is made from an extract of the patient's own cancer cells, and IL-2 is delivered by proteoliposomes. Two cholesteryl pullulan-based cancer vaccines, CHP-NY-ESO-1 and CHP-HER2, elicited antigen-specific immune responses against NY-ESO-1 and HER2 in the presence of adjuvant OK-432 in esophageal cancer patients [45].

Nanomaterials, such as PLGA, iron oxide nanoparticles, virus-like particles (VLP) and conjugated polymers, can enhance the uptake of APC cells and stimulate the immune response [46]. Meian-A VLP used for the treatment of stage III-IV malignant melanoma is in phase III clinical trials [47]. The VLP Melan-A vaccine composed of a protein coat derived from bacteriophage Qbeta, CpG, and a peptide antigen from melanoma cells elicited greater than twofold increase in antigen-specific T-cell responses in 76% of patients. In some other cases, nanoparticles are also designed as an important component of the final product in order to facilitate the effect of tumor antigens on the host immune system.

Another strategy avoids the need to escape from endosomes and provides efficient T-cell activation and tumor eradication by designing aAPC based on the modification of nanosized particles, including magnetic beads, liposomes, polymeric and paramagnetic nanoparticles [48, 49]. aAPC mainly contain two signals for the T-cell activation, that is, the MHC-I-antigen complex and a costimulatory signal, such as anti-CD28 and anti-CD3 Abs [50]. They can be administered intravenously *in vivo* or used in ACT *ex vivo*.

Many studies conducted in recent years have shown that combining immunotherapy with other anticancer approaches, such as chemotherapy, phototherapy, and radiation therapy, has a synergistic effect and significantly improves therapeutic efficacy against a wide range of malignancies [51, 52]. Chemotherapeutic agents or external influences (light and radiation) not only directly destroy tumors, but participate in the immune process, causing the death of immunogenic (ICD) tumor cells.

The concept of ICD proposed in recent years demonstrates that dying tumor cells (DTCs) can generate a mass of antigens and increase the formation of damage-associated molecular patterns (DAMP), such as adenosine triphosphate, CRT, heat shock proteins and high mobility groups. DAMP provide the “*eat me*” signals for antigen recognition and phagocytosis by DC and trigger the activation of the adaptive immune response [53]. More importantly, ICD-derived tumor antigens can be controlled by the immune system and pose threat to abscopal and metastatic tumors, which is called the “abscopal effect” [51, 54].

Chemotherapy is the preferred therapeutic regimen in the clinic, but its application is seriously hampered by its notorious side effects and tumor recurrence. Chemotherapy in combination

with immunotherapy can reduce toxicity and improve the therapeutic effect. In chemoimmunotherapy, low-dose chemotherapy is able to induce ICD of tumor cells and lead to the release of tumor antigen, thus preventing serious side effects. At the same time, immunoregulatory agents provide a favorable environment for highly efficient antigen presentation and activation of APC and cytotoxic T-cells. Many studies, in which chemo/immunotherapeutic agents are encapsulated in nanoscale drug delivery systems, have been successful [13, 39, 55].

For example, the FEN group [13] loaded the TLR9 agonist CpG into a nanodepot platform (NDP) consisting of cationic liposomes and thiolated hyaluronic acid. CpG-NDP was then conjugated to the surface of immunogenic DTC induced by mitoxantrone, an anthracenedione antitumor agent. The experiment showed that DTC-CpG-NDP vaccination significantly stimulated the generation of tumor antigen-specific CD8+T cells and strongly protected against melanoma infection.

It should be noted that some of the traditional chemotherapeutic agents unexpectedly exert an immunoregulatory effect on immune cells. For example, the chemotherapeutic drug paclitaxel (PTX) has a modulating effect on the polarization of macrophages according to the ML-based phenotype at low concentrations [56]. Unlike free PTX, NP-PTX can be efficiently endocytosed by macrophages and stimulate the macrophage polarization in a dose-dependent manner without causing obvious toxicity to immune cells. Although the mechanism underlying this phenomenon is not fully understood, it represents an unconventional strategy for investigating the immunomodulatory function of chemotherapeutic agents.

Many attractive characteristics of nanoparticles in cancer immunotherapy are also applicable to prevent or counteract bacterial and viral infections, such as human immunodeficiency virus (HIV), influenza, encephalitis, hepatitis, Ebola, pneumonia, etc. [7, 57]. For the prevention of these diseases, anti-infective vaccines used certain antigenic components instead of whole microbes to increase the immune efficiency. However, these antigens are more easily broken down by enzymes and removed from the bloodstream. Moreover, they usually require the help of adjuvants to effectively activate the immune system. In addition, DNA vaccines have also shown a great potential in recent years, but their use in clinical practice is limited due to their low

safety and efficacy. Nanotechnology opens up the possibilities of a new generation of anti-infective vaccines. Currently, nanovaccines based on virosomes and liposomes against infectious diseases have shown good effectiveness. Two nanoparticle-based vaccines, Inflexal V and Epaxal, are FDA approved for the prevention of malaria, influenza and hepatitis A. Nanoparticles of appropriate size can deliver antigens and adjuvants to immune cells by encapsulation or surface conjugation. Nanoparticles are also designed as a reservoir for the slow release of antigens to increase the exposure of APC. For DNA vaccines, nanoparticles provide a non-viral delivery strategy that transports genetic material in a site-specific manner. Ample evidence has supported the promising effects of nanotechnology-based vaccines against infectious diseases, which benefit from the improved delivery efficiency, convenient nanoparticle engineering and the intrinsic adjuvant function. Immunomodulatory systems using nanoparticles for the prevention and treatment of infectious diseases include a vaccine with nanoparticles against HIV, influenza, bacterial infection and other infectious diseases.

Nanoparticles, including inorganic and polymeric nanoparticles, as effective delivery vehicles have shown effective immunization to protect against bacteria and infections. Thus, gold nanoparticles are better for preparing a nanovaccine due to good biocompatibility, a simple synthesis process and, most importantly, the adjuvant activity. For example, gold nanoparticles conjugated to *Pseudomonas aeruginosa* flagellin showed antibody titer against flagellin compared to flagellin formulated in Freund's adjuvant [58]. In another study, *Vetro et al.* [59] developed a glycoconjugate nanoparticle vaccine that modified gold nanoparticles with pneumococcal capsular polysaccharide antigens, which were an important component of the current commercial vaccine and also required for pneumococcal infection. A glucose derivative was added as an internal component of the gold nanoparticles to increase water solubility, and the T-helper peptide OVA was also loaded on to the gold nanoparticles. This glycoconjugate vaccine induced a potent and specific IgG-Ab-dependent immune response against *Streptococcus pneumoniae* in mice. Many other studies have highlighted the improved outcome of fighting infections due to the use of nanotechnology for the delivery of antigen and/or adjuvants [60, 61]. Next, it is interesting to focus on the design and application

of biomimetic nanoparticles with a modified surface as a vaccine against bacterial infection. Nanoparticle platforms, designed with their inherent ability to neutralize toxins and enhance immunity, have superior properties over traditional methods due to the increased safety and more efficient removal of toxins or antigens.

The next area of improving medicine is the development of DNA vaccination. However, despite the low cost and rapid production of DNA vaccines, their low stability and insufficient immunogenicity limit their use in the prevention and treatment of various infectious diseases. Nanotechnology provides a new opportunity in the development of nanoparticle platforms containing DNA vaccines for controlled and targeted delivery to specific cells. *Draz et al.* [57] reported DNA vaccination against a model hepatitis C virus using plasma gold nanoparticles that could be activated by specific electrical pulses to facilitate pore formation in the adjacent cell membrane and increase membrane permeability for DNA transfection. In this case, the absorption of the DNA vaccine by myocytes significantly increases after the joint administration of the free DNA plasmid and gold nanoparticles to the animals, which allowed more efficient expression of the encoded genes. Moreover, due to the low electric field required for this process, cell destruction or lysis can be avoided.

In addition to the ability to enhance the pro-inflammatory immune response, nanoparticle platforms have also been used to induce immune tolerance against chronic or acute inflammation, autoimmune diseases, transplant rejection and allergy. Unlike cancer and infections, which enter the human body through an insufficient immune response, these diseases arise as a result of an improper overreaction of the immune system to autoantigens, allogeneic antigens during transplantation, or environmental factors. Considering the fact that nanotechnological immunostimulation has attracted much attention, monitoring the immunosuppressive properties of nanomaterials is equally important to alleviate the immune-mediated burden. Immunosuppressants, mostly with small molecules, have shown improved therapeutic efficacy in recent years. However, long-term treatment can lead to severe systemic toxicity or immunodeficiency [62]. Many immunosuppressants, such as methotrexate, rapamycin and dexamethasone, are hydrophobic drugs and have a limited biological activity. These agents are randomly and widely

distributed in the body after introduction, leading to serious side effects in non-target tissues and causing damage of the liver, muscles and the gastrointestinal tract.

Anti-inflammatory cytokines, such as IL-4, have been widely studied in the treatment of various autoimmune diseases. However, their short half-life determines the introduction of high doses and inevitable systemic toxicity. The therapeutic delivery of microRNAs (miRNAs) for symptom control can also be challenging due to limited efficacy, low stability, and the lack of targeting. Nanotechnology overcomes the existing shortcomings of immunosuppressants through multiple aspects, such as providing protection against degradation, prolonging blood circulation and facilitating the immune cell-targeted delivery [63]. The nanoparticle itself can also be converted into an immunomodulatory component, and nanoparticles delivering the antigen-MHC complex can expand antigen-specific Treg to control inflammatory disorders.

■ Conclusions

Nanotechnology opens up great opportunities for the prevention and treatment of infectious diseases since the coded delivery of antigens and adjuvants significantly increases the immunogenicity of microbial components and demonstrates higher efficacy than conventional vaccines using whole microbes.

Thus, nanomaterial-based immunotherapy is rapidly developing and will show significant potential over the past few decades. Thanks to constantly improved production methods and design strategies, nanotechnology is successfully used to control and prevent many diseases

through immune regulation. As discussed above, the data presented highlight excellent tumor treatment outcomes due to the activation of APC and T-cells, regulation of Treg, TAM and MDSC in immunosuppressive TME and the synergism with chemotherapy, phototherapy and radiotherapy. In the prevention and eradication of infectious viruses and bacteria, the nanoparticle-based vaccine provides higher absorption of APC and induces improved T and B cell responses. In addition, the coded delivery of tumor antigens and adjuvants in nanosized carriers increases the effectiveness of anticancer vaccines. A new trend in cancer immunotherapy involves the recognition of tumor neoantigens, which originate from patient-specific cancer mutations and can be identified as “foreign” by the immune system. Although a tumor neoantigen may be an ideal candidate for personalized cancer immunotherapy, it is rare in some cancers with low mutations, and therefore, a combination with radiation therapy or chemotherapy is preferable to increase the burden of mutations, as well as tumor neoantigens. In addition, the process of identification and synthesis of neoantigen peptides is time-consuming, and new techniques and methods are urgently needed to reduce this time period [64].

Then nanomaterials have emerged as a new antibacterial weapon in addition to antibiotics in protecting against various microbial infections, including resistant bacteria. It is known that nanomaterials cause lethality in two ways, namely, the destruction of cell membranes and the production of ROS. However, it has been found that nanomaterials have the increased antimicrobial activity with lower toxicity and do not cause drug resistance compared to antibiotics.

■ References

- Pearson, R. M.; Casey, L. M.; Hughes, K. R.; Miller, S. D.; Shea, L. D. *In vivo* reprogramming of immune cells: Technologies for induction of antigen-specific tolerance. *Adv. Drug Deliv. Rev.* **2017**, *114*, 240–255. <https://doi.org/10.1016/j.addr.2017.04.005>.
- Tazaki, T.; Tabata, K.; Aina, A.; Ohara, Y.; Kobayashi, S.; Ninomiya, T.; Orba, Y.; Mitomo, H.; Nakano, T.; Hasegawa, H.; Ijiro, K.; Sawa, H.; Suzuki, T.; Niikura, K. Shape-dependent adjuvanticity of nanoparticle-conjugated RNA adjuvants for intranasal inactivated influenza vaccines. *RSC Adv.* **2018**, *8* (30), 16527–16536. <https://doi.org/10.1039/C8RA01690A>.
- Kim, H.; Niu, L.; Larson, P.; Kucaba, T. A.; Murphy, K. A.; James, B. R.; Ferguson, D. M.; Griffith, T. S.; Panyam, J. Polymeric nanoparticles encapsulating novel TLR7/8 agonists as immunostimulatory adjuvants for enhanced cancer immunotherapy. *Biomaterials* **2018**, *164*, 38–53. <https://doi.org/10.1016/j.biomaterials.2018.02.034>.
- Chen, J.; Ding, J.; Xu, W.; Sun, T.; Xiao, H.; Zhuang, X.; Chen, X. Receptor and Microenvironment Dual-Recognizable Nanogel for Targeted Chemotherapy of Highly Metastatic Malignancy. *Nano Lett.* **2017**, *17* (7), 4526–4533. <https://doi.org/10.1021/acs.nanolett.7b02129>.
- Xu, W.; Ding, J.; Chen, X. Reduction-Responsive Polypeptide Micelles for Intracellular Delivery of Antineoplastic Agent. *Biomacromolecules* **2017**, *18* (10), 3291–3301. <https://doi.org/10.1021/acs.biomac.7b00950>.
- Zhang, Y.; Cai, L.; Li, D.; Lao, Y.-H.; Liu, D.; Li, M.; Ding, J.; Chen, X. Tumor microenvironment-responsive hyaluronate-calcium carbonate hybrid nanoparticle enables effective chemotherapy for primary and advanced osteosarcomas. *Nano Res.* **2018**, *11* (9), 4806–4822. <https://doi.org/10.1007/s12274-018-2066-0>.
- Gao, S.; Tang, G.; Hua, D.; Xiong, R.; Han, J.; Jiang, S.; Zhang, Q.; Huang, C. Stimuli-responsive bio-based polymeric systems and their applications. *J. Mater. Chem. B* **2019**, *7* (5), 709–729. <https://doi.org/10.1039/c8tb02491j>.

8. Musetti, S.; Huang, L. Nanoparticle-Mediated Remodeling of the Tumor Microenvironment to Enhance Immunotherapy. *ACS Nano* **2018**, *12* (12), 11740–11755. <https://doi.org/10.1021/acsnano.8b05893>.
9. Yang, H.-W.; Ye, L.; Guo, X. D.; Yang, C.; Compans, R. W.; Prausnitz, M. R. Ebola Vaccination Using a DNA Vaccine Coated on PLGA-PLL/PGA Nanoparticles Administered Using a Microneedle Patch. *Adv. Healthcare Mater.* **2017**, *6* (1), 1600750. <https://doi.org/10.1002/adhm.201600750>.
10. Li, S.; Feng, X.; Wang, J.; He, L.; Wang, C.; Ding, J.; Chen, X. Polymer nanoparticles as adjuvants in cancer immunotherapy. *Nano Res.* **2018**, *11* (11), 5769–5786. <https://doi.org/10.1007/s12274-018-2124-7>.
11. Xiao, H.; Yan, Lesan; Dempsey, E. M.; Song, W.; Qi, R.; Li, W.; Huang, Y.; Jing, X.; Zhou, D.; Ding, J.; Chen, X. Recent progress in polymer-based platinum drug delivery systems. *Prog. Polym. Sci.* **2018**, *87*, 70–106. <https://doi.org/10.1016/j.progpolymsci.2018.07.004>.
12. Wang, Y.; Jiang, Z.; Xu, W.; Yang, Y.; Zhuang, X.; Ding, J.; Chen, X. Chiral Polypeptide Thermogels Induce Controlled Inflammatory Response as Potential Immunoadjuvants. *ACS Appl. Mater. Interfaces* **2019**, *11* (9), 8725–8730. <https://doi.org/10.1021/acsnano.9b01872>.
13. Fan, Y.; Kuai, R.; Xu, Y.; Ochyl, L. J.; Irvine, D. J.; Moon, J. J. Immunogenic Cell Death Amplified by Co-localized Adjuvant Delivery for Cancer Immunotherapy. *Nano Lett.* **2017**, *17* (12), 7387–7393. <https://doi.org/10.1021/acsnano.7b03218>.
14. Song X.; Xu J.; Liang C.; Chao Y.; Jin Q.; Wang C.; Chen M.; Liu Z. Self-Supplied Tumor Oxygenation through Separated Liposomal Delivery of H₂O₂ and Catalase for Enhanced Radio-Immunotherapy of Cancer. *Nano Lett.* **2018**, *18* (10), 6360–6368. <https://doi.org/10.1021/acsnano.8b02720>.
15. He, L.; Xu, W.; Wang, X.; Wang, C.; Ding, J.; Chen, X. Polymer micro/nanocarrier-assisted synergistic chemohormonal therapy for prostate cancer. *Biomater. Sci.* **2018**, *6*, 1433–1444. <https://doi.org/10.1039/C8BM00190A>.
16. Wang, J.; Xu, W.; Li, S.; Qiu, H.; Li, Z.; Wang, C.; Wang X., Ding, J. Polylactide-Cholesterol Stereocomplex Micelle Encapsulating Chemotherapeutic Agent for Improved Antitumor Efficacy and Safety. *J. Biomed. Nanotechnol.* **2018**, *14* (12), 2102–2113. <https://doi.org/10.1166/jbn.2018.2624>.
17. Guo, H.; Li, F.; Xu, W.; Chen, J.; Hou, Y.; Wang, C.; Ding, J.; Chen, X. Mucoadhesive Cationic Polypeptide Nanogel with Enhanced Penetration for Efficient Intravesical Chemotherapy of Bladder Cancer. *Adv. Sci.* **2018**, *5* (6), 1800004. <https://doi.org/10.1002/advs.201800004>.
18. Zhang, Y.; Wang, F.; Li, M.; Yu, Z.; Qi, R.; Ding, J.; Zhang, Z.; Chen, X. Self-Stabilized Hyaluronate Nanogel for Intracellular Codelivery of Doxorubicin and Cisplatin to Osteosarcoma. *Adv. Sci.* **2018**, *5* (5), 1700821. <https://doi.org/10.1002/advs.201700821>.
19. Luo, L.; Zhu, C.; Yin, H.; Jiang, M.; Zhang, J.; Qin, B.; Luo, Z.; Yuan, X.; Yang, J.; Li, W.; Du, Y.; You, J. Laser Immunotherapy in Combination with Perdurable PD-1 Blocking for the Treatment of Metastatic Tumors. *ACS Nano* **2018**, *12* (8), 7647–7662. <https://doi.org/10.1021/acsnano.8b00204>.
20. Nam, J.; Son, S.; Ochyl, L. J.; Kuai, R.; Schwendeman, A.; Moon, J. J. Chemo-photothermal therapy combination elicits anti-tumor immunity against advanced metastatic cancer. *Nat. Commun.* **2018**, *9* (1), 1074. <https://doi.org/10.1038/s41467-018-03473-9>.
21. Wang, C.; Ye, Y.; Hu, Q.; Bellotti, A.; Gu, Z. Tailoring Biomaterials for Cancer Immunotherapy: Emerging Trends and Future Outlook. *Adv. Mater.* **2017**, *29* (29). <https://doi.org/10.1002/adma.201606036>.
22. Stead, S. O.; Kireta, S.; McInnes, S. J. P.; Kette, F. D.; Sivanathan, K. N.; Kim, J.; Cueto-Diaz, E. J.; Cunin, F.; Durand, J. O.; Drogemuller, C. J.; Carroll, R. P.; Voelcker, N. H.; Coates, P. T. Murine and Non-Human Primate Dendritic Cell Targeting Nanoparticles for in Vivo Generation of Regulatory T-Cells. *ACS Nano* **2018**, *12* (7), 6637–6647. <https://doi.org/10.1021/acsnano.8b01625>.
23. Yang, R.; Xu, J.; Xu, L.; Sun, X.; Chen, Q.; Zhao, Y.; Peng, R.; Liu, Z. Cancer Cell Membrane-Coated Adjuvant Nanoparticles with Mannose Modification for Effective Anticancer Vaccination. *ACS Nano* **2018**, *12* (6), 5121–5129. <https://doi.org/10.1021/acsnano.7b09041>.
24. Yang, M.; Ding, J.; Feng, X.; Chang, F.; Wang, Y.; Gao, Z.; Zhuang, X.; Chen, X. Scavenger Receptor-Mediated Targeted Treatment of Collagen-Induced Arthritis by Dextran Sulfate-Methotrexate Prodrug. *Theranostics* **2017**, *7* (1), 97–105. <https://doi.org/10.7150/thno.16844>.
25. Bahmani, B.; Uehara, M.; Jiang, L.; Ordikhani, F.; Banouni, N.; Ichimura, T.; Solhjoui, Z.; Furtmüller, G. J.; Brandacher, G.; Alvarez, D.; von Andrian, U. H.; Uchimura, K.; Xu Q.; Vohra, I.; Yilmam, O. A.; Haik, Y.; Azzi, J.; Kasinath, V.; Bromberg, J. S.; McGrath, M. M.; Abdi, R. Targeted delivery of immune therapeutics to lymph nodes prolongs cardiac allograft survival. *J. Clin. Invest.* **2018**, *128* (11), 4770–4786. <https://doi.org/10.1172/JCI120923>.
26. Ou, W.; Thapa, R. K.; Jiang, L.; Soe, Z. C.; Gautam, M.; Chang, J. H.; Jeong, J. H.; Ku, S. K.; Choi, H. G.; Yong, C. S.; Kim, J. O. Regulatory T cell-targeted hybrid nanoparticles combined with immuno-checkpoint blockade for cancer immunotherapy. *J. Controlled Release* **2018**, *281*, 84–96. <https://doi.org/10.1016/j.jconrel.2018.05.018>.
27. Heo, R.; You, D. G.; Um, W.; Choi, K. Y.; Jeon, S.; Park, J. S.; Choi, Y.; Kwon, S.; Kim, K.; Kwon, I. C.; Jo, D. G.; Kang, Y. M.; Park, J. H. Dextran sulfate nanoparticles as a theranostic nanomedicine for rheumatoid arthritis. *Biomaterials* **2017**, *131*, 15–26. <https://doi.org/10.1016/j.biomaterials.2017.03.044>.
28. Jiang, Z.; Chen, J.; Cui, L.; Zhuang, X.; Ding, J.; Chen, X. Advances in Stimuli-Responsive Polypeptide Nanogels. *Small Methods* **2018**, *2* (3), 1700307 <https://doi.org/10.1002/smt.201700307>.
29. Ding, J.; Feng, X.; Jiang, Z.; Xu, W.; Guo, H.; Zhuang, X.; Chen, X. Polymer-Mediated Penetration-Independent Cancer Therapy. *Biomacromolecules* **2019**, *20* (12), 4258–4271. <https://doi.org/10.1021/acsbio.9b01263>.
30. Li, D.; Han, J.; Ding, J.; Chen, L.; Chen, X. Acid-sensitive dextran prodrug: A higher molecular weight makes a better efficacy. *Carbohydr. Polym.* **2017**, *161*, 33–41. <https://doi.org/10.1016/j.carbpol.2016.12.070>.
31. Feng, X.; Li, D.; Han, J.; Zhuang, X.; Ding, J. Schiff base bond-linked polysaccharide–doxorubicin conjugate for upregulated cancer therapy. *Materials Science and Engineering: C* **2017**, *76*, 1121–1128. <https://doi.org/10.1016/j.msec.2017.03.201>.
32. Zhang, C.; Shi, G.; Zhang, J.; Song, H.; Niu, J.; Shi, S.; Huang, P.; Wang, Y.; Wang, W.; Li, C.; Kong, D. Targeted antigen delivery to dendritic cell via functionalized alginate nanoparticles for cancer immunotherapy. *J. Controlled Release* **2017**, *256*, 170–181. <https://doi.org/10.1016/j.jconrel.2017.04.020>.
33. Cheng, K.; Ding, Y.; Zhao, Y.; Ye, S.; Zhao, X.; Zhang, Y.; Ji, T.; Wu, H.; Wang, B.; Anderson, G. J.; Ren, L.; Nie, G. Sequentially Responsive Therapeutic Peptide Assembling Nanoparticles for Dual-Targeted Cancer Immunotherapy. *Nano Lett.* **2018**, *18* (5), 3250–3258. <https://doi.org/10.1021/acsnano.8b01071>.
34. Li, D.; Zhang, G.; Xu, W.; Wang, J.; Wang, Y.; Qiu, L.; Ding, J.; Yang, X. Investigating the Effect of Chemical Structure of Semiconducting Polymer Nanoparticle on Photothermal Therapy and Photoacoustic Imaging. *Theranostics* **2017**, *7* (16), 4029–4040. <https://doi.org/10.7150/thno.19538>.
35. Madan, R. A.; Turkbey, B.; Lepone, L. M.; Donahue, R. N.; Grenga, I.; Borofsky, S.; Pinto, P. A.; Citrin, D. E.; Kaushal, A.; Krauze, A. V.; McMahon, S.; Rauchhorst, M.; Couvillon, A.; Falk, M. H.; Eggleton, P.; Choyke, P. L.; Dahut, W. L.; Schlom, J.; Gulley, J. Changes in

- multiparametric prostate MRI and immune subsets in patients (Pts) receiving neoadjuvant immunotherapy and androgen deprivation therapy (ADT) prior to radiation. *J. Clin. Oncol.* **2017**, *35* (6_suppl), 30–30. https://doi.org/10.1200/JCO.2017.35.6_suppl.30.
36. Oyen, D.; Torres, J. L.; Wille-Reece, U.; Ockenhouse, C. F.; Emerling, D.; Glanville, J.; Volkmoth, W.; Flores-Garcia, Y.; Zavala, F.; Ward, A. B.; King, C. R.; Wilson, I. A. Structural basis for antibody recognition of the NANP repeats in *Plasmodium falciparum* circumsporozoite protein. *Proc. Natl. Acad. Sci. U. S. A.* **2017**, *114* (48), E10438–E10445. <https://doi.org/10.1073/pnas.1715812114>.
 37. Witte, D.; Cunliffe, N. A.; Turner, A. M.; Ngulube, E.; Ofori-Anyinam, O.; Vekemans, J.; Chimpeni, Ph.; Lievens, M.; Wilson, T. P.; Njiram'madzi, J.; Mendoza, Y. G.; Leach, A. Safety and Immunogenicity of Seven Dosing Regimens of the Candidate RTS,S/AS01_e Malaria Vaccine Integrated Within an Expanded Program on Immunization Regimen. A Phase II, Single-Center, Open, Controlled Trial in Infants in Malawi. *The Pediatric Infectious Disease Journal* **2018**, *37* (5), 483–491. <https://doi.org/10.1097/INF.0000000000001937>.
 38. Dang, B. N.; Kwon, T. K.; Lee, S.; Jeong, J. H.; Yook, S. Nanoparticle-based immunoengineering strategies for enhancing cancer immunotherapy. *J. Controlled Release* **2024**, *365*, 773–800. <https://doi.org/10.1016/j.jconrel.2023.12.007>.
 39. Feng, B.; Zhou, F.; Hou, B.; Wang, D.; Wang, T.; Fu, Y.; Ma, Y.; Yu, H.; Li, Y. Binary Cooperative Prodrug Nanoparticles Improve Immunotherapy by Synergistically Modulating Immune Tumor Microenvironment. *Adv. Mater.* **2018**, *30* (38), e1803001. <https://doi.org/10.1002/adma.201803001>.
 40. Fesnak, A. D.; June, C. H.; Levine, B. L. Engineered T cells: the promise and challenges of cancer immunotherapy. *Nat. Rev. Cancer* **2016**, *16* (9), 566–581. <https://doi.org/10.1038/nrc.2016.97>.
 41. Zhang, Q.; Wei, W.; Wang, P.; Zuo, L.; Li, F.; Xu, J.; Xi, X.; Gao, X.; Ma, G.; Xie, H. Y. Biomimetic Magnetosomes as Versatile Artificial Antigen-Presenting Cells to Potentiate T-Cell-Based Anticancer Therapy. *ACS Nano* **2017**, *11* (11), 10724–10732. <https://doi.org/10.1021/acsnano.7b04955>.
 42. Chiang, C. S.; Lin, Y. J.; Lee, R.; Lai, Y. H.; Cheng, H. W.; Hsieh, C. H.; Shyu, W. C.; Chen, S. Y. Combination of fucoidan-based magnetic nanoparticles and immunomodulators enhances tumour-localized immunotherapy. *Nat. Nanotechnol.* **2018**, *13* (8), 746–754. <https://doi.org/10.1038/s41565-018-0146-7>.
 43. Sun, Q.; Zhou, Z.; Qiu, N.; Shen, Y. Rational Design of Cancer Nanomedicine: Nanoproperty Integration and Synchronization. *Adv. Mater.* **2017**, *29* (14). <https://doi.org/10.1002/adma.201606628>.
 44. Qiu, F.; Becker, K. W.; Knight, F. C.; Baljon, J. J.; Sevimli, S.; Shae, D.; Gilchuk P.; Joyce, S.; Wilson, J. T. Poly(propylacrylic acid)-peptide nanoplexes as a platform for enhancing the immunogenicity of neoantigen cancer vaccines. *Biomaterials* **2018**, *182*, 82–91. <https://doi.org/10.1016/j.biomaterials.2018.07.052>.
 45. Jabulowsky, R. A.; Loquai, C.; Derhovanessian, E.; Grabbe, S.; Türeci, Ö.; Sahin, U. A first-in-human phase I/II clinical trial assessing novel mRNA-lipoplex nanoparticles encoding shared tumor antigens for immunotherapy of malignant melanoma. *Ann. Oncol.* **2018**, *29*, VIII439. <https://doi.org/10.1093/annonc/mdy288.109>.
 46. Zhao, J.; Yang, H.; Li, J.; Wang, Y.; Wang, X. Fabrication of pH-responsive PLGA(UCNPs/DOX) nanocapsules with upconversion luminescence for drug delivery. *Scientific reports* **2017**, *7* (1), 18014. <https://doi.org/10.1038/s41598-017-16948-4>.
 47. Cohen, A. D.; Lendvai, N.; Nataraj, S.; Imai, N.; Jungbluth, A. A.; Tsakos, I.; Rahman, A.; Mei, A. H.; Singh, H.; Zarychta, K.; Kim-Schulze, S.; Park, A.; Venhaus, R.; Alpaugh, K.; Gnjatich, S.; Cho, H. J. Autologous Lymphocyte Infusion Supports Tumor Antigen Vaccine-Induced Immunity in Autologous Stem Cell Transplant for Multiple Myeloma. *Cancer Immunol. Res.* **2019**, *7* (4), 658–669. <https://doi.org/10.1158/2326-6066.CIR-18-0198>.
 48. Dreno, B.; Thompson, J. F.; Smithers, B. M.; Santinami, M.; Jouary, T.; Gutzmer, R.; Levchenko, E.; Rutkowski, P.; Grob, J. J.; Korovin, S.; Drucis, K.; Grange, F.; Machet, L.; Hersey, P.; Krajsova, I.; Testori, A.; Conry, R.; Guillot, B.; Kruit, W. H. J.; Demidov, L.; Thompson, J. A.; Bondarenko, I.; Jaroszek, J.; Puig, S.; Cinat, G.; Hauschild, A.; Goeman, J. J.; van Houwelingen, H. C.; Ulloa-Montoya, F.; Callegaro, A.; Dizier, B.; Spiessens, B.; Debois, M.; Brichard, V. G.; Louahed, J.; Therasse, P.; Debruyne, C.; Kirkwood, J. M. MAGE-A3 immunotherapeutic as adjuvant therapy for patients with resected, MAGE-A3-positive, stage III melanoma (DERMA): a double-blind, randomised, placebo-controlled, phase 3 trial. *Lancet Oncol.* **2018**, *19* (7), 916–929. [https://doi.org/10.1016/S1470-2045\(18\)30254-7](https://doi.org/10.1016/S1470-2045(18)30254-7).
 49. McQuade, J. L.; Homsy, J.; Torres-Cabala, C. A.; Bassett, R.; Popuri, R. M.; James, M. L.; Vence, L. M.; Hwu, W. J. A phase II trial of recombinant MAGE-A3 protein with immunostimulant AS15 in combination with high-dose Interleukin-2 (HDIL2) induction therapy in metastatic melanoma. *BMC Cancer* **2018**, *18* (1), 1274. <https://doi.org/10.1186/s12885-018-5193-9>.
 50. Kosmides, A. K.; Meyer, R. A.; Hickey, J. W.; Aje, K.; Cheung, K. N.; Green, J. J.; Schneck, J. P. Biomimetic biodegradable artificial antigen presenting cells synergize with PD-1 blockade to treat melanoma. *Biomaterials* **2017**, *118*, 16–26. <https://doi.org/10.1016/j.biomaterials.2016.11.038>.
 51. Min, Y.; Roche, K. C.; Tian, S.; Eblan, M. J.; McKinnon, K. P.; Caster, J. M.; Chai, S.; Herring, L. E.; Zhang, L.; Zhang, T.; DeSimone, J. M.; Tepper, J. E.; Vincent, B. G.; Serody, J. S.; Wang, A. Z. Antigen-capturing nanoparticles improve the abscopal effect and cancer immunotherapy. *Nat. Nanotechnol.* **2017**, *12* (9), 877–882. <https://doi.org/10.1038/nnano.2017.113>.
 52. Zheng, D. W.; Chen, J. L.; Zhu, J. Y.; Rong, L.; Li, B.; Lei, Q.; Fan, J. X.; Zou, M. Z.; Li, C.; Cheng, S. X.; Xu, Z.; Zhang, X. Z. Highly Integrated Nano-Platform for Breaking the Barrier between Chemotherapy and Immunotherapy. *Nano Lett.* **2016**, *16* (7), 4341–4347. <https://doi.org/10.1021/acs.nanolett.6b01432>.
 53. Velpurisiva, P.; Gad, A.; Piel, B.; Jadia, R.; Rai, P. Nanoparticle Design Strategies for Effective Cancer Immunotherapy. *Journal of Biomedicine* **2017**, *2*, 64–77. <https://doi.org/10.7150/jbm.18877>.
 54. Viswanath, D.; Park, J.; Misra, R.; Pizzuti, V. J.; Shin, S.-H.; Doh, J.; Won, Y.-Y. Nanotechnology-enhanced radiotherapy and the abscopal effect: Current status and challenges of nanomaterial-based radio-immunotherapy. *Wiley Interdiscip. Rev.: Nanomed. Nanobiotechnol.* **2024**, *16* (1), e1924. <https://doi.org/10.1002/wnan.1924>.
 55. Song, W.; Shen, L.; Wang, Y.; Liu, Q.; Goodwin, T. J.; Li, J.; Dorosheva, O.; Liu, T.; Liu, R.; Huang, L. Synergistic and low adverse effect cancer immunotherapy by immunogenic chemotherapy and locally expressed PD-L1 trap. *Nat. Commun.* **2018**, *9* (1), 2237. <https://doi.org/10.1038/s41467-018-04605-x>.
 56. Tang, W.; Yang, J.; Yuan, Y.; Zhao, Z.; Lian, Z.; Liang, G. Paclitaxel nanoparticle awakens immune system to fight against cancer. *Nanoscale* **2017**, *9* (19), 6529–6536. <https://doi.org/10.1039/c6nr09895a>.
 57. Draz, M. S.; Wang, Y.-J.; Chen, F. F.; Xu, Y.; Shafiee, H. Electrically Oscillating Plasmonic Nanoparticles for Enhanced DNA Vaccination against Hepatitis C Virus. *Adv. Funct. Mater.* **2017**, *27* (5), 1604139. <https://doi.org/10.1002/adfm.201604139>.
 58. Dakterzada, F.; Mohabati Mobarez, A.; Habibi Roudkenar, M.; Mohsenifar, A. Induction of humoral immune response against *Pseudomonas aeruginosa* flagellin(1-161) using gold nanoparticles as an adjuvant. *Vaccine* **2016**, *34* (12), 1472–1479. <https://doi.org/10.1016/j.vaccine.2016.01.041>.
 59. Vetro, M.; Safari, D.; Fallarini, S.; Salsabila, K.; Lahmann, M.; Penadés, S.; Lay, L.; Marradi, M.; Compostella, F. Preparation and immunogenicity of gold glyco-nanoparticles as antipneumococcal vaccine model. *Nanomedicine* **2017**, *12* (1), 13–23. <https://doi.org/10.2217/nnm-2016-0306>.

60. Chien-Wei Lin, L.; Chattopadhyay, S.; Lin, J.-C.; Hu, C.-M. J. Advances and Opportunities in Nanoparticle- and Nanomaterial-Based Vaccines against Bacterial Infections. *Adv. Healthcare Mater.* **2018**, *7* (13), 1701395. <https://doi.org/10.1002/adhm.201701395>.
61. Pavot, V.; Climent, N.; Rochereau, N.; Garcia, F.; Genin, C.; Tiraby, G.; Vernejoul, F.; Perouzel, E.; Lioux, T.; Verrier, B.; Paul, S. Directing vaccine immune responses to mucosa by nanosized particulate carriers encapsulating NOD ligands. *Biomaterials* **2016**, *75*, 327–339. <https://doi.org/10.1016/j.biomaterials.2015.10.034>.
62. Gargett, T.; Abbas, M. N.; Rolan, P.; Price, J. D.; Gosling, K. M.; Ferrante, A.; Ruszkiewicz, A.; Atmosukarto, I. I. C.; Altin, J.; Parish, C. R.; Brown, M. P. Phase I trial of Lipovaxin-MM, a novel dendritic cell-targeted liposomal vaccine for malignant melanoma. *Cancer Immunol. Immunother.* **2018**, *67* (9), 1461–1472. <https://doi.org/10.1007/s00262-018-2207-z>.
63. Pujol, J. L.; De Pas, T.; Rittmeyer, A.; Vallières, E.; Kubisa, B.; Levchenko, E.; Wiesemann, S.; Masters, G. A.; Shen, R.; Tjulandin, S. A.; Hofmann, H. S.; Vanhoutte, N.; Salaun, B.; Debois, M.; Jarnjak, S.; De Sousa Alves, P. M.; Louahed, J.; Brichard, V. G.; Lehmann, F. F. Safety and Immunogenicity of the PRAME Cancer Immunotherapeutic in Patients with Resected Non-Small Cell Lung Cancer: A Phase I Dose Escalation Study. *J. Thorac. Oncol.* **2016**, *11* (12), 2208–2217. <https://doi.org/10.1016/j.jtho.2016.08.120>.
64. Zhu, G.; Zhang, F.; Ni, Q.; Niu, G.; Chen, X. Efficient Nanovaccine Delivery in Cancer Immunotherapy. *ACS Nano* **2017**, *11* (3), 2387–2392. <https://doi.org/10.1021/acsnano.7b00978>.

Information about the authors:

Oleksandr F. Piminov, D.Sci. in Pharmacy, Professor, Director of the Institute for Advanced Training of Pharmacy Specialists of the National University of Pharmacy of the Ministry of Health of Ukraine; <https://orcid.org/0000-0003-4369-907X>.

Rita V. Sahaidak-Nikitiuk (*corresponding author*), D.Sci. in Pharmacy, Professor, Head of the Department of Pharmaceutical Technology, Standardization and Certification of Drugs, Institute for Advanced Training of Pharmacy Specialists of the National University of Pharmacy of the Ministry of Health of Ukraine; <https://orcid.org/0000-0002-9337-7741>; e-mail for correspondence: sahaidak_rita@ukr.net; tel. +380667899940.

Anna I. Kvitchata, Ph.D. in Medicine, Associate Professor of the Department of Clinical Pharmacology, Institute for Advanced Training of Pharmacy Specialists of the National University of Pharmacy of the Ministry of Health of Ukraine; <https://orcid.org/0000-0001-8093-2569>.

Svitlana M. Rolik-Attia, Ph.D. in Pharmacy, Associate Professor of the Department of Pharmaceutical Technology, Standardization and Certification of Drugs, Institute for Advanced Training of Pharmacy Specialists of the National University of Pharmacy of the Ministry of Health of Ukraine; <https://orcid.org/0000-0002-0299-5895>.

UDC 547.821.2+542.06

T. M. Sokolenko¹, Yu. L. Yagupolskii^{1,2}¹Institute of Organic Chemistry of the National Academy of Sciences of Ukraine,
5 Academician Kukhar str., 02660 Kyiv, Ukraine²Enamine Ltd., 78 Winston Churchill str., 02094 Kyiv, Ukraine

5-Trifluoromethoxy-substituted Nicotinic Acid, Nicotinamide and Related Compounds

Abstract

A practical and convenient method for synthesizing nicotinic acid and nicotinamide with the trifluoromethoxy group in position 5 of the ring has been developed. A series of related compounds, for example, nicotinic aldehyde and nicotinic alcohol, have been synthesized. It has been shown that 3-bromo-5-trifluoromethoxypyridine is a convenient and efficient synthon for palladium-catalyzed coupling reactions. The trifluoromethoxy group has been found to be remarkably stable against hydroiodic acid in contrast to the methoxy group.

Keywords: nicotinic acid; nicotinamide; trifluoromethoxy group; antimony trifluoride; fluorination

T. M. Соколенко¹, Ю. Л. Ягупольський^{1,2}

¹Інститут органічної хімії Національної академії наук України,
вул. Академіка Кухаря, 5, м. Київ, 02660, Україна

²ТОВ НВП «Єнамін», вул. Вінстона Черчилля, 78, м. Київ, 02094, Україна

5-Трифлуорометоксизаміщена нікотинова кислота, нікотинамід і споріднені сполуки

Анотація

Розроблено практичний і зручний метод синтезу нікотинової кислоти та нікотинаміду з трифлуорометоксигрупою в положенні 5 кільця. Було синтезовано деякі споріднені сполуки, наприклад, нікотинний альдегід і нікотинний спирт. З'ясовано, що 3-бромо-5-трифлуорометоксипіридин є зручним синтоном для каталізованих паладієм реакцій сполучення. Визначено, що, на відміну від метоксигрупи, трифлуорометоксигрупа є надзвичайно стійка до дії йодоводневої кислоти.

Ключові слова: нікотинова кислота; нікотинамід; трифлуорометоксигрупа; стибій трифлуорид; флуорування

Citation: Sokolenko, T. M.; Yagupolskii, Yu. L. 5-Trifluoromethoxy-substituted Nicotinic Acid, Nicotinamide and Related Compounds. *Journal of Organic and Pharmaceutical Chemistry* **2024**, *22* (1), 22–30.

<https://doi.org/10.24959/ophcj.24.302435>

Supporting information: Copies of ¹H, ¹³C and ¹⁹F NMR spectra of the synthesized compounds.

Received: 24 February 2024; **Revised:** 11 April 2024; **Accepted:** 15 April 2024

Copyright © 2024, T. M. Sokolenko, Yu. L. Yagupolskii. This is an open access article under the CC BY license (<http://creativecommons.org/licenses/by/4.0>).

Funding: The authors received no specific funding for this work.

Conflict of interests: The authors have no conflict of interests to declare.

■ Introduction

A fluorine atom has a privileged position within the halogen family for drugs and agrochemicals design due to its unique properties – small size, high electronegativity, and the ability to form a strong C-F bond. In 2020, about 20% of the commercial pharmaceuticals were fluorine-containing drugs, and their total quantity was 340 compounds. Commonly, they were fluoro-

substituted arenes (167 compounds) or heterocycles (20 compounds), as well as trifluoromethylated arenes and heteroarenes (64 compounds). Fluorinated ethers were an important group of pharmaceuticals represented by 18 compounds, among them four were trifluoromethoxylated arenes, namely riluzole (treatment of amyotrophic lateral sclerosis), pretomanid and delamanid (treatment of tuberculosis), and sonidegib (treatment of basal cell carcinoma) [1].

Nitrogen-containing heterocycles are the most popular compounds for drug design. At least 85% of pharmaceuticals contain such a fragment in their structure. Therefore, it seems unexpected that a small number of drugs with a fluorine-containing heterocyclic ring is known (42 compounds). Moreover, only single fluorine atom or the trifluoromethyl group represent fluorinated substituents [1]. Such circumstances can be explained by the absence of practical and cheap synthetic ways to heterocycles with other fluorinated groups, in particular fluorinated ethers [2]. Methodologies for the synthesis of fluorinated ethers are significantly different from methods for the preparation of alkyl ethers. It is impossible to use trifluoromethyl iodide or trifluoromethyl triflate for direct trifluoromethylation of oxygen nucleophiles in the same way as methyl iodide or methyl triflate. This is due to the strong electronegativity of a fluorine atom that results in reverse polarity of I-CF₃ and TfO-CF₃ bonds as compared to I-CH₃ and TfO-CH₃ [2, 3]. A few different strategies can be applied for the preparation of fluorinated ethers. The first method was based on the ether fluorination. It was incorporated into organic chemistry by *Lev Yagupolskii* in 1955 [4]. The main limitation of this method is the harsh conditions of the fluorination stage. Nevertheless, this approach was successfully applied to the synthesis of trifluoromethoxy substituted heterocycles [5–7]. Pyridines with the trifluoromethoxy group in various positions of the ring – α -, β - and γ -substituted pyridines – were obtained by this method. However, this reaction successfully occurred only when at least one α -position of the ring was occupied by a chlorine atom. The same feature was also found to be characteristic for pyrazine derivatives [7]. The second approach to trifluoromethoxylated heterocycles is the cyclization of the fluorinated precursors [8, 9]. A novel route to trifluoromethoxy substituted heterocycles is based on trifluoromethylation of the hydroxyl group by the action of hypervalent iodine reagents or direct trifluoromethoxylation [10]. Although the examples of direct trifluoromethoxylation are known from the literature [11], these methods are promising for preparing the α -substituted pyridine ring mainly, at the same time, the synthesis of β -trifluoromethoxypyridine in such a manner is controversial. Direct introduction of the trifluoromethoxy group occurred under more mild reaction conditions than fluorination. Therefore, it can be applied to a wide range of substrates. From the other hand, these methods

require expensive reagents that are used in a large excess.

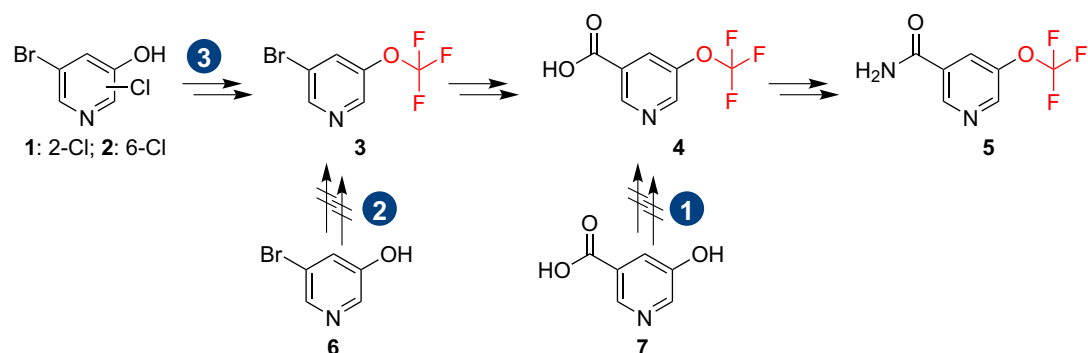
It can be summarized that each of the above-mentioned strategies – fluorination of ethers, nucleophilic substitution or direct trifluoromethylation of hydroxy-compounds – requires some improvements before it becomes a practical method. In the current study, we concentrated our attention on the scalable synthesis of nicotinic acid and related compounds with the trifluoromethoxy group in position 5.

■ Results and discussion

A series of trifluoromethoxysubstituted pyridines was prepared earlier [6]. The method used in this paper was based on chlorination-fluorination techniques that allowed to obtain a series of α -chloropyridines with the OCF₃-group in various positions. These compounds were used for the preparation of pyridines with different functional groups: amines, aldehydes, acids, silanes, etc. However, 5-trifluoromethoxy substituted nicotinic acid or any suitable precursors for its preparation were not described in this research.

Key compounds for the synthesis of nicotinic acid **4** and nicotinamide **5** with trifluoromethoxy substituent are shown in **Scheme 1**. We found that transformation of 5-hydroxynicotinic acid **7** (or its methyl ester) into the corresponding chlorothionoformate or methylxanthate with further chlorination-fluorination gave no positive results (*route 1*). Similarly, our attempts to transform bromopyridinol **6** to 3-bromo-5-trifluoromethoxypyridine in such a manner failed, despite such transformation was well documented for pyridines with halogen atoms in α -position (*route 2*) [5, 6]. Taking into account this feature of the pyridine ring, α -chloro-substituted pyridines **1** and **2** were used as starting compounds (**Scheme 1**, *route 3*).

We tried to prepare pyridines **10** and **11** according to [6] and found that this procedure was suitable for trichloromethoxysubstituted pyridine **10**, but gave poor results for pyridine **11**. Modifications of the method (reversed mixing of the reagents) allowed us to increase the yield of **11** from 15 to 78% (**Scheme 2**). It should be noted that chlorothionoformates **8** and **9** were used for further transformations without isolation in a pure state. Thus, the methodology proposed is very attractive in terms of handling such toxic compounds. Further fluorination of **10** and **11** by



Scheme 1. Potential routes to 5-(trifluoromethoxy)nicotinic acid and nicotinamide

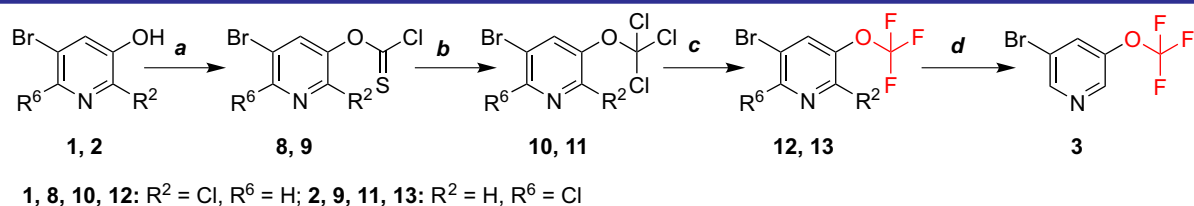
antimony trifluoride led to trifluoromethoxysubstituted pyridines **12** and **13**, respectively, in high yields.

For hydrodechlorination reaction of **12** and **13**, we used “red phosphorus / HI” as a reducing agent, and 3-bromo-5-trifluoromethoxypyridine (**3**) was prepared in a high yield. It is noteworthy that the reaction can be performed in a 50 g scale. It is worth mentioning that this reaction required the use of hydroiodic acid as a solvent. However, in contrast to the methoxy group that easily cleaves under these conditions (*Zeisel* determination of ethers [12]), trifluoromethoxy one remains intact even after prolonged heating. No evidence of this group destruction was found in ^{19}F NMR spectra of the reaction mixture. Thus, both isomers **12** and **13** were successfully transformed into **3** in the same yields. With this in mind, we also used the mixture of chloropyridines **1** and **2** for preparing pyridine **3**.

This mixture can be easily obtained by chlorination of 5-bromopyridin-3-ol (**6**) with sodium hypochlorite [13] and, as a result, is more available than individual isomers **1**, **2**.

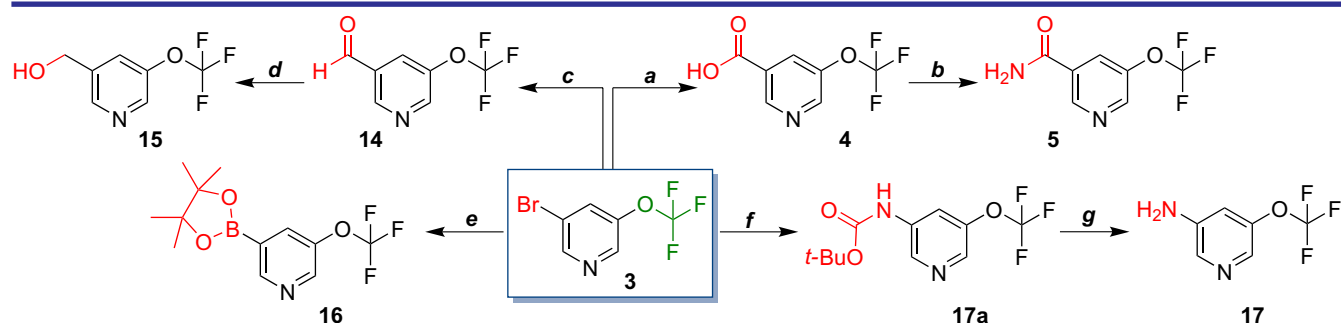
We have found that 3-bromo-5-trifluoromethoxypyridine (**3**) is a convenient starting material for a wide range of 5-trifluoromethoxysubstituted pyridines (**Scheme 3**). Bromopyridine **3** can be readily lithiated by the action of *n*-butyllithium, and after the treatment with carbon dioxide, nicotinic acid **4** was formed in almost quantitative yield. This acid was used for preparing 5-trifluoromethoxynicotinamide (**5**) by common methods with a high yield. Lithiated pyridine **3** readily reacted with ethyl formate yielding nicotinic aldehyde **14**. This aldehyde was reduced to alcohol **15** with a high yield.

Bromopyridine **3** was also used in palladium-catalyzed cross-coupling reactions. Bromine was substituted with boronic ester under $\text{Pd}(\text{dppf})\text{Cl}_2$,



Scheme 2. The synthesis of 3-bromo-5-(trifluoromethoxy)pyridine (**3**)

Reagents and conditions: (a) CSCl_2 , NaOH, $\text{CHCl}_3/\text{H}_2\text{O}$, 0°C ; (b) Cl_2 , CHCl_3 , r.t.; (c) SbF_3 , SbCl_5 , $145\text{--}150^\circ\text{C}$; (d) P, aq 57% HI, reflux



Scheme 3. The reactivity of 3-bromo-5-(trifluoromethoxy)pyridine

Reagents and conditions: (a) *n*BuLi, -90°C , then CO_2 , 85% yield; (b) SOCl_2 , 70°C , then NH_4OH , 0°C , 85% yield; (c) *n*BuLi, -90°C , then EtOCHO, 64% yield; (d) NaBH_4 , EtOH, r.t., then aq HCl, r.t., 89% yield; (e) B_2pin_2 , $\text{Pd}(\text{dppf})\text{Cl}_2$, KOAc, dioxane, 100°C , 80% yield; (f) $t\text{BuOCONH}_2$, Pd_2dba_3 , Xantphos, Cs_2CO_3 , dioxane, 100°C , 69% yield; (g) CF_3COOH , CH_2Cl_2 , r.t., 72% yield

catalysis to form pyridine **16**. Compound **3** readily reacted with *tert*-butyl carbamate under Pd₂dba₃ catalysis yielding Boc-protected amine **17a**. After deprotection, aminopyridine **17** was obtained in 50% yield in two steps.

Alternatively, we investigated the metalation of chloro-substituted pyridine **13** using *n*-butyllithium (Scheme 4). We found that a mixture of nicotinic and isonicotinic acids was formed after treating lithium derivatives with carbon dioxide. If the reaction mixture was saturated by gaseous CO₂ at -95–-100°C, a mixture of acids **18–19** (1:1) was obtained. When lithiated pyridine was poured onto solid carbon dioxide (-78 °C), the main product was isonicotinic acid **18** (5:1). We supposed that the rearrangement of the initially formed 3-lithium isomer into 4-isomer occurred at temperatures higher than -78 °C due to a strong α -effect of the OCF₃ group.

In contrast to nicotinic acids **18** and **19**, nicotinic aldehyde **20** was formed selectively and obtained in a high yield of 79% by the reaction of 3-bromo-2-chloro-5-trifluoromethoxypyridine (**13**) with *n*-butyllithium and further treatment with DMF. In this case isomerization did not occur, probably because the interaction of lithiated pyridine with DMF proceeded faster than with carbon dioxide.

It was shown that this aldehyde **20** could be reduced to alcohol **21** by sodium borohydride or oxidized by potassium permanganate yielding nicotinic acid **19**. In both cases, the target products were obtained in almost quantitative yields. 2-Chloronicotinic acid **19** was used for preparing 5-trifluoromethoxynicotinic acid (**4**). A chlorine atom was reduced by Pd catalysed hydrogenation. This reaction occurred at atmospheric

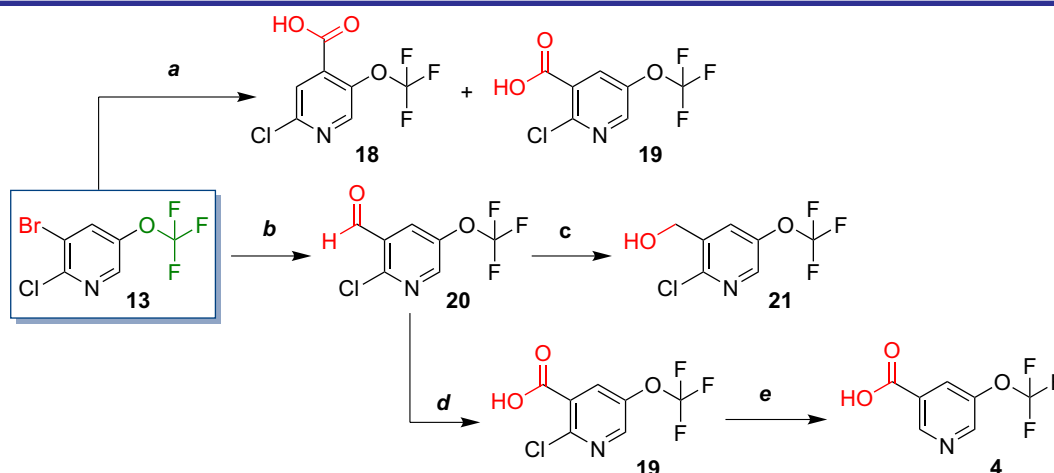
pressure, and the product was obtained in a high yield.

Conclusion

A synthetic approach based on chlorination-fluorination of the chlorothionoformate group in the pyridine core is a convenient and practical route for trifluoromethoxylated pyridines. The presence of a chlorine atom in α -position of pyridine (either 2 or 6) is necessary for successful transformation, and in both cases 2- or 6-chloro-3-bromo-5-trifluoromethoxypyridines are obtained in high yields. In contrast to methoxy group, the trifluoromethoxy one is stable to the hydroiodic acid action. This remarkable property of the trifluoromethoxy group allows to reduce a chlorine atom in α -position of the pyridine ring selectively without destruction of the OCF₃ group and reduction of a bromine atom in β -position of the ring. 3-Bromo-5-trifluoromethoxy pyridine is a promising building block demonstrated by metalation reactions and Pd-catalyzed syntheses. Using this precursor, analogues of natural products– nicotinic acid and nicotinamide with trifluoromethoxy group have been synthesized.

Experimental part

¹H NMR spectra were recorded using a Varian VXR-300 instrument at 300 MHz, a Bruker AVANCE DRX 500 spectrometer at 500 MHz, or a Varian UNITY-Plus 400 instrument at 400 MHz. ¹³C NMR spectra (proton decoupled) were recorded on a Bruker AVANCE DRX 500 instrument at 125 MHz, or a Varian UNITY-Plus 400 spectrometer at 100 MHz, or a Varian VXR-300



Scheme 4. The synthetic potential of 3-bromo-2-chloro-5-trifluoromethoxypyridine

Reagents and conditions: (a) *n*BuLi, -90 °C, then CO₂; (b) *n*BuLi, -90 °C, then DMF, 79% yield; (c) NaBH₄, EtOH, r.t., then HCl aq, r.t., 94% yield; (d) KMnO₄, H₂O, 60 °C, 80% yield; (e) H₂, 10% Pd/C, HCOONH₄, MeOH, r.t., 79% yield

instrument at 75 MHz. ^{19}F NMR spectra were recorded at 376 MHz using a Varian UNITY-Plus 400 spectrometer or at 188 MHz using a Mercury VX 200 Varian instrument. The chemical shifts are given in ppm relative to TMS and CCl_3F , respectively, as internal or external standards. The LC-MS spectra were registered on an Agilent 1100 instrument with a diode-matrix and an Agilent 1100 LS/MSD SL mass-selective detector. The GC-MS spectra were registered on a Hewlett-Packard HP GC/MS 5890/5972 instrument (EI 70 eV). The melting points were determined in open capillaries using an SMP3 instrument. The elemental analysis was performed in the Analytical Laboratory of the Institute of Organic Chemistry of mass-selective detector NASU.

For the column chromatography, Merck Kieselgel 60 silica gel was used. Thin-layer chromatography (TLC) was carried out on aluminium-backed plates coated with silica gel (Merck Kieselgel 60 F254).

Unless otherwise stated, commercially available reagents were purchased from Enamine Ltd. (Kyiv, Ukraine) and were used without purification. The solvents were purified according to the standard procedures. Antimony trifluoride was sublimed immediately prior to use. Chlorination of 5-bromopyridin-3-ol with sodium hypochlorite was performed according to [13]. Pure 5-bromo-2-chloro-pyridin-3-ol (M. p. 188 °C) was obtained by SiO_2 column chromatography with the mixture of hexane/ethyl acetate (1:4) as an eluent (R_f 0.5).

Trichloromethoxy-pyridines (10) and (11). The general procedure

Method A. The solution of thiophosgene (41.4 g, 0.36 mol) in 300 mL of chloroform was added dropwise to the vigorously stirred mixture of hydroxypyridine **1** or **2** (75 g, 0.36 mol) and sodium hydroxide (15.1 g, 0.38 mol) in 300 mL of water at 0 °C, and the mixture was stirred for 2 h at the same temperature. The organic layer was separated, washed with water, and dried over MgSO_4 . Prepared in such a manner the chloroform solution of chlorothionoformate was saturated with chlorine and stirred for 48 h at room temperature. The excess of chlorine was then removed with N_2 gas stream. The solvent was distilled off under reduced pressure (300 mbar), and the residue was distilled in a vacuum yielding the corresponding trichloromethoxy-pyridine **10** or **11**.

Method B. Sodium hydroxide (15.8 g, 0.40 mol) in 300 mL of water was added dropwise to the vigorously stirred mixture of hydroxypyridine **1** or **2** (75 g, 0.36 mol) and thiophosgene (41.4 g,

0.36 mol) in chloroform at 0 °C, and the mixture was stirred for 2 h at the same temperature. The organic layer was separated, washed with water, and dried over MgSO_4 . Prepared in such a manner the chloroform solution of chlorothionoformate was saturated with chlorine and stirred for 48 h at room temperature. The excess of chlorine was removed with N_2 gas stream. The solvent was distilled off under reduced pressure (300 mbar), and the residue was distilled in a vacuum yielding the corresponding trichloromethoxy-pyridine **10** or **11**.

5-Bromo-2-chloro-3-trichloromethoxy-pyridine (10)

A colorless oil or a low melted solid. Yield – 64.5 g, 55% (Method A); 72.7 g, 62% (Method B). B. p. 115–117 °C at 0.5 mbar; M. p. 32 °C. Anal. Calcd for $\text{C}_6\text{H}_2\text{BrCl}_4\text{NO}$, %: C 22.12, H 0.62, N 4.30. Found, %: C 21.97, H 0.85, N 4.08. ^1H NMR (400 MHz, CDCl_3), δ , ppm: 8.15 (1H, d, $^3J_{\text{HH}} = 2.4$ Hz, 4-PyH), 8.41 (1H, d, $^3J_{\text{HH}} = 2.4$ Hz, 6-PyH). ^{13}C NMR (100 MHz, CDCl_3), δ , ppm: 111.5, 117.8, 132.7, 143.7, 144.7, 147.5.

3-Bromo-2-chloro-5-trichloromethoxy-pyridine (11)

A colorless oil or a low melted solid. B. p. 120–122 °C at 0.5 mbar; M. p. 45 °C. Yield – 17.7 g, 15% (Method A); 91.5 g, 78% (Method B). Anal. Calcd for $\text{C}_6\text{H}_2\text{BrCl}_4\text{NO}$, %: C 22.12, H 0.62, N 4.30. Found, %: C 22.01, H 0.80, N 4.12. ^1H NMR (400 MHz, CDCl_3), δ , ppm: 8.02 (1H, d, $^3J_{\text{HH}} = 2.4$ Hz, 4-PyH), 8.43 (1H, d, $^3J_{\text{HH}} = 2.4$ Hz, 6-PyH). ^{13}C NMR (100 MHz, CDCl_3), δ , ppm: 112.1, 119.9, 136.3, 142.2, 147.0, 149.0.

Trifluoromethoxy-pyridines (12) and (13). The general procedure

The corresponding trichloromethoxy-pyridine **10** or **11** (81.5 g, 0.25 mol) was added in portions to the mixture of SbF_3 (134 g, 0.75 mol) and SbCl_5 (7.5 g, 0.025 mol) at 100 °C. The mixture was stirred for 5 h at 145–150 °C, cooled to room temperature, mixed with 650 mL of CH_2Cl_2 , and then quenched with an aqueous solution of K_2CO_3 (517 g, 3.75 mol in 2.5 L of water) and KF (653 g, 11.25 mol in 1.25 L of water). The precipitate was filtered off, the organic layer was separated, washed with water, and dried with MgSO_4 . The solvent was distilled off, and the residue was distilled in a vacuum yielding the corresponding trifluoromethoxy-pyridine **12** or **13**.

5-Bromo-2-chloro-3-trifluoromethoxy-pyridine (12)

A colorless oil. Yield – 58.1 g (84%). B. p. 90–92 °C at 20 mbar. Anal. Calcd for $\text{C}_6\text{H}_2\text{BrClF}_3\text{NO}$, %:

C 26.07, H 0.73, Cl 12.82. Found, %: C 25.88, H 0.50, Cl 13.04. ^1H NMR (400 MHz, CDCl_3), δ , ppm: 7.78 (1H, s, 4-PyH), 8.41 (1H, s, 6-PyH). ^{13}C NMR (100 MHz, CDCl_3), δ , ppm: 118.6, 120.3 (q, $^2J_{\text{CF}} = 262.5$ Hz, OCF_3), 133.1, 142.0, 143.5, 148.4. ^{19}F NMR (300 MHz, CDCl_3), δ , ppm: -57.55 (s, OCF_3). GC-MS, m/z (I_{rel} , %): 277 (100) $[\text{M}^{(79}\text{Br}^{37}\text{Cl})/^{(81}\text{Br}^{35}\text{Cl})]^+$, 275 (79) $[\text{M}^{(79}\text{Br}^{35}\text{Cl})]^+$, 279 (24) $[\text{M}^{(81}\text{Br}^{37}\text{Cl})]^+$.

3-Bromo-2-chloro-5-trifluoromethoxypyridine (13)

A colorless oil. Yield – 63.1 g (91%). B. p. – 105–107 °C at 20 mbar. Anal. Calcd for $\text{C}_6\text{H}_2\text{BrClF}_3\text{NO}$, %: C 26.07, H 0.73, Cl 12.82. Found, %: C 25.80, H 0.55, Cl 12.49. ^1H NMR (300 MHz, CDCl_3), δ , ppm: 7.86 (1H, dd, $^3J_{\text{HH}} = 2.4$ Hz, $^4J_{\text{HF}} = 1.8$ Hz, 4-PyH), 8.32 (1H, dd, $^3J_{\text{HH}} = 2.4$ Hz, $^4J_{\text{HF}} = 1.8$ Hz, 6-PyH). ^{13}C NMR (100 MHz, CDCl_3), δ , ppm: 120.2 (q, $^1J_{\text{CF}} = 260.5$ Hz, OCF_3), 120.3, 134.6, 140.7, 144.4, 148.9. ^{19}F NMR (300 MHz, CDCl_3), δ , ppm: -58.93 (s, OCF_3). GC-MS, m/z (I_{rel} , %): 277 (100) $[\text{M}^{(79}\text{Br}^{37}\text{Cl})/^{(81}\text{Br}^{35}\text{Cl})]^+$, 275 (79) $[\text{M}^{(79}\text{Br}^{35}\text{Cl})]^+$, 279 (24) $[\text{M}^{(81}\text{Br}^{37}\text{Cl})]^+$.

The synthesis of 3-bromo-5-trifluoromethoxypyridine (3)

The mixture of 3-bromo-2-chloro-5-trifluoromethoxypyridine (13) (63.0 g, 0.23 mol) and red phosphorus (85.0 g, 2.75 mol) in 1 L of 57% aqueous HI was refluxed for 48 h. The progress of the reaction was monitored by ^{19}F NMR spectra. The excess of phosphorus was filtered off *via* a glass filter, and the resulting solution was poured into the solution of Na_2CO_3 (400 g, 3.8 mol) in 2.5 L of water. The product was extracted with CH_2Cl_2 (6×400 mL), the extract obtained was washed with water (3×250 mL), and dried with MgSO_4 . The solvent was distilled off, and the residue was distilled in a vacuum yielding pyridine 3 (50.2 g, 90%).

5-Bromo-2-chloro-3-trifluoromethoxypyridine (12) (63 g, 0.23 mol) was used for preparing pyridine 3 (46.2 g, 83%) by the same procedure. When the mixture of chlorinated pyridines 12 and 13 in the ratio of 4:1 (50 g, 0.18 mol) was used for this reaction, bromopyridine 3 was obtained in 83% yield (36.3 g).

A colorless oil. B. p. 100–105 °C at 70 mbar. Anal. Calcd for $\text{C}_6\text{H}_3\text{BrF}_3\text{NO}$, %: C 29.78, H 1.25, Br 33.02. Found, %: C 29.88, H 1.53, Br 32.85. ^1H NMR (400 MHz, CDCl_3), δ , ppm: 7.73 (1H, s, 4-PyH), 8.48 (1H, s, 2/6-PyH), 8.63 (1H, s, 2/6-PyH). ^{13}C NMR (75 MHz, CDCl_3), δ , ppm: 120.3 (q, $^1J_{\text{CF}} = 260.7$ Hz, OCF_3), 120.4, 131.4, 141.1, 145.9, 149.4. ^{19}F NMR (300 MHz, CDCl_3), δ , ppm:

-58.74 (s, OCF_3). GC-MS, m/z (I_{rel} , %): 241 (100) $[\text{M}^{(79}\text{Br})]^+$, 243 (98) $[\text{M}^{(81}\text{Br})]^+$.

The preparation of 5-trifluoromethoxynicotinic acid (4) from bromopyridine (3)

n-Butyllithium (2.5 M solution in hexane, 7 mL, 17.4 mmol) was added to 25 mL of vigorously stirred toluene at -70– -65 °C. After the addition was completed, bromopyridine 3 (4 g, 16.5 mmol) was added at the same temperature, and the mixture was stirred for additional 30 min. Then the mixture was cooled to -85– -90 °C, and 12 mL of THF were added. The reaction mixture was stirred for 15 min, then poured into crushed dry ice (*ca.* 15 g). The product was extracted with aqueous sodium hydroxide solution (2 g, 50 mmol in 40 mL of water), washed with MTBE, and acidified with 3% aqueous hydrochloric acid to pH 5.5. The precipitate was filtered and crystallized (water/ethanol 5-to-1 mixture) yielding nicotinic acid 4 (2.9 g, 85%).

The preparation of 5-trifluoromethoxynicotinic acid (4) from 2-chloro-5-(trifluoromethoxy)nicotinic acid (19)

The mixture of 2-chloronicotinic acid 19 (0.5 g, 2 mmol), ammonium formate (0.2 g, 3 mmol) and 10% Pd on charcoal (0.2 g) in methanol (10 mL) was stirred in hydrogen atmosphere for 24 h. The mixture was filtered, the solvent was evaporated in a vacuum, and the residue was diluted with 3% hydrochloric acid and extracted with ethyl acetate. The organic solution was dried with MgSO_4 , evaporated in a vacuum yielding nicotinic acid 4 (0.33 g, 79%).

5-Trifluoromethoxynicotinic acid (4)

A colorless powder. M. p. 148–149 °C. Anal. Calcd for $\text{C}_7\text{H}_4\text{F}_3\text{NO}_3$, %: C 40.60, H 1.95. Found, %: C 40.48, H 2.13. ^1H NMR (500 MHz, $\text{DMSO}-d_6$), δ , ppm: 8.19 (1H, s, 4-PyH), 8.90 (1H, s, 2/6-PyH), 9.08 (1H, s, 2/6-PyH). ^{13}C NMR (125 MHz, $\text{DMSO}-d_6$), δ , ppm: 120.4 (q, $^1J_{\text{CF}} = 257.7$ Hz, OCF_3), 128.6, 129.4, 145.5, 146.8, 149.4, 165.3. ^{19}F NMR (470 MHz, $\text{DMSO}-d_6$), δ , ppm: -58.38 (s, OCF_3). LC-MS, m/z (CI): 207 $[\text{M}]^+$.

The synthesis of 5-(trifluoromethoxy)nicotinamide (5)

Nicotinic acid 4 (1 g, 4.8 mmol) was added in portions to thionyl chloride (2.9 g, 24 mmol) at 0 °C. The mixture was stirred at 70 °C for 2 h until the evolution of gas was completed. The excess of thionyl chloride was distilled off in a vacuum, and the residue was dissolved in MTBE (10 mL). A concentrated aqueous solution of ammonia (2 mL) was added dropwise to the solution at 0 °C, and the precipitate formed was filtered and dried in a vacuum.

A colorless powder. Yield – 0.85 g (85%). M. p. 147–148 °C. Anal. Calcd for $C_7H_5F_3N_2O_2$, %: C 40.79, H 2.45, N 13.59. Found, %: C 40.60, H 2.55, N 13.70. 1H NMR (400 MHz, DMSO- d_6), δ , ppm: 7.82 (1H, s, NH₂), 8.22 (1H, s, 4-PyH), 8.32 (1H, s, NH₂), 8.83 (1H, s, 2/6-PyH), 9.07 (1H, s, 2/6-PyH). ^{13}C NMR (125 MHz, DMSO- d_6), δ , ppm: 120.4 (q, $^1J_{CF}$ = 257.7 Hz, OCF₃), 128.6, 129.4, 145.5, 146.8, 149.4, 165.3. ^{19}F NMR (376 MHz, DMSO- d_6), δ , ppm: -57.68 (s, OCF₃). LC-MS, m/z (CI): 207 [M+H]⁺.

The procedure for 5-trifluoromethoxy-nicotinaldehyde (14)

n-Butyllithium (2.5 M solution in hexane, 7 mL, 17.4 mmol) was added to 25 mL of vigorously stirred toluene at -70–-65 °C. After the addition was completed, the solution of bromopyridine **3** (4 g, 16.5 mmol) in toluene (10 mL) was added to the mixture at the same temperature, and the mixture was stirred for further 30 min. The reaction mixture was cooled to -85–-90 °C, 12 mL of THF was added, the reaction mixture was stirred for 15 min, ethyl formate (1.5 g, 20 mmol) was added dropwise at the same temperature. After the addition was completed, the mixture was warmed to -10 °C, and the solution of NaHSO₄ (4 g, 33 mmol) in 10 mL of water was added. The product was extracted with MTBE, the extract obtained was washed with a brine, and dried with MgSO₄. The solvent was distilled off, and the residue was distilled in a vacuum yielding nicotinic aldehyde **14** as a colorless oil.

Yield – 2 g (64%). B. p. 50–52 °C at 0.5 mbar. Anal. Calcd for $C_7H_4F_3NO_2$, %: C 43.99, H 2.11, N 7.33. Found, %: C 42.71, H 2.35, N 7.12. 1H NMR (300 MHz, CDCl₃), δ , ppm: 8.01 (1H, s, 4-PyH), 8.77 (1H, s, 6-PyH), 9.02 (1H, s, 2-PyH), 10.15 (1H, s, CHO). ^{13}C NMR (100 MHz, CDCl₃), δ , ppm: 120.3 (q, $^2J_{CF}$ = 260.5 Hz, OCF₃), 126.7, 132.3, 146.5, 147.9, 149.9, 189.0. ^{19}F NMR (188 MHz, CDCl₃), δ , ppm: -58.38 (s, OCF₃). GC-MS, m/z (I_{rel} , %): 191 (100) [M]⁺.

The preparation of 5-trifluoromethoxy-pyridin-3-yl-methanol (15)

Sodium borohydride (0.6 g, 15 mmol) was added to the solution of 5-(trifluoromethoxy)nicotinaldehyde (**14**) (1 g, 5 mmol) in ethanol (30 mL) at 0 °C, and the mixture was stirred at room temperature for 4 h. The solvent was evaporated in vacuum, and 10 mL of water was added to the mixture. The mixture was acidified with 10% aqueous HCl to pH 1–2, stirred at room temperature for 12 h, and then neutralized with NaHCO₃. The product was extracted with MTBE, the extract

was dried over MgSO₄. The solvent was distilled off, and the residue was distilled in a vacuum to give alcohol **15** as a colorless oil.

Yield – 0.85 g (89%). B. p. 92–93 °C at 0.5 mbar. Anal. Calcd for $C_7H_6F_3NO_2$, %: C 43.53, H 3.13, N 7.25. Found, %: C 43.37, H 3.33, N 7.22. 1H NMR (300 MHz, CDCl₃), δ , ppm: 4.06 (1H, br. s, OH), 4.73 (2H, s, CH₂OH), 7.60 (1H, s, 4-PyH), 8.33 (1H, s, 2/6-PyH), 8.40 (1H, s, 2/6-PyH). ^{13}C NMR (100 MHz, CDCl₃), δ , ppm: 61.3 (CH₂OH), 120.3 (q, $^1J_{CF}$ = 260.0 Hz, OCF₃), 127.0, 138.6, 141.3, 146.0, 146.3. ^{19}F NMR (188 MHz, CDCl₃), δ , ppm: -58.66 (s, OCF₃). GC-MS, m/z (I_{rel} , %): 193 (100) [M]⁺.

The preparation of 3-(4,4,5,5-Tetramethyl-1,3,2-dioxaborolan-2-yl)-5-trifluoromethoxy-pyridine (16)

The mixture of bromopyridine **3** (6 g, 25 mmol), bis(pinacolato)diboron (8.2 g, 32 mmol), potassium acetate (9.7 g, 100 mmol) and Pd(dppf)Cl₂·CH₂Cl₂ (1 g, 1.2 mmol) in 90 mL of dioxane was stirred for 24 h at 95–100 °C under argon atmosphere. The mixture was cooled to room temperature, filtered through a SiO₂ pad, diluted with water (150 mL), and extracted with MTBE. The product was purified by SiO₂ column chromatography using a mixture of hexane/MTBE in 3:1 as an eluent (R_f 0.3).

A colorless powder. Yield – 5.8 g (80%). M. p. 35–37 °C. Anal. Calcd for $C_{12}H_{15}BF_3NO_3$, %: C 49.86, H 5.23. Found, %: C 50.01, H 5.40. 1H NMR (300 MHz, CDCl₃), δ , ppm: 1.35 (12H, s, 4×CH₃), 7.90 (1H, s, 4-PyH), 8.59 (1H, s, 2/6-PyH), 8.86 (1H, s, 2/6-PyH). ^{13}C NMR (150 MHz, CDCl₃), δ , ppm: 24.6 (CH₃), 84.6 (C(CH₃)₂), 118.3, 120.3 (q, $^1J_{CF}$ = 260.1 Hz, OCF₃), 133.9, 145.0, 145.8, 153.4. ^{19}F NMR (300 MHz, CDCl₃), δ , ppm: -58.0 (s, OCF₃). GC-MS, m/z (I_{rel} , %): 289 (100) [M(¹¹B)]⁺, 288 (26) [M(¹⁰B)]⁺.

tert-Butyl 5-(trifluoromethoxy)pyridin-3-yl-carbamate (17a)

The mixture of bromopyridine **3** (4.8 g, 20 mmol), *tert*-butyl carbamate (3.5 g, 30 mmol), caesium carbonate (13 g, 40 mmol), Pd₂dba₃ (0.9 g, 1 mmol) and Xantphos (0.6 g, 1 mmol) in 50 mL of dioxane were stirred for 24 h at 95–100 °C under argon atmosphere. The mixture was cooled to room temperature, filtered through a SiO₂ pad, diluted with water (150 mL), and extracted with MTBE. The product was purified by SiO₂ column chromatography using the mixture of hexane/ethyl acetate (5:1) as an eluent (R_f 0.2).

A colorless powder. Yield – 3.8 g (69%). M. p. 60–62 °C. Anal. Calcd for $C_{11}H_{13}F_3N_2O_3$, %: C 47.49,

H 4.71, N 10.07. Found, %: C 47.28, H 4.88, N 10.24. ^1H NMR (400 MHz, CDCl_3), δ , ppm: 1.55 (9H, s, *t*-Bu), 7.38 (1H, s, 4-PyH), 8.22 (1H, s, 2/6-PyH), 8.48 (1H, s, NH). ^{13}C NMR (125 MHz, CDCl_3), δ , ppm: 28.2 ($\text{C}(\text{CH}_3)_3$), 81.8 ($\text{C}(\text{CH}_3)_3$), 118.3, 120.4 (q, $^1J_{\text{CF}} = 260.2$ Hz, OCF_3), 135.9, 137.2, 137.5, 146.4, 152.7. ^{19}F NMR (300 MHz, CDCl_3), δ , ppm: -58.54 (s, OCF_3).

3-Amino-5-trifluoromethoxy pyridin (17)

The mixture of compound **Boc-17** (3.8 g, 14 mmol) and trifluoroacetic acid in CH_2Cl_2 were stirred at room temperature for 20 h. The mixture was neutralized with sodium carbonate, washed with water, and dried with MgSO_4 . The solvent was distilled off, and the residue was distilled in a vacuum to yield pyridine **17** as a colorless solid.

Yield – 1.8 g (72%). B. p. 60–62 °C at 1 mbar; M. p. 35–37 °C. Anal. Calcd for $\text{C}_6\text{H}_5\text{F}_3\text{N}_2\text{O}$, %: C 40.46, H 2.83, N 15.73. Found, %: C 40.31, H 3.01, N 15.55. ^1H NMR (400 MHz, CDCl_3), δ , ppm: 4.09 (2H, s, NH), 6.87 (1H, s, 4-PyH), 7.95 (1H, s, 2/6-PyH), 8.06 (1H, s, 2/6-PyH). ^{13}C NMR (125 MHz, CDCl_3), δ , ppm: 118.0, 120.5 (q, $^1J_{\text{CF}} = 260.0$ Hz, OCF_3), 136.0, 137.0, 137.5, 146.6, 152.7. ^{19}F NMR (300 MHz, CDCl_3), δ , ppm: -58.5 (s, OCF_3). GC-MS, m/z (I_{rel} , %): 178 (100) [M] $^+$.

2-Chloro-5-trifluoromethoxy-nicotinaldehyde (20)

n-Butyllithium (2.5 M solution in hexane, 4.6 mL, 11.5 mmol) was added to 20 mL of vigorously stirred toluene at -70–65 °C. After the addition was complete, the solution of pyridine **13** (3 g, 10.8 mmol) in toluene (10 mL) was added to the mixture at the same temperature, and the mixture was stirred for further 30 min. The reaction mixture was cooled to -90–85 °C, and 10 mL of THF was added, the reaction mixture was stirred for 15 min, then DMF (2.4 g, 30 mmol) was added dropwise at the same temperature. After the addition was completed, the mixture was warmed to -10 °C, and the solution of NaHSO_4 (2.9 g, 20 mmol) in 10 mL of water was added. The product was extracted with MTBE, the extract was washed with a brine, dried over MgSO_4 . The solvent was distilled off, and the residue was distilled in a vacuum to give chloronicotinic aldehyde **20** as a colorless oil.

Yield – 1.9 g (79%). B. p. 65–66 °C at 1 mbar. Anal. Calcd for $\text{C}_7\text{H}_3\text{ClF}_3\text{NO}_2$, %: C 37.28, H 1.34, N 6.21. Found, %: C 37.30, H 1.55, N 6.12. ^1H NMR (500 MHz, CDCl_3), δ , ppm: 8.05 (1H, s, 4-PyH), 8.51 (1H, s, 6-PyH), 10.37 (1H, s, CHO).

^{13}C NMR (125 MHz, CDCl_3), δ , ppm: 120.1 (q, $^1J_{\text{CF}} = 261.5$ Hz, OCF_3), 129.2, 129.5, 145.6, 146.9, 150.6, 178.8. ^{19}F NMR (188 MHz, CDCl_3), δ , ppm: -57.92 (s, OCF_3). GC-MS, m/z (I_{rel} , %): 225 (100) [$\text{M}^{(35)\text{Cl}}$] $^+$, 227 (30) [$\text{M}^{(35)\text{Cl}}$] $^+$.

2-Chloro-5-(trifluoromethoxy)pyridin-3-yl-methanol (21)

Sodium borohydride (0.95 g, 25 mmol) was added to the solution of 2-chloro-5-(trifluoromethoxy)nicotinaldehyde (**20**) (1.9 g, 8.4 mmol) in ethanol (40 mL) at 0 °C, and the mixture was stirred at room temperature for 4 h. The solvent was evaporated in a vacuum, and 10 mL of water was added to the mixture. The mixture was acidified with 10% aqueous HCl to pH 1–2, stirred at room temperature for 12 h, and then neutralized with NaHCO_3 . The product was extracted with MTBE, the extract was dried with MgSO_4 . The solvent was distilled off, and the residue was distilled in a vacuum to give alcohol **23** as a colorless oil.

Yield – 1.8 g (94%). B. p. 101–102 °C at 0.5 mbar. Anal. Calcd for $\text{C}_7\text{H}_5\text{F}_3\text{NO}_2$, %: C 36.95, H 2.21, Cl 15.58. Found, %: C 36.90, H 2.28, Cl 15.55. ^1H NMR (400 MHz, CDCl_3), δ , ppm: 2.25 (1H, br. s, OH), 4.78 (2H, s, CH_2OH), 7.83 (1H, s, 4-PyH), 8.22 (1H, s, 6-PyH). ^{13}C NMR (100 MHz, CDCl_3), δ , ppm: 61.2 (CH_2OH), 120.3 (q, $^1J_{\text{CF}} = 260.0$ Hz, OCF_3), 127.0, 138.6, 141.3, 146.0, 146.3. ^{19}F NMR (188 MHz, CDCl_3), δ , ppm: -58.84 (s, OCF_3). GC-MS, m/z (I_{rel} , %): 227 (100) [$\text{M}^{(35)\text{Cl}}$] $^+$, 225 (30) [$\text{M}^{(35)\text{Cl}}$] $^+$.

2-Chloro-5-(trifluoromethoxy)nicotinic acid (19)

Potassium permanganate (0.46 g, 3 mmol) was added to a mixture of aldehyde **20** (1 g, 4.4 mmol) and potassium carbonate (0.11 g, 0.8 mmol) in water (10 mL) at 50–60 °C. The mixture was stirred for 1 h at 60 °C, cooled to room temperature, filtered, and the water solution was acidified to pH 6 with 3% aqueous hydrochloric acid. The product was filtered off, washed with water, and dried in a vacuum.

A colorless powder. Yield – 0.85 g (80%). M. p. 142–143 °C. Anal. Calcd for $\text{C}_7\text{H}_3\text{ClF}_3\text{NO}_3$, %: C 34.81, H 1.25, Cl 14.68. Found, %: C 34.50, H 1.55, Cl 14.82. ^1H NMR (300 MHz, $\text{DMSO}-d_6$), δ , ppm: 8.24 (1H, s, 4-PyH), 8.89 (1H, s, 6-PyH), 13.76 (1H, br. s, COOH). ^{13}C NMR (75 MHz, $\text{DMSO}-d_6$), δ , ppm: 116.4 (q, $^1J_{\text{CF}} = 260.5$ Hz, OCF_3), 125.2, 128.1, 131.7, 147.0, 148.8, 164.2. ^{19}F NMR (188 MHz, $\text{DMSO}-d_6$), δ , ppm: -57.34 (s, OCF_3). LC-MS, m/z (CI): 241 [$\text{M}^{(35)\text{Cl}}+\text{H}$] $^+$, 243 [$\text{M}^{(35)\text{Cl}}+\text{H}$] $^+$.

The metalation of 3-bromo-2-chloro-5-trifluoromethoxy-pyridine (**13**) using *n*-butyllithium with the formation of the mixture of isonicotinic (**18**) and nicotinic acids (**19**)

n-Butyllithium (2.5 M solution in hexane, 4.6 mL, 11.5 mmol) was added to 20 mL of vigorously stirred toluene at -70–65 °C. After the addition was completed, the solution of pyridine **13** (3 g, 10.8 mmol) in toluene (10 mL) was added to the mixture at the same temperature, and the resulting mixture was stirred for further 30 min. The reaction mixture was cooled to -90–85 °C, and 10 mL of THF was added, the reaction mixture was stirred for 15 min, then gaseous CO₂ (4.8 g, 0.11 mol) was bubbled through the reaction mixture at -90–85 °C. After the addition was

completed, the mixture was warmed to room temperature, washed with MTBE, acidified with 5% hydrochloric acid to pH 2. The products were filtered off, washed with water, and dried in a vacuum.

The yield of the mixture of isonicotinic **18** and nicotinic **19** acids (1:1) was 1.95 g (75%). In the case when the reaction mixture after the addition of THF and stirring for 15 min at -90–85 °C was poured into crushed dry ice, the yield of the mixture of acids **18** and **19** (5:1) was 2.2 g (84%). The structures of products were determined by ¹H and ¹⁹F NMR and LC-MS methods. They were in good agreement with [6] for 2-chloro-5-(trifluoromethoxy)isonicotinic acid (**18**), and the sample of pure 2-chloro-5-(trifluoromethoxy)nicotinic acid (**19**) prepared by oxidation of aldehyde **20**.

References

- Inoue, M.; Sumii, Y.; Shibata, N. Contribution of Organofluorine Compounds to Pharmaceuticals. *ACS Omega* **2020**, *5* (19), 10633–10640. <https://doi.org/10.1021/acsomega.0c00830>.
- Davydova, Yu. A.; Sokolenko, T. M.; Yahupolskyi, Yu. L. Five-membered heterocyclic compound with fluoroalkoxy substituents. *Ukrainian Chemistry Journal* **2015**, *81* (7–8), 3–24 [in Ukrainian].
- Kolomeitsev, A. A.; Vorobyev, M.; Gillandt, H. Versatile application of trifluoromethyl triflate. *Tetrahedron Lett.* **2008**, *8* (3), 449–454. <https://doi.org/10.1016/j.tetlet.2007.11.105>.
- Yagupolskii, L. M. Synthesis of derivatives of phenyl trifluoromethyl ethers. *Dokl. Acad. Nauk SSSR* **1955**, *105*, 100–102. [Chem. Abstr. **1956**, *50*, 11270b]
- Fuss, A.; Koch, V. Chemistry of 3-Hydroxypyridine Part 3: Synthesis of Substituted 3-[Fluoro(chloro)alkoxy]pyridines from Halo- or Amino-3-hydroxypyridines. *Synthesis* **1990**, *7*, 604–608. <https://doi.org/10.1055/s-1990-26956>.
- Manteau, B.; Genix, P.; Brelot, L.; Vors, J.-P.; Pazenok, S.; Giornal, F.; Leuenberger, C.; Leroux, F. R. A General Approach to (Trifluoromethoxy)-pyridines: First X-ray Structure Determinations and Quantum Chemistry Studies. *Eur. J. Org. Chem.* **2010**, *31*, 6043–6066. <https://doi.org/10.1002/ejoc.201000958>.
- Sokolenko, T.M.; Yagupolskii, Y.L. Trifluoromethoxypyrazines: Preparation and Properties. *Molecules* **2020**, *25*, 2226. <https://doi.org/10.3390/molecules25092226>.
- Sokolenko, T. M.; Davydova, Y. A.; Yagupolskii, Y. L. Efficient synthesis of 5'-fluoroalkoxythiazoles via α -bromo- α -fluoroalkoxyacetophenones Hantzsch type cyclization with thioureas or thioamides. *J. Fluorine Chem.* **2012**, *136*, 20–25. <https://doi.org/10.1016/j.jfluchem.2012.01.005>.
- Davydova, Y. A.; Sokolenko, T. M.; Yagupolskii, Y. L. Polyfluoro- and perfluoroalkoxyenaminones in syntheses of nitrogen containing heterocycles. *J. Fluorine Chem.* **2014**, *157*, 58–62. <https://doi.org/10.1016/j.jfluchem.2013.11.007>.
- Tlili, A.; Toulgoat, F.; Billard, T. Synthetic Approaches to Trifluoromethoxy-Substituted Compounds. *Angew. Chem. Int. Ed.* **2016**, *55*, 2–12. <https://doi.org/10.1002/anie.201603697>.
- Yang, Y.-M.; Yao, J.-F.; Yan, W.; Luo, Z.; Tang, Z.-Y. Silver-Mediated Trifluoromethoxylation of (Hetero)aryldiazonium Tetrafluoroborates. *Org. Lett.* **2019**, *21* (19), 8003–8007. <https://doi.org/10.1021/acs.orglett.9b03000>.
- Wang, Z. Zeisel Determination. In *Comprehensive Organic Name Reactions and Reagents*; Wang, Z., Ed. John Wiley & Sons, 2010; pp 3115–3118. <https://doi.org/10.1002/9780470638859.conrr689>.
- Morgentin, R.; Jung, F.; Lamorlette, M.; Maudet, M.; Ménard, M. Plé, P.; Pasquet, G.; Renaud, F. An efficient large-scale synthesis of alkyl 5-hydroxy-pyridin- and pyrimidin-2-yl acetate. *Tetrahedron* **2009**, *65* (4), 757–764. <https://doi.org/10.1016/j.tet.2008.11.064>.

Information about the authors:

Taras M. Sokolenko (corresponding author), Ph.D. in Chemistry, Senior Researcher, Organofluorine Compounds Chemistry Department, Institute of Organic Chemistry of the National Academy of Sciences of Ukraine; <https://orcid.org/0000-0002-3944-5571>; e-mail for correspondence: taras_sk@ukr.net.

Yurii L. Yagupolskii, Dr.Sci. in Chemistry, Professor, Chief of Organofluorine Compounds Chemistry Department, Institute of Organic Chemistry of the National Academy of Sciences of Ukraine; Scientific advisor, Enamine Ltd.; <https://orcid.org/0000-0002-5179-4096>.

UDC [547.759+547.83]:54.057

V. V. Voloshchuk^{1,2}, S. P. Ivonin¹¹ Institute of Organic Chemistry of the National Academy of Sciences of Ukraine,
5 Academician Kukhar str., 02098 Kyiv, Ukraine² Enamine Ltd., 78 Winston Churchill str., 02094 Kyiv, Ukraine

Recent Advances in the Synthesis and Biological Activity of Pyrrolo[2,3-*c*]pyridines

Abstract

Pyrrolo[2,3-*c*]pyridines (6-azaindoles) are the most promising nitrogen-containing heterocyclic compounds in the field of drug development. Exhibiting extraordinary versatility as pharmacophores, they are widely used in the development of kinase inhibitors, antiproliferative agents, and as potential therapeutic agents for the treatment of various diseases, including cancer and Alzheimer's disease. A large number of works focusing on new methods and approaches in the synthesis of 6-azaindoles, as well as on the study of their biological activity, have been published worldwide. In our review, we tried to classify all currently known strategies for the construction of the 6-azaindole core, which were published within the last 15 years, the chemical diversity of the derivatives obtained, and their therapeutic potential in the context of medicinal chemistry. We hope that this work will generalize and facilitate the understanding of the strategy for the synthesis of pyrrolo[2,3-*c*]pyridines, as well as help scientists in their further research in the direction of 6-azaindoles.

Keywords: pyrrolo[2,3-*c*]pyridines; 6-azaindoles; biological activity; medicinal chemistry; heterocyclic compounds; drug development

В. В. Волощук^{1,2}, С. П. Івонін¹

¹ Інститут органічної хімії Національної академії наук України,
вул. Академіка Кухаря, 5, м. Київ, 02660, Україна

² ТОВ НВП «Енамін», вул. Вінстона Черчилля, 78, м. Київ, 02094, Україна

Останні досягнення в синтезі та біологічній активності піроло[2,3-*c*]піридинів

Анотація

Піроло[2,3-*c*]піридини (6-азаіндоли) є одними з найперспективніших серед азотовмісних гетероциклічних сполук у сфері розробки ліків. Виявляючи надзвичайну універсальність як фармакофори, вони відіграють ключову роль у розробці інгібіторів кіназ, антипроліферативних агентів та постають потенційними терапевтичними агентами для лікування різноманітних захворювань, зокрема раку та хвороби Альцгеймера. У світі опубліковано велику кількість робіт, зосереджених на нових методиках та підходах у синтезі 6-азаіндолів, а також на дослідженні їхньої біологічної активності. У нашому огляді ми намагалися класифікувати всі відомі на сьогодні стратегії конструювання 6-азаіндольного ядра, опубліковані за останні 15 років, розглянути хімічне різноманіття одержаних похідних та їх терапевтичний потенціал у контексті медичної хімії. Ми сподіваємось, що ця робота узагальнить та полегшить розуміння стратегій синтезу піроло[2,3-*c*]піридинів, а також допоможе науковцям у їхніх подальших дослідженнях 6-азаіндолів.

Ключові слова: піроло[2,3-*c*]піридини; 6-азаіндоли; біологічна активність; медична хімія; гетероциклічні сполуки; розробка ліків

Citation: Voloshchuk, V. V.; Ivonin, S. P. Recent advances in the synthesis and biological activity of pyrrolo[2,3-*c*]pyridines.

Journal of Organic and Pharmaceutical Chemistry **2024**, *22* (1), 33–56.

<https://doi.org/10.24959/ophcj.24.303972>

Received: 13 April 2024; Revised: 7 May 2024; Accepted: 10 May 2024

Copyright© 2024, V. V. Voloshchuk, S. P. Ivonin. This is an open access article under the CC BY license (<http://creativecommons.org/licenses/by/4.0>).

Funding: The authors received no specific funding for this work.

Conflict of interests: The authors have no conflict of interests to declare.

■ Introduction

Nitrogen-containing heterocyclic compounds play one of the central roles in the realm of drug development, mainly thanks to their inherent molecular polarity, water solubility, and the ability to permeate cellular membranes. The analysis of FDA-approved drugs reveals that an astonishing 59 % of unique small-molecule drugs contain at least one nitrogen heterocycle, which demonstrates their importance in drug design and discovery [1]. This predominance is attributed not only to the versatility of nitrogen heterocycles in mimicking the biological landscape, but also to their structural diversity, which offers myriad possibilities for the modulation of pharmacokinetic and pharmacodynamic properties.

Among all of the nitrogen-containing heterocycles, pyrrolo[2,3-*c*]pyridines stand out as a very promising scaffold due to its unique structural features and considerable biological activity. This class of compounds with the condensed pyrrole and pyridine ring has long attracted a widespread interest from the research community. This interest is demonstrated by the vast list of literature on synthetic methodologies, structural modifications, and the study of the medicinal and biological potential of the 6-azaindole core. The review by *Popowycz et al.* (2007) meticulously summarized this data, highlighting the versatility of 6-azaindoles in drug development and underscoring the synthesis of compounds *via* diverse strategies, including the *Reisert*, *Batcho-Leimgruber*, *Hemetsberger-Knittel* syntheses, and their functionalization in various positions to enhance the biological activity [2]. It delves into the design of 6-azaindoles as biological targets and demonstrates their potential across a range of applications, from therapeutic agents to key synthetic intermediates.

However, since 2007, the synthesis and functionalization capabilities of pyrrolo[2,3-*c*]pyridines have significantly expanded due to advancements in synthetic chemistry, the availability of new reagents, increased technical capabilities, and so on. This synthetic versatility combined with the inherent biological relevance of the pyrrolo[2,3-*c*]pyridine core has led to the emergence of an immense amount of research, publications, and scientific works over the past 17 years.

Therefore, it seems to be very reasonable to complement the work of *Popowycz*, conduct a thorough analysis of all the new scientific achievements and provide a fresh thorough overview

of the current state of research on pyrrolo[2,3-*c*]pyridines, encompassing their synthesis, structural modifications, and pharmacological potential. By studying the current scientific developments in this field and identifying promising areas for future research, we hope to contribute to the ongoing efforts to use pyrrolo[2,3-*c*]pyridines in the search for new therapeutic agents.

■ Results and discussion

Pyrrolo[2,3-*c*]pyridines and their annulated derivatives can be synthesized by various synthetic strategies. However, it makes sense to highlight three main principal approaches that stand out due to their efficiency and versatility: (1) the annulation of the pyrrole nucleus to the pyridine cycle; (2) the annulation of the pyridine nucleus to the pyrrole cycle; (3) the synchronous formation of the 6-azaindole system where both the pyrrole and pyridine rings are constructed in a single, concerted step. Each of these methods offers its own unique advantages in terms of reaction conditions, functional group tolerance, and overall yield.

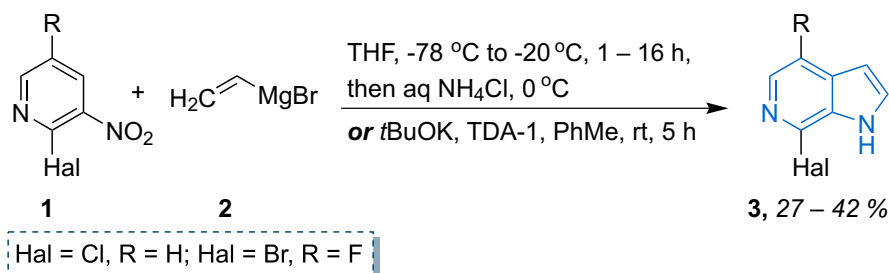
Initially, we propose focusing on the first method, namely the annulation of the pyridine nucleus to the pyrrole cycle.

1. Annulation of the pyrrole nucleus to the pyridine cycle

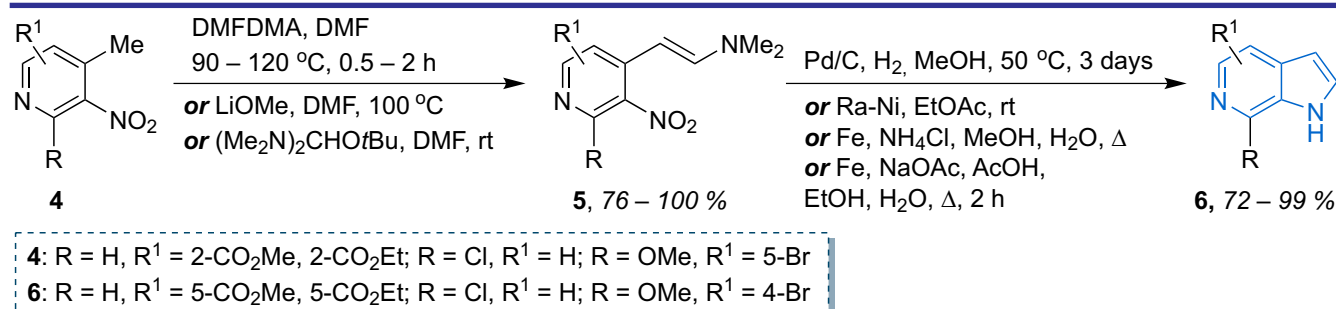
The first and one of the most common methods for forming the pyrrolo[2,3-*c*]pyridine framework **3** involves the *Bartoli* reaction of 2-halogen-3-nitropyridines **1** with vinyl magnesium bromide **2** in the THF solution [3–6] or using toluene as a solvent in the presence of a base [7] (**Scheme 1**).

The widespread application of this method can be attributed to its versatility, the high yields of targeted compounds it can achieve, and, of course, the possibility of using halogenated nitropyridines as precursors. The *Bartoli* reaction is a classic, described in an immense number of scientific studies and publications.

However, a two-step alternative approach allows the synthesis of 2,3-unsubstituted 6-azaindoles with much higher yields. For example, the reaction of 4-methyl-3-nitropyridines **4** with dimethylacetamide dimethyl acetal (DMFDMA) [8–11], lithium methylate in the DMF solution [12] or 1-*tert*-butoxy-*N,N,N',N'*-tetramethylmethanedi-amine [13] gives enamines **5**, which reductive cyclization leads to the target pyrrolo[2,3-*c*]pyridines (**Scheme 2**) with up to 100 % yields.



Scheme 1. The “classic” *Bartoli* reaction of nitropyridines with a vinyl Grignard reagent



Scheme 2. The alternative two-step approach for increasing the yields to 2,3-unsubstituted 6-azaindoles

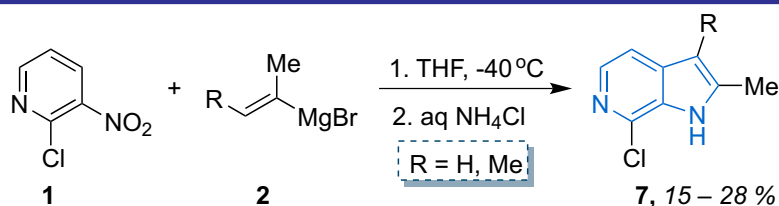
The *Bartoli* reaction is also used and described for synthesizing 2-alkyl-substituted or 2,3-dialkyl-substituted pyrrolo[2,3-*c*]pyridines **7**, among the functionalized derivatives of which potent potassium-competitive acid blockers (P-CABs) have been identified (**Scheme 3**) [14].

It is worth noting that this approach facilitates the incorporation of versatile alkyl groups in critical positions of the pyrrolopyridine core, allowing to fine-tune the molecule interaction with the H⁺/K⁺-ATPase enzyme. The subsequent functionalization of these derivatives has led to the identification of compounds exhibiting remarkable *in vitro* and *in vivo* inhibitory activities against gastric acid secretion, positioning them as promising leads for the development of new therapies for diseases associated with the increased stomach acid production.

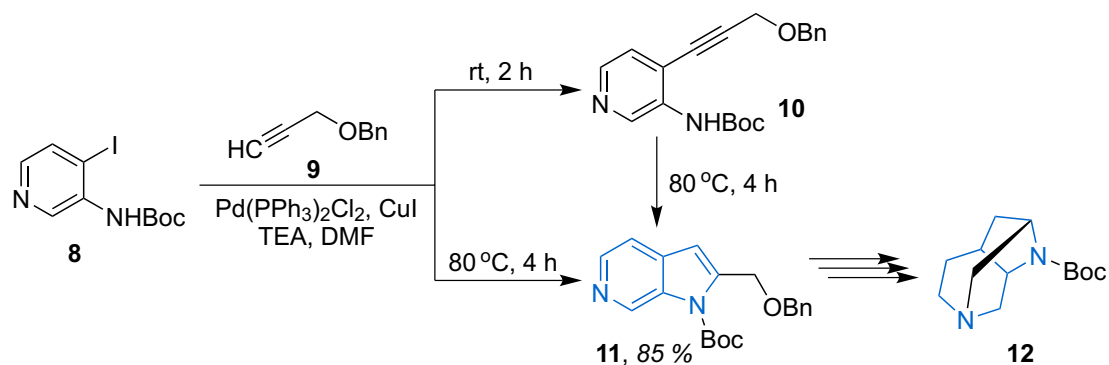
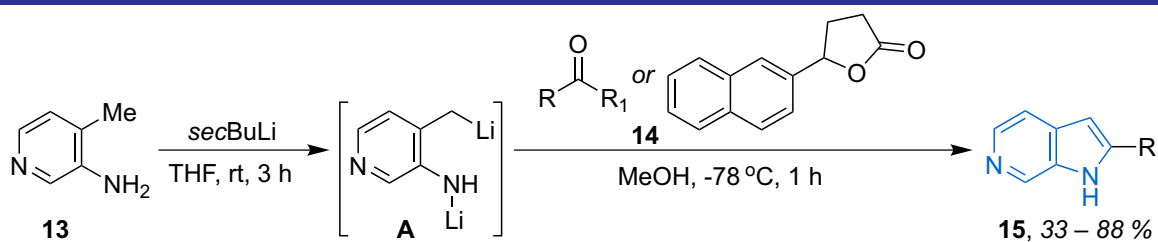
Thus, the utility of the *Bartoli* reaction consists not only in constructing complex nitrogen-containing heterocycles, but also in enabling the targeted modification of these molecules to enhance their pharmacological profiles, thereby offering a valuable strategy for the discovery and optimization of novel P-CABs.

The next described method for constructing the 6-azaindole core is the *Sonogashira* reaction. The interaction of *tert*-butyl (4-iodopyridine-3-yl) carbamate **8** with a terminal alkyne **9** at room temperature gave the alkylation product **10**; its heating at 80 °C provided a smooth cyclization to 2-benzyl-oxymethylpyrrolo[2,3-*c*]pyridine **11**, from which a new tricyclic diamine **12** could be synthesized by further functionalization [15]. In addition, to implement a tandem *Sonogashira* coupling/intramolecular cyclization reaction and obtain 6-azaindole **11** in one stage, the reaction mixture of iodopyridine **8** with a terminal alkyne **9** was heated (**Scheme 4**).

Undoubtedly, our review would be incomplete without mentioning the study from 2005 [16] where the authors described a one-step method for constructing a combinatorial library of 6-azaindole derivatives **15**, it involves the direct dilithiation of unprotected 3-amino-4-picoline **13**. The condensation of the dianion **A** obtained with carboxylic acid esters, thioester, or dihydrofuranone **14** led to a number of 2-substituted pyrrolo[2,3-*c*]pyridines with quite good and competitive yields (**Scheme 5**).

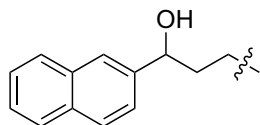


Scheme 3. The use of *Bartoli* reaction for P-CABs synthesis

Scheme 4. The *Sonogashira* reaction in the synthesis of 6-azaindole core

14: R = Me, R¹ = OMe; R = *t*Bu, R¹ = OMe; R = BnCH₂, R¹ = OMe; R = adamantan-1-yl, R¹ = OEt; R = Ph, R¹ = OEt; R = 4-BrC₆H₄, R¹ = OMe; R = 4-CF₃C₆H₄, R¹ = OMe; R = 2-naphthyl, R¹ = OMe; R = 3-furyl, R¹ = OEt; R = 3-thienyl, R¹ = OEt; R = 2-furyl, R¹ = SMe

15: R = Me, *t*Bu, BnCH₂, adamantan-1-yl, Ph, 4-BrC₆H₄, 4-CF₃C₆H₄, 2-naphthyl, 2-furyl, 3-furyl, 3-thienyl



Scheme 5. The scheme of the synthesis of the combinatorial library of 6-azaindole derivatives

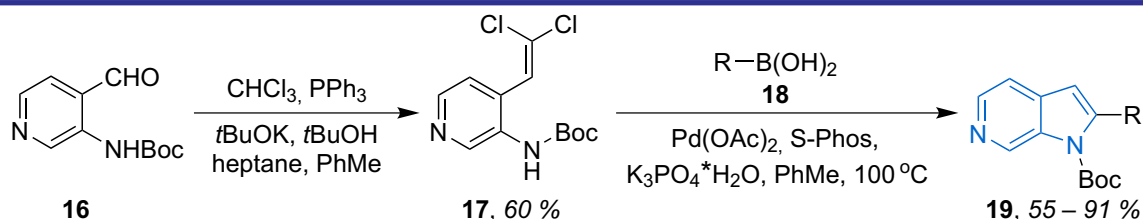
Another convenient method for synthesizing 2-alkyl(aryl, heteroaryl)-substituted 6-azaindoles **19** is the palladium-catalyzed reaction of *gem*-dichloro olefins **17** and boronic acids **18**, which includes a tandem intramolecular C–N coupling and the intermolecular *Suzuki* process (Scheme 6) [17].

In work [18] an example of obtaining 2-phenyl-1*H*-pyrrolo[2,3-*c*]pyridine **15** using a Pd-catalyzed and carbon monoxide mediated reductive cyclization of 3-nitro-4-styrylpyridine **20** (Scheme 7) was described. In a similar transformation,

authors of work [19] used phenyl formate as a CO source (Scheme 7).

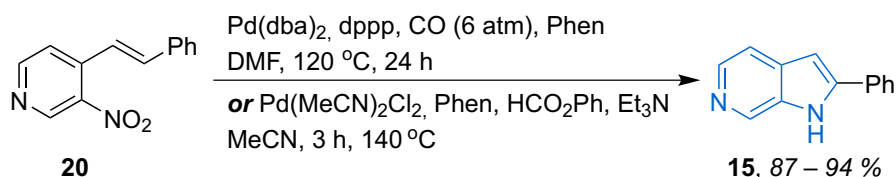
Another example of the Pd-catalyzed synthesis of 6-azaindoles **25** was developed based on the *Sonogashira* reaction followed by a tandem C–N coupling and cyclization with amines. The interaction of 3,4-dibromopyridine **21** with alkynes **22** led to 3-bromo-4-(arylethynyl)pyridines **23**, the treatment with aromatic amines produced a range of pyrrolo[2,3-*c*]pyridines **25** (Scheme 8) [20].

The work documented in [21] outlines a one-pot method for synthesizing 3-substituted

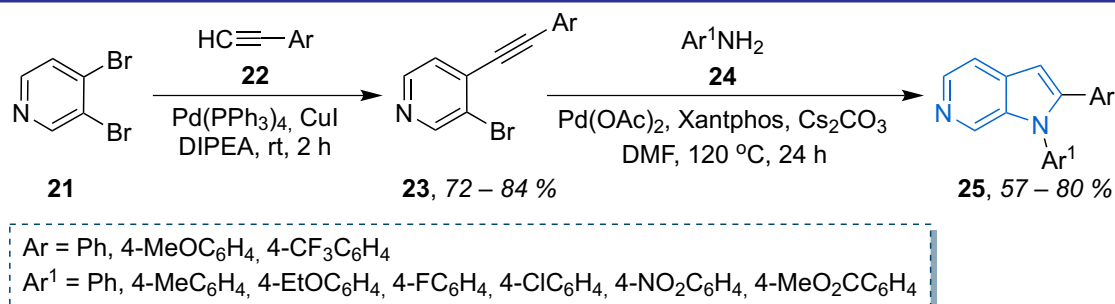


R = *n*PrCH=CH, Ph, 2-MeC₆H₄, 4-MeOC₆H₄, 4-CF₃C₆H₄, 2-naphthyl, 3-thienyl

Scheme 6. The alternative approach to 2-alkyl(aryl, heteroaryl)-substituted 6-azaindoles



Scheme 7. The synthesis of 2-phenyl-1H-pyrrolo[2,3-c]pyridine with the reductive cyclization



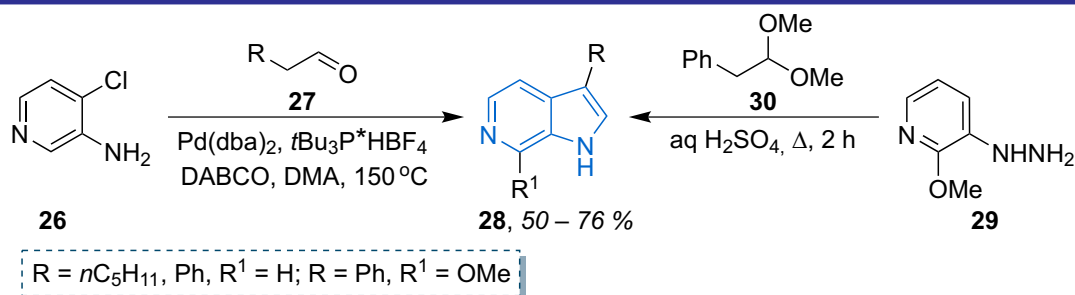
Scheme 8. The method for the synthesis of aryl substituted pyrrolo[2,3-c]pyridines

6-azaindoles **28** by the Pd-catalyzed direct annulation of *ortho*-chloroaminopyridine **26** with aldehydes **27** (Scheme 9). It is noteworthy that the authors of [22] used the Fischer cyclization of 3-hydrazinyl-2-methoxypyridine **29** and protected phenylacetaldehyde **30** as an alternative metal-free method for obtaining 3-phenyl-6-azaindole **28** (Scheme 9).

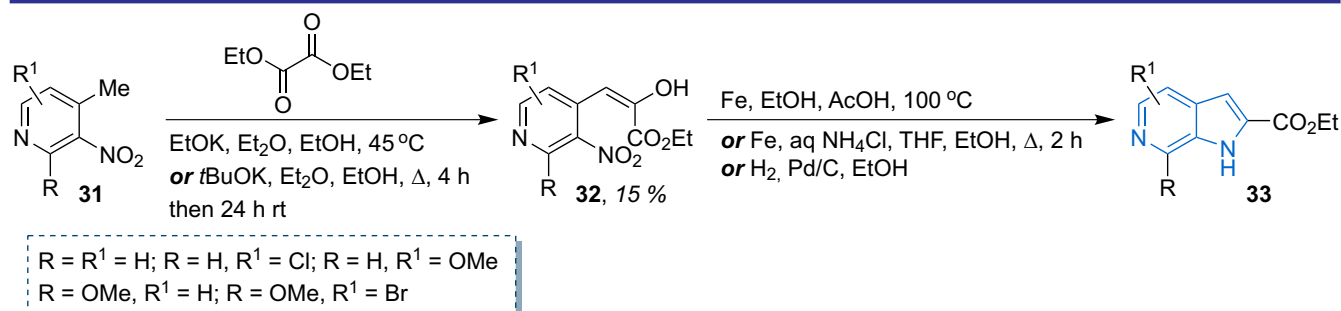
A series of works [23–25] describe the condensation of nitropyridines **31** with diethyl oxalate followed by the reductive cyclization of the resulting product **32** to yield ethyl 1H-pyrrolo[2,3-c]pyridine-2-carboxylates **33**, which are used

as building blocks in the synthesis of an immense range of biologically active compounds (Scheme 10).

The synthesis of isomeric ethyl 1H-pyrrolo[2,3-c]pyridine-3-carboxylates **36** was achieved by the condensation of 3- and 5-nitropyridines **34** with diethyl malonate in the presence of NaH in the DMF solution, yielding the corresponding diethyl 2-pyridylmalonates **35**. The reduction of the nitro group in these compounds followed by the heterocyclization with 25 % aqueous ammonia solution *in situ* led to the formation of the target products **36** (Scheme 11). Derivatives of



Scheme 9. The one-pot method for the synthesis of 3-substituted 6-azaindoles



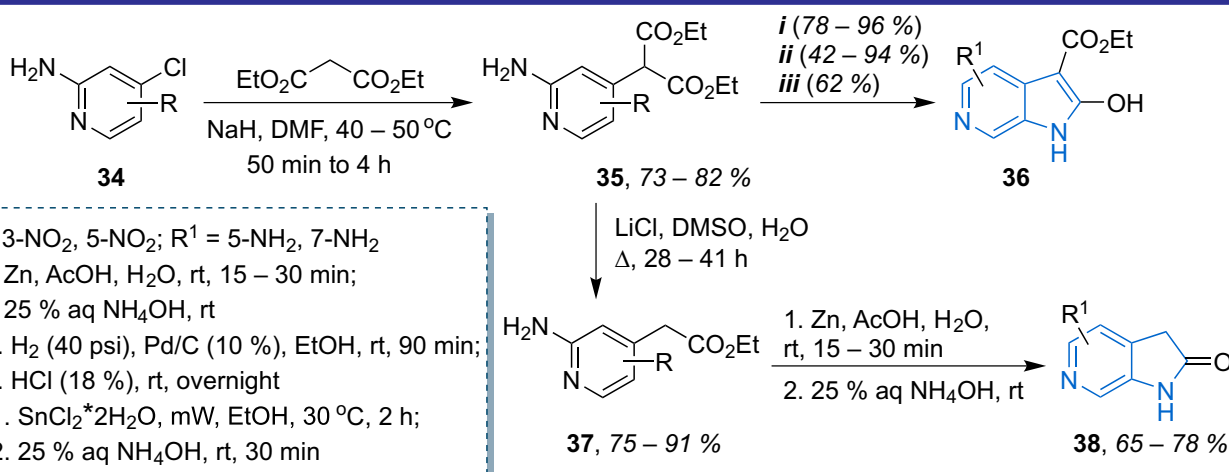
Scheme 10. The synthesis of 1H-pyrrolo[2,3-c]pyridine-2-carboxylates as the starting building block for obtaining the biologically active compounds

diethyl malonates **35** were converted into ethyl esters of acetic acid **37** by the decarboxylation treated with LiCl in a water/DMSO mixture at reflux. The reductive cyclization of derivatives **37** with zinc in acetic acid produced 5-amino- and 7-amino-6-azaindoles **38** (Scheme 11) [26]. On the example of the synthesis of ethyl 5-amino-2-hydroxy-1*H*-pyrrolo[2,3-*c*]pyridine-3-carboxylate **36**, the authors of work [27] tried the heterocyclization in a Parr hydrogenator using a catalytic amount of Pd on carbon in ethanol and the treatment with the 18 % solution of hydrochloric acid, as well as treating diethyl malonate **35** with an excess of SnCl₂·H₂O in ethanol under ultrasound activation (Scheme 11) [27].

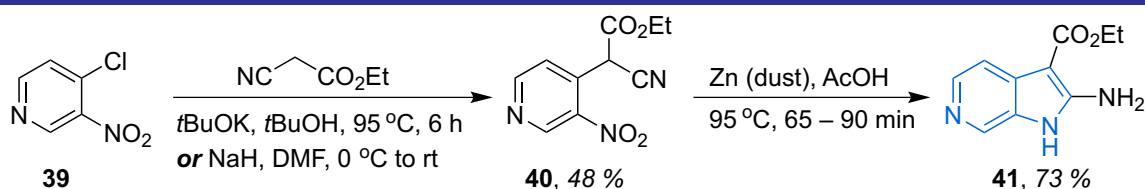
Meanwhile, the condensation of 4-chloro-3-nitropyridine **39** with ethyl cyanoacetate yielded ethyl 2-cyano-2-(3-nitropyridin-4-yl)acetate **40**; its intramolecular cyclization upon the treatment with powdered zinc in acetic acid led to the formation of ethyl 2-amino-1*H*-6-azaindole-3-carboxylate **41** (Scheme 12) [28, 29].

The Pd-catalyzed cyclization of *tert*-butyl 2-(5-nitropyridin-4-yl)acrylate **43** obtained by the condensation of the corresponding ethanoate **42** with 1,3,5-trioxane in the presence of calcium oxide and potassium carbonate yielded the expected *tert*-butyl 6-azaindole-3-carboxylate (Scheme 13) [30].

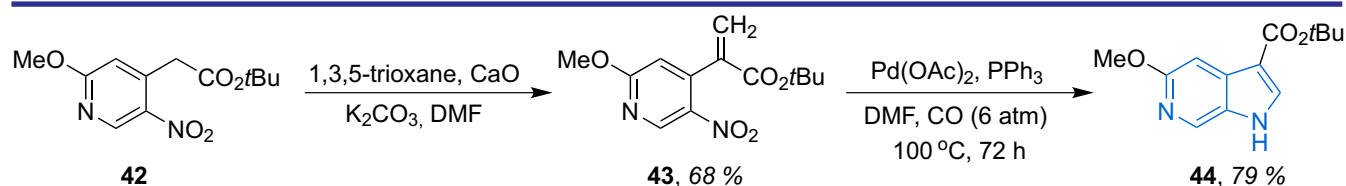
The authors of work [31] developed a one-pot variant for the synthesis of 2-trifluoromethyl-6-azaindoles **46**. The acylation of 2-methoxy-3-nitropyridine **45** with ethyl trifluoroacetate led to the formation of the intermediate 1,1,1-trifluoro-3-(3-nitropyridin-4-yl)propan-2-one (**A**) cyclized under the action of Zn in acetic acid to 2-(trifluoromethyl)-6-azaindole **46_1**. In contrast, the reaction of 2-chloro derivative **45** resulted in a mixture of 6-azaindole **46_2** (yield 33 %) and cyclic hemiaminal **47** (yield 49 %). An improvement in the yield of the target 7-chloropyrrolo[2,3-*c*]pyridine **46_2** was achieved by dehydration by stirring the mixture of products in glacial acetic acid for 3 days (Scheme 14).



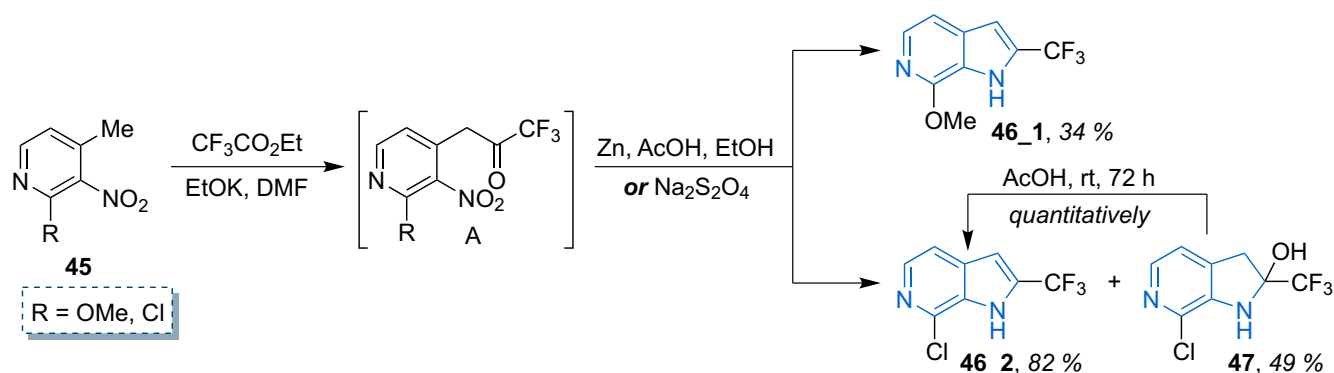
Scheme 11. The example of the synthesis of isomeric ethyl 1*H*-pyrrolo[2,3-*c*]pyridine-3-carboxylates



Scheme 12. The synthesis of 2-amino-1*H*-6-azaindole-3-carboxylate



Scheme 13. The synthesis of *tert*-butyl 6-azaindole-3-carboxylate



Scheme 14. The synthesis of 2-trifluoromethyl-6-azaindoles

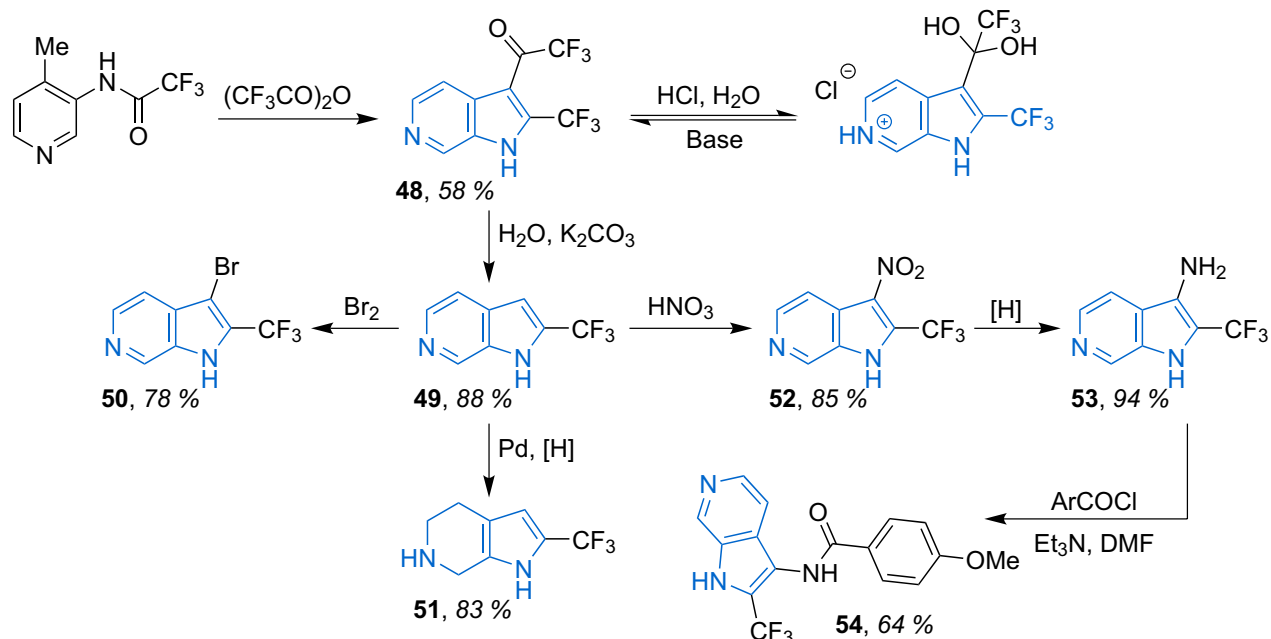
Another convenient approach to 3-trifluoromethyl-6-azaindoles was described in 2020 [32]. The hydration of trifluoroacetyl derivative **48** in hydrochloric acid at 80 °C for 16 hours gave easy removing of the trifluoroacetyl group to give 3-H 2-trifluoromethyl 6-azaindole. This efficient scalable synthetic route to 2-trifluoromethyl 6-azaindole made possible the synthesis of a variety of 3-substituted 2-trifluoromethyl 6-azaindoles and their partially saturated derivatives **49–54** (**Scheme 15**).

In 1970, the synthesis of 3-formyl-6-azaindole by the *Vilsmeier-Haack* formylation in 19% yield was described for the first time. However, in 2024, this work was expanded and supplemented by a study concerning the scope and limitations of the synthesis of 3-formyl-6-azaindoles **56** via the *Vilsmeier-Haack* formylation of the corresponding 3-amino-4-methyl pyridines **55** (**Scheme 16**) [33].

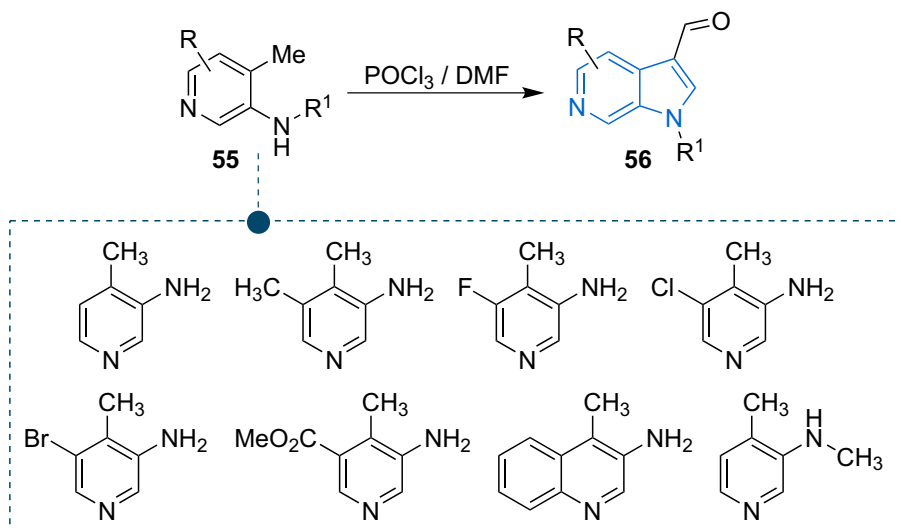
This method was demonstrated to be very effective, scalable, and regioselective, requiring no catalysts and quite easy to perform.

Also, the same year, the synthesis of 6-azaindoles *via* the formal electrophilic [4+1]-cyclization of 3-amino-4-methyl pyridines from the whole set of 3-amino-4-methylpyridine derivatives was described in detail (**Scheme 17**) [34]. The essential difference compared to all similar reactions previously known is the absence of the activation of the methyl group by a strong base. It allows to provide the cyclization in mildly acidic conditions and significantly enlarges its scope. 3-Methylamino-4-methylpyridine and 3-hydroxy-4-methylpyridine were preparatively entered into the reaction, giving the corresponding fused pyrrolo-/furno-derivatives though in hydrated form.

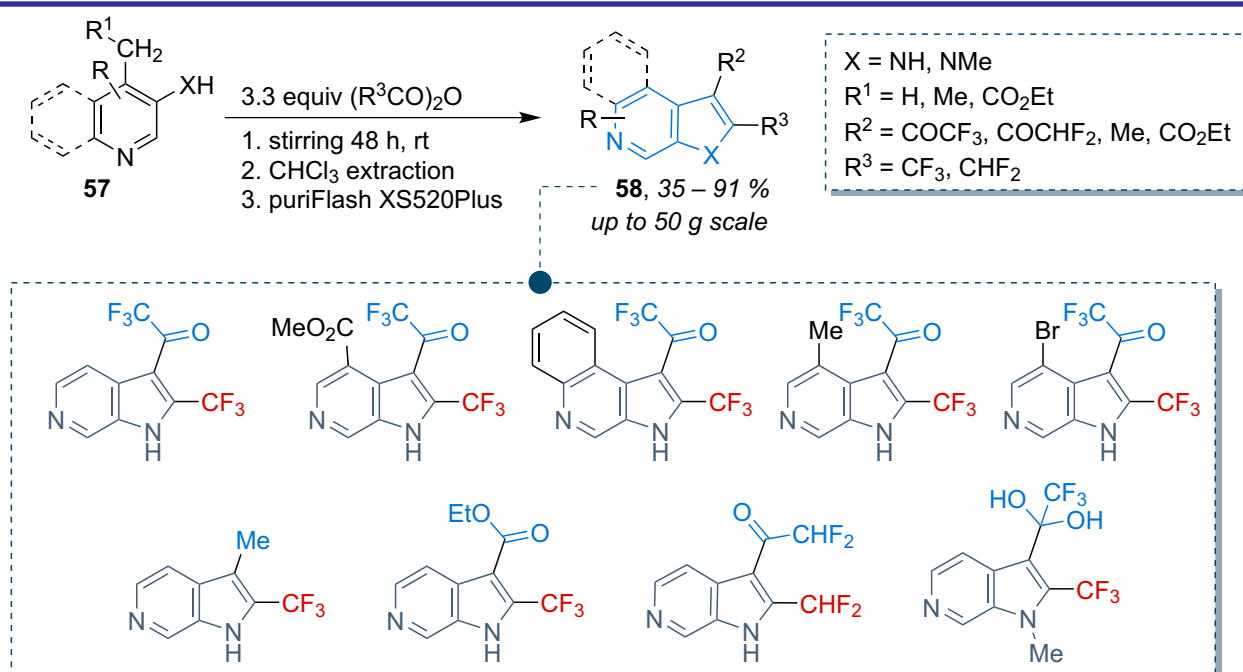
While pyrrolo[2,3-*c*]pyridines themselves are of substantial interest mainly due to their potential as pharmacophores, the move towards synthesizing their annulated derivatives opens new possibilities in drug design. Approaches to them include strategies, such as intramolecular cyclization reactions, the use of transition metal-catalyzed cross-coupling reactions, and employing



Scheme 15. An efficient way to 2-trifluoromethyl 6-azaindole and its derivatives



Scheme 16. The synthesis of 3-formyl-6-azaindoles via the Vilsmeier-Haack formylation



Scheme 17. The [4+1]-cyclization of 3-amino-4-methylpyridines

heteroatom insertions. Each method offers its own set of advantages in terms of selectivity, yield, and the types of annulated structures that can be achieved.

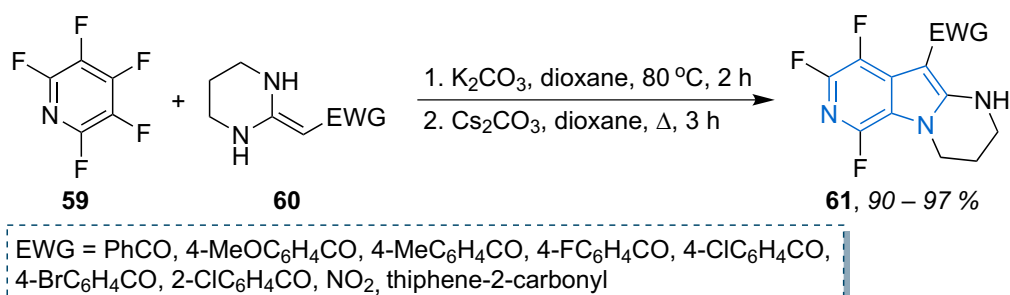
A one-pot, two-step method for synthesizing highly functionalized derivatives of 6-azaindole **61** was developed based on the nucleophilic aromatic substitution reaction of perfluoropyridine **59** with heterocyclic ketene aminals **60** promoted by two bases, K₂CO₃ and Cs₂CO₃ (**Scheme 18**) [35].

A convenient route for obtaining condensed derivatives of 6-azaindoles **63** and **64** is based on a simple four-step cascade sequence; its key stages are Cu-catalyzed coupling of boronic acids **62** with *di-tert*-butyl diazodicarboxylate (DBAD) and the Fischer indolization (**Scheme 19**) [36].

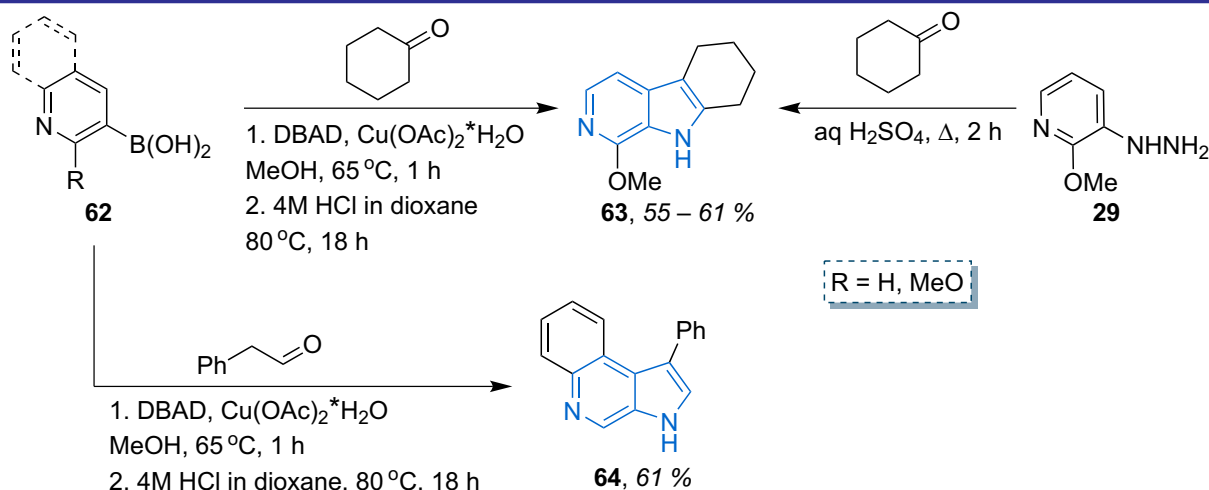
The interaction of 3-hydrazinyl-2-methoxypyridine **29** with cyclohexanone under the Fischer cyclization conditions was also effective for the annulation of the tricyclic system **63** (**Scheme 19**) [22].

An effective method for obtaining β -carboline **68** involved directed lithiation of 3-fluoropyridines **65** followed by zincation and the Negishi cross-coupling with 2-halogenanilines **66**, leading to the formation of 2-aminobiaryls **67**. Further treatment of derivatives **53** with an excess of NaHMDS facilitated the intramolecular aromatic substitution, yielding the target 9*H*-pyrido[3,4-*b*]indoles **68** (**Scheme 20**) [37].

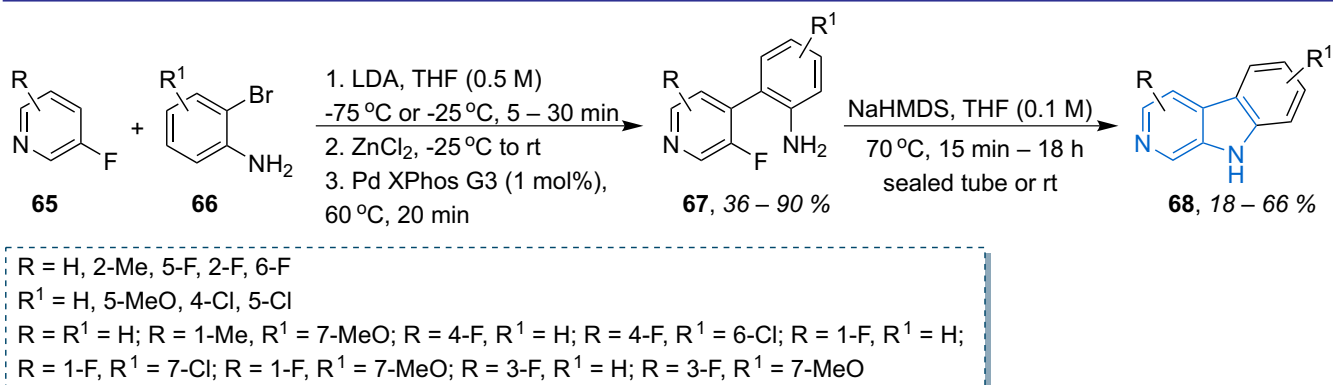
Another convenient approach to the synthesis of β -carboline **71** is based on a double C–N coupling catalyzed by copper of 3,4-dibromopyridine **69** with



Scheme 18. The method for the synthesis of annulated pyrrolo[2,3-c]pyridines with EWG in the pyrrole cycle



Scheme 19. The synthesis of condensed 6-azaindoles via the Cu-catalyzed coupling of boronic acids



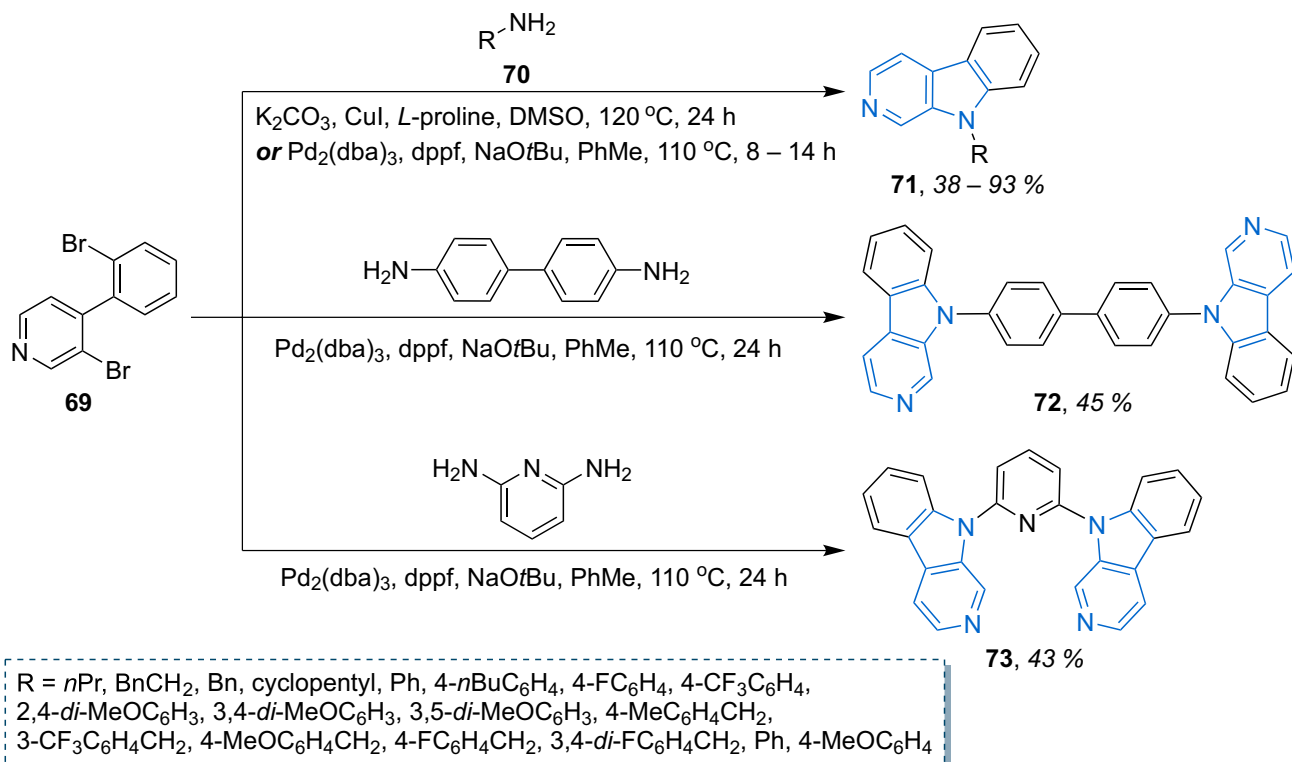
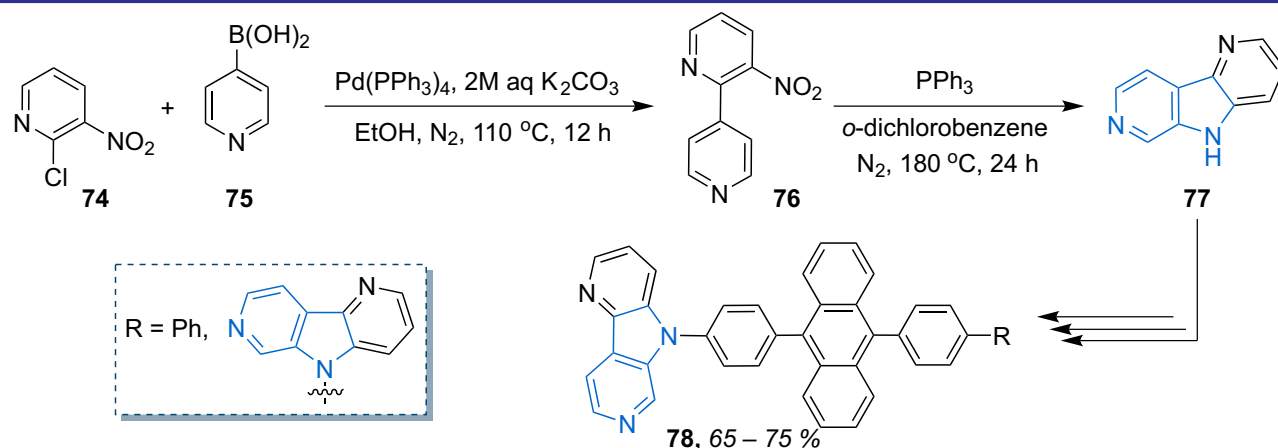
Scheme 20. An effective method for the synthesis of β -carbolines

a series of amines **70** (Scheme 21) [38]. In turn, the authors of work [39] successfully used the Pd-catalyzed *Buchwald-Hartwig* reaction to obtain β -carbolines **71**, and dicarbolines **72** and **73** (Scheme 21).

In work [40], the synthesis of a new electron-deficient 2,5-diazacarbazole (2,5-NCz) (**77**) was reported for the first time. The synthetic pathway involved the interaction of 2-chloro-3-nitropyridine (**74**) with boronic acid **75** and the cyclization of the resulting 3-nitro-2,4'-bipyridine (**76**) to 2,5-NCz (**77**). It is worth noting that compound **77** synthesized possesses a high level of the triplet energy $T_1 = 2.77$ eV and a potential

for creating organic electronic materials in the photoelectric field. Through structural modification of product **77**, two new materials for electron transport (ETM), *p*-S25NCzDPA and *p*-D25NCzDPA **78**, were developed and used to manufacture sky-blue fluorescent OLEDs (Scheme 22).

For the synthesis of pyrido[4',3':4,5]pyrrolo[2,3-*d*]pyrimidine derivatives **82**, among which a dual inhibitor of the FMS-like tyrosine kinase 3 (FLT3) and cyclin-dependent kinase 4 (CDK4) were identified, 5-(3-chloropyridin-4-yl)pyrimidine-2,4-diamine **81** was introduced into the *Buchwald-Hartwig* reaction. This compound was

Scheme 21. An alternative route to β -carbolines

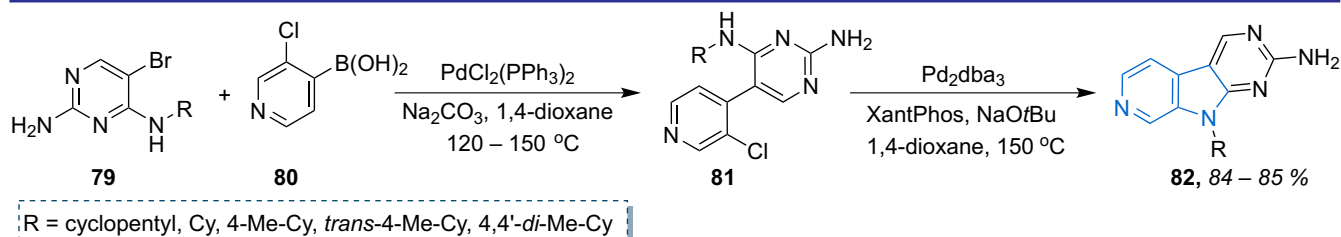
Scheme 22. The synthesis of new electron-deficient 2,5-diazacarbazole

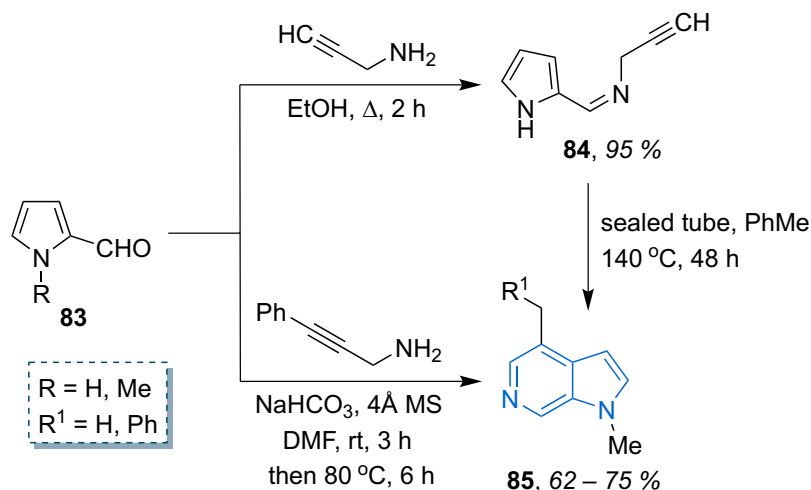
obtained by the *Negishi* cross-coupling of 5-bromopyrimidine-2,4-diamine **79** with boronic acid **80** (Scheme 23) [41].

2. Annulation of the pyridine nucleus to the pyrrole cycle

The next strategy for the synthesis of the pyrolopyridine core is through the annulation of the

pyridine nucleus onto the pyrrole cycle. In work [42] a regioselective approach to the synthesis of pyrrolo[2,3-*c*]pyridine **85** was demonstrated by interacting 1*H*-pyrrole-2-carbaldehydes **83** with propargylamine to form propargylimine **84**, the reaction of 6*π*-electrocyclization of which at high temperature gave the target product **85**

Scheme 23. The synthesis of pyrido[4',3':4,5]pyrrolo[2,3-*d*]pyrimidine derivatives



Scheme 24. A regioselective approach to pyrrolo[2,3-*c*]pyridines

(**Scheme 24**). Also, an effective variant B for obtaining 6-azaindole **85** was implemented by heating 1-methyl-1*H*-pyrrole-2-carbaldehyde **83** and phenylpropargylamine in the presence of molecular sieves (**Scheme 24**) [43].

A method for constructing highly functionalized 6-azaindoles **87** involved the iodine-mediated electrophilic cyclization of 2-alkynyl-1-methylene azides **86** (**Scheme 25**) [44].

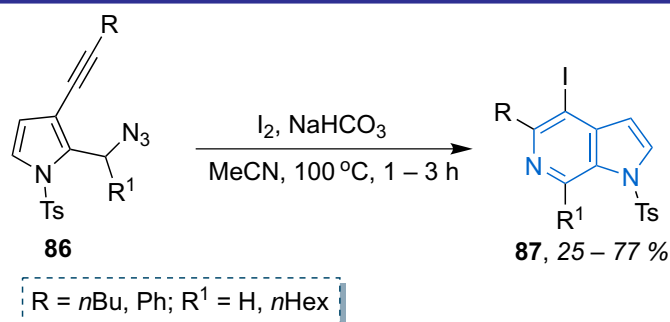
The intramolecular cyclization of the poly-substituted 6-azaindole **90** obtained from the reaction of ethyl 1*H*-pyrrole-3-carboxylate **88** and *N*-Ts-glycine **89** under LiHMDS treatment led to the highly functionalized pyrrolo[2,3-*c*]pyridine **91** (**Scheme 26**) [45].

The Ir(III)-catalyzed reaction of pyrroloxime **92** and α -diazocarbonyl derivative **93** proved to be effective for the synthesis of *N*-oxide pyrrolo-

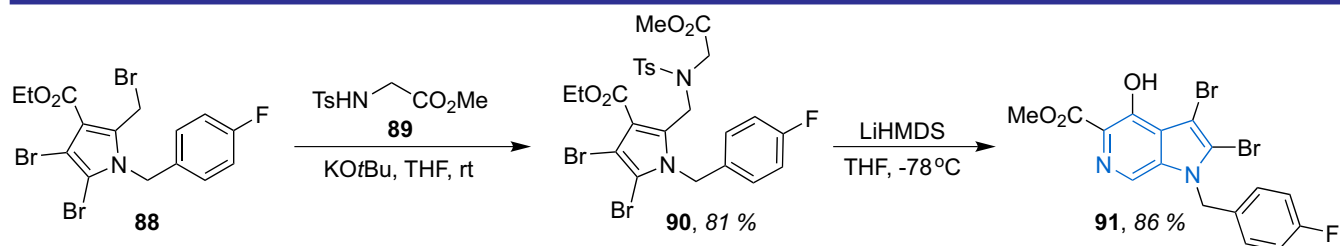
[2,3-*c*]pyridine **94**. It is worth noting that this represents a straightforward method for the synthesis of phosphorylated heterocycles, which are highly important in the organic synthesis and medicinal chemistry (**Scheme 27**) [46].

In terms of the synthesis of β -carboline derivatives through the annulation of the pyridine nucleus onto the pyrrole cycle, the *Pictet-Spengler* cyclization is one of the most common methods. The interaction of tryptamine or serotonin **95** with aldehydes in acetic acid led to the formation of tetrahydro- β -carbolines **96**; its structural modification yielded derivatives **97** and **98** – potential phosphodiesterase-4 inhibitors (**Scheme 28**) [47].

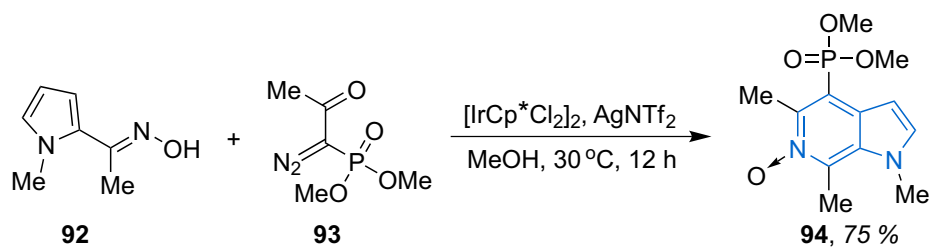
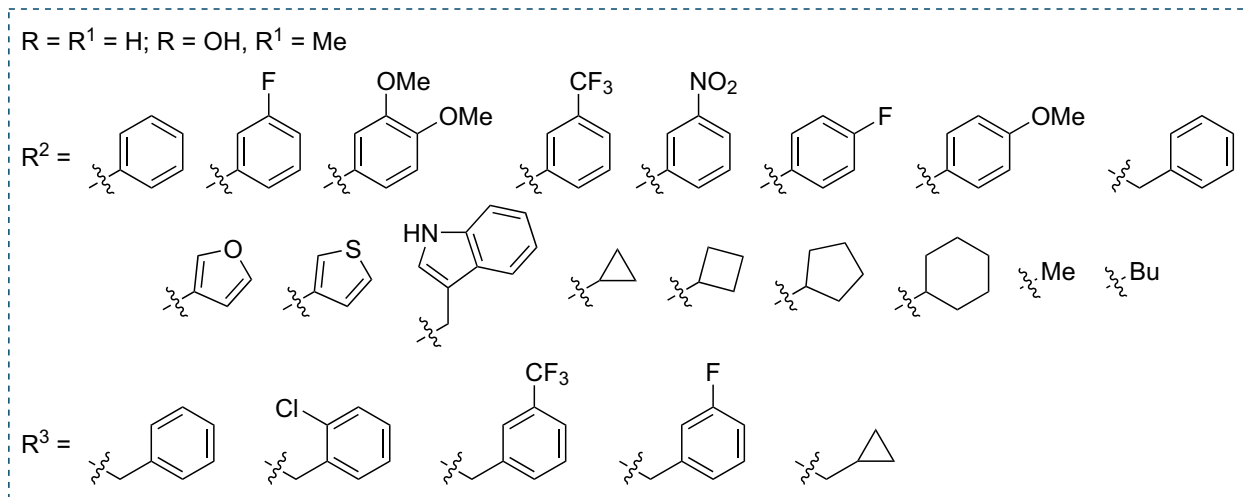
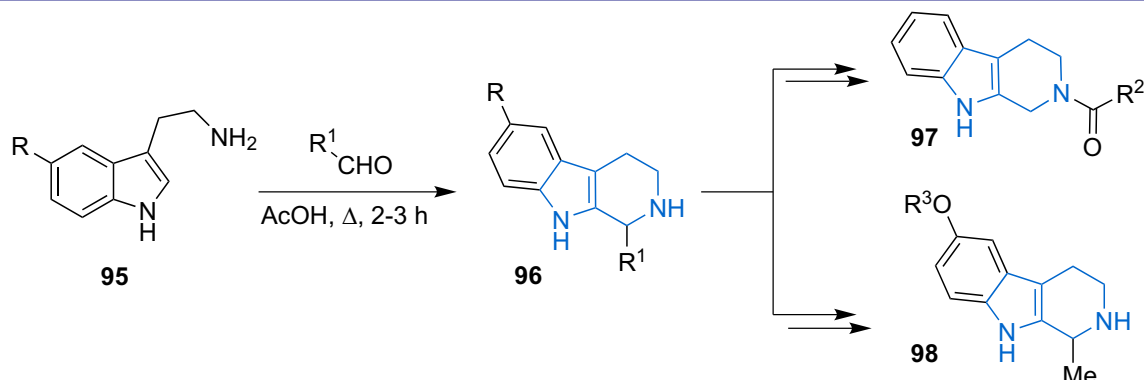
A series of tetrahydro- β -carbolines and methyl tetrahydropyrido[3,4-*b*]indole-3-carboxylates **100** synthesized from tryptamine or the methyl ester of tryptophan **99** and aldehydes were



Scheme 25. The method for obtaining highly functionalized 6-azaindoles



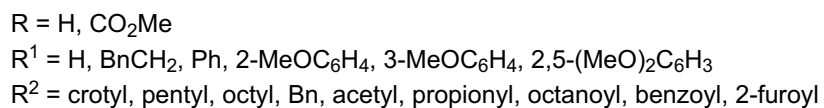
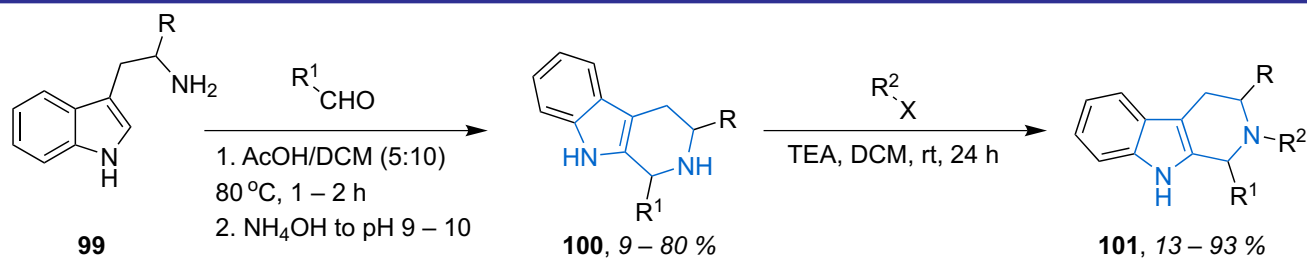
Scheme 26. Another approach to highly functionalized 6-azaindoles

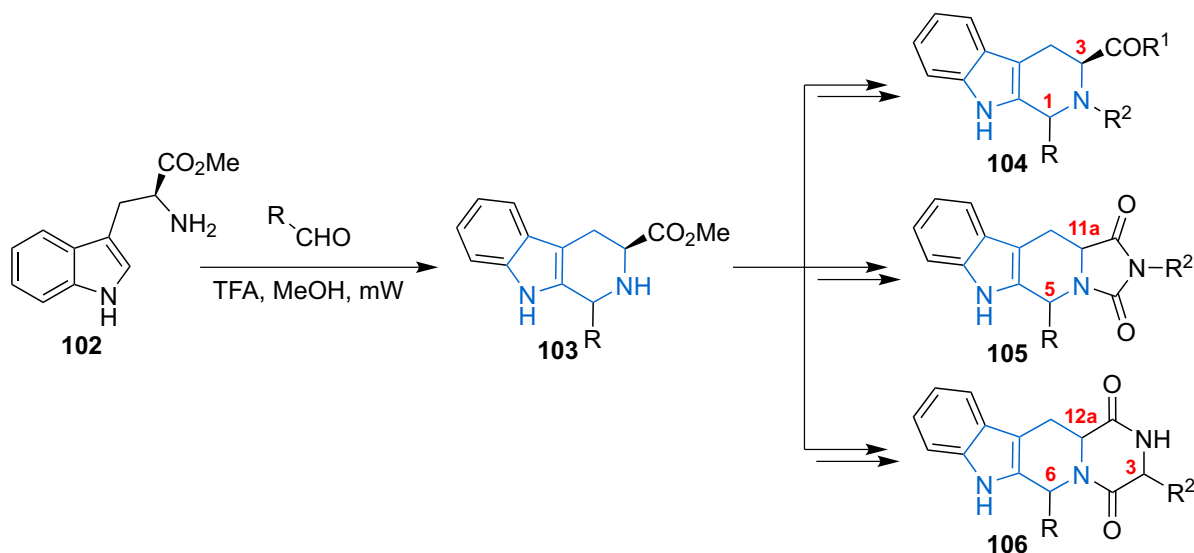

Scheme 27. The synthesis of pyrrolo[2,3-*c*]pyridine *N*-oxide

Scheme 28. The synthesis of β -carboline derivatives through the *Pictet-Spengler* cyclization

alkylated and acylated in position 2 to obtain potential antimicrobial agents **101** (**Scheme 29**) [48].

Tetrahydro- β -carbolines **103** were synthesized *via* a microwave-assisted version of the *Pictet-*

Spengler reaction from the methyl ester of tryptophan **102** and aldehydes in methanol in the presence of trifluoroacetic acid (TFA). The intermediate products **103** were transformed into the


Scheme 29. The synthesis of tetrahydro- β -carbolines



104: R, R¹, R²; Ph, OMe, Bn (1*R*,3*S*); Ph, OMe, Bn (1*S*,3*S*); H, NHCH₂(4-F)Ph, H (3*S*); *i*Bu, NHCH₂(4-F)Ph, H (1*R*,3*S*); *i*Bu, NHCH₂(4-F)Ph, H (1*S*,3*S*); CH₂CH₂CO₂Me, NHCH₂(4-F)Ph, H (1*R*,3*S*); CH₂CH₂CO₂Me, NHCH₂(4-F)Ph, H (1*S*,3*S*); CH₂CH₂CO₂H, NHCH₂(4-F)Ph, H (1*R*,3*S*); CH₂CH₂CO₂H, NHCH₂(4-F)Ph, H (1*S*,3*S*); H, OMe, COCH₂CH₂NH₂ (3*S*)

105, 106: R, R²; H, H (12*aS*); H, Bn (3*S*,12*aS*); H, Bn (3*S*,12*aS*); *i*Bu, Bn (3*S*,6*R*,12*aS*); *i*Bu, Bn (3*S*,6*S*,12*aS*); 4-Cl-C₆H₄, H (6*R*,12*aS*); 4-Cl-C₆H₄, H (6*S*,12*aS*); H, CH₂4-F-C₆H₄ (11*aS*); *i*Bu, CH₂4-OMe-C₆H₄ (5*R*,11*aS*); *i*Bu, CH₂4-OMe-C₆H₄ (5*S*,11*aR*); 4-Cl-C₆H₄, CH₂4-Me-C₆H₄ (5*R*,11*aS*); 4-Cl-C₆H₄, CH₂4-Me-C₆H₄ (5*S*,11*aR*); 4-Cl-C₆H₄, CH₂4-F-C₆H₄ (5*R*,11*aS*); 4-Cl-C₆H₄, CH₂4-Me-C₆H₄ (5*R*,11*aS*); 4-F-C₆H₄, Bn (5*R*,11*aS*); 4-F-C₆H₄, Bn (5*S*,11*aR*); 4-F-C₆H₄, (CH₂)₃NH₂ (5*R*,11*aS*); 4-F-C₆H₄, (CH₂)₃NH₂ (5*S*,11*aR*); 4-F-C₆H₄, 3-CF₃-C₆H₄ (5*R*,11*aS*); 4-F-C₆H₄, 3-CF₃-C₆H₄ (5*S*,11*aR*); 4-F-C₆H₄, 2-F-C₆H₄ (5*R*,11*aS*); 4-F-C₆H₄, 2-F-C₆H₄ (5*S*,11*aR*); 4-F-C₆H₄, 4-F-C₆H₄ (5*R*,11*aS*); 4-F-C₆H₄, 4-F-C₆H₄ (5*S*,11*aR*)

Scheme 30. The synthesis of tetrahydro- β -carbolines via the microwave-assisted Pictet-Spengler reaction

corresponding *N*-substituted tetrahydro- β -carbolines **104**, hydantoin **105**, and pyrazine **106** condensed derivatives (**Scheme 30**) [49].

The β -carboline derivatives **104–106** obtained were analyzed as potential analgesics and antagonists of TRPM8 binding sites (transient receptor potential melastatin 8 ion channel) [49].

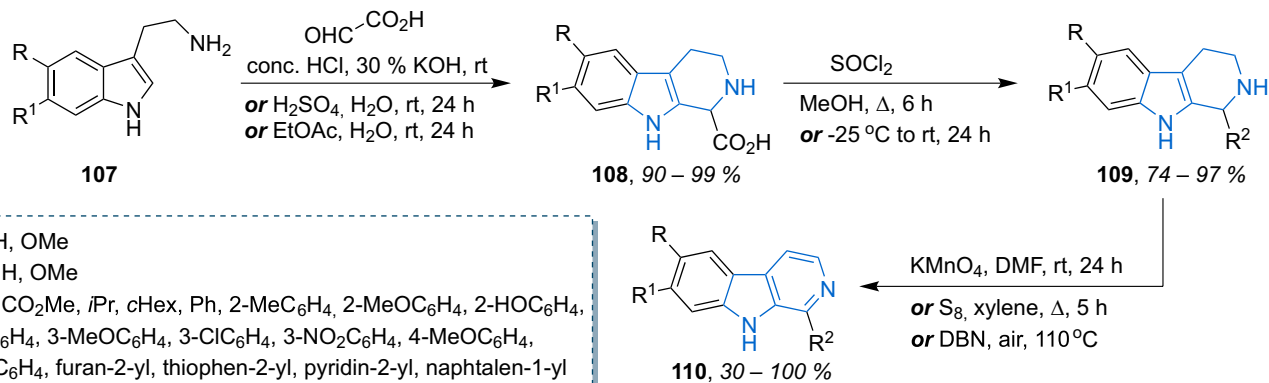
2,3,4,9-Tetrahydro-1*H*-pyrido[3,4-*b*]indole-1-carboxylic acids **108** were obtained by the reaction of tryptamines **107** with glyoxylic acid [50–52]. The subsequent esterification of acids **108** in the presence of thionyl chloride in methanol yielded methyl tetrahydropyrido[3,4-*b*]indole-1-carboxylates **109**; its aromatization with potassium permanganate or sulfur in refluxing xylene led to methyl 9*H*-pyrido[3,4-*b*]indole-1-carboxylates **110** (**Scheme 31**). Otherwise, the authors of [53] used DBN in the air to oxidize alkyl-, aryl-, and heteroaryl-substituted β -carbolines **109** (**Scheme 31**).

In a series of studies [54–58], a general approach to the synthesis of methyl 9*H*-pyrido[3,4-*b*]indole-3-carboxylates **114** is described. This approach includes the Pictet-Spengler reaction of tryptophan **111** and aldehydes **99**, esterification

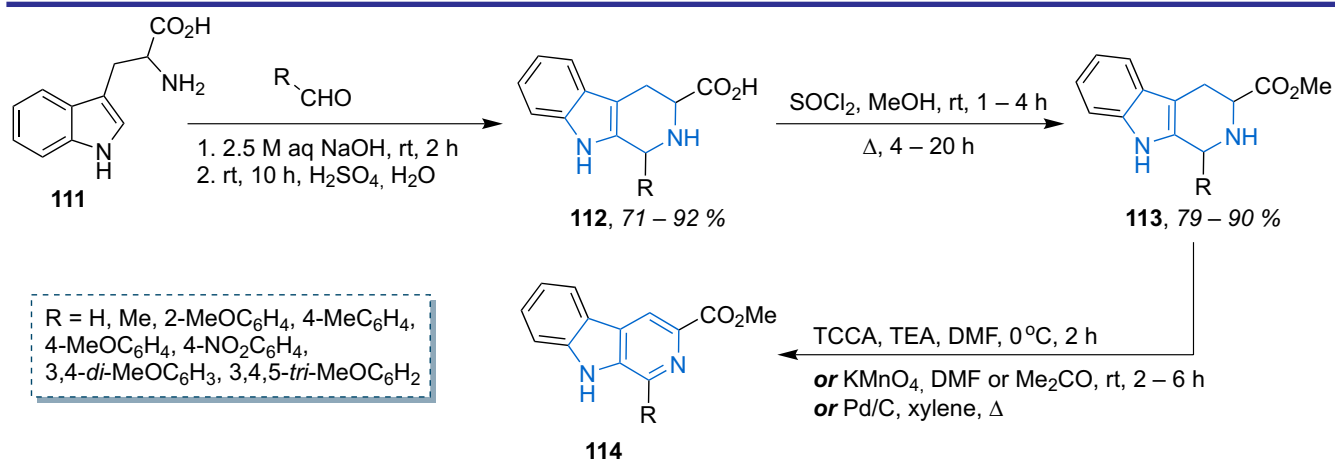
of acids **112**, and oxidation of tetrahydro- β -carbolines **113** (**Scheme 32**). A similar synthetic pathway was used to obtain (3*S*)-methyl-1*H*-pyrido[3,4-*b*]indole-3-carboxylates [59, 51].

On the other hand, the authors of study [60] initiated the construction of the β -carboline core **118** by esterifying *L*-tryptophan **115** with methanol in the presence of SOCl₂ to obtain hydrochloride **116**, which was subjected to the Mannich reaction with formaldehyde in an acidic media, yielding tetrahydro- β -carboline-3-carboxylate **117**. The oxidation of the latter with trichloroisocyanuric acid (TCCA) in DMF produced methyl 9*H*-pyrido[3,4-*b*]indole-3-carboxylate **118** (**Scheme 33**).

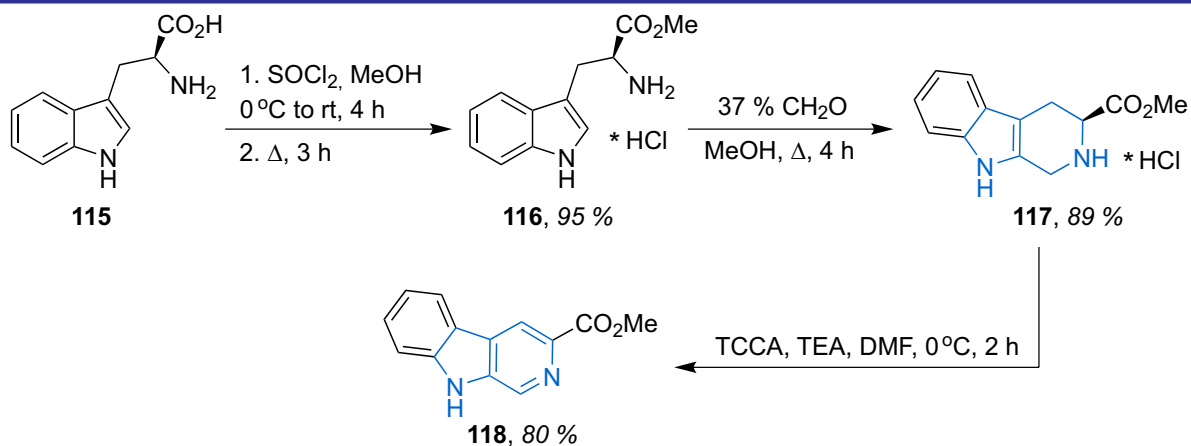
A one-pot method for the synthesis of β -carboline **121** was developed through the reaction of tryptamine **119** and pyridine-2-carboxaldehyde **120** in refluxing anisole followed by reduction with the Pd/C system (**Scheme 34**). It is noteworthy that the copper(II) complexes **122** based on 1-(pyridin-2-yl)-9*H*-pyrido[3,4-*b*]indole **121** were tested for the antitumor activity against myeloid leukemia 1 (Mcl-1) [61, 62].



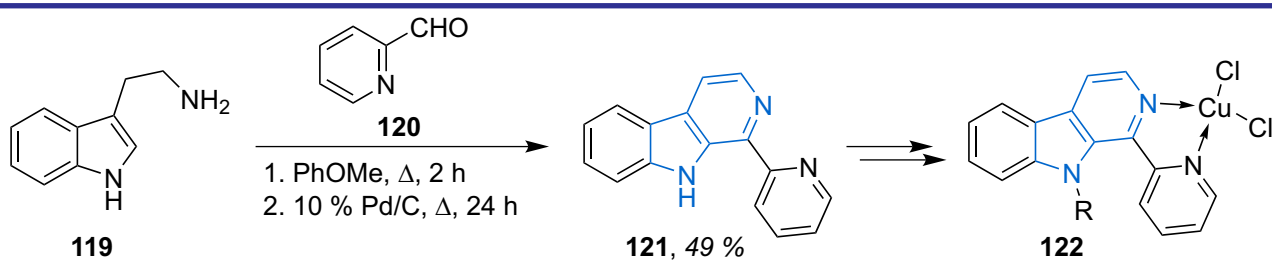
Scheme 31. The synthesis of tetrahydro-1*H*-pyrido[3,4-*b*]indole-1-carboxylic acids



Scheme 32. The approach to the synthesis of methyl 9*H*-pyrido[3,4-*b*]indole-3-carboxylates



Scheme 33. The synthesis of the β -carboline core through the Mannich reaction



Scheme 34. The one-pot method for the synthesis of β -carboline

The authors of work [63] developed a one-step method for synthesizing β -carboline derivatives **124** from substituted methyl ester of tryptophan **123** and aldehydes in a methylene chloride solution in the presence of catalytic amounts of TFA at room temperature, followed by further treatment of the reaction mixture with trichloroisocyanuric acid (Scheme 35).

The biomimetic approach is a convenient alternative to the methods involving the stepwise synthesis of β -carbolines. Treating a mixture of substituted tryptophan **125** and amino acids with molecular iodine and trifluoroacetic acid successively undergoes decarboxylation, deamination, the *Pictet-Spengler* reaction, and oxidation, resulting in the formation of target β -carbolines **127** (Scheme 36). In contrast, the reaction of tryptophan hydrochloride **126** leads to the formation of methyl 9*H*-pyrido[3,4-*b*]indole-3-carboxylate **127**. This indicates that the carboxylic group esterification in tryptophan blocks the decarboxylation, but does not impede other reactions in the process [64].

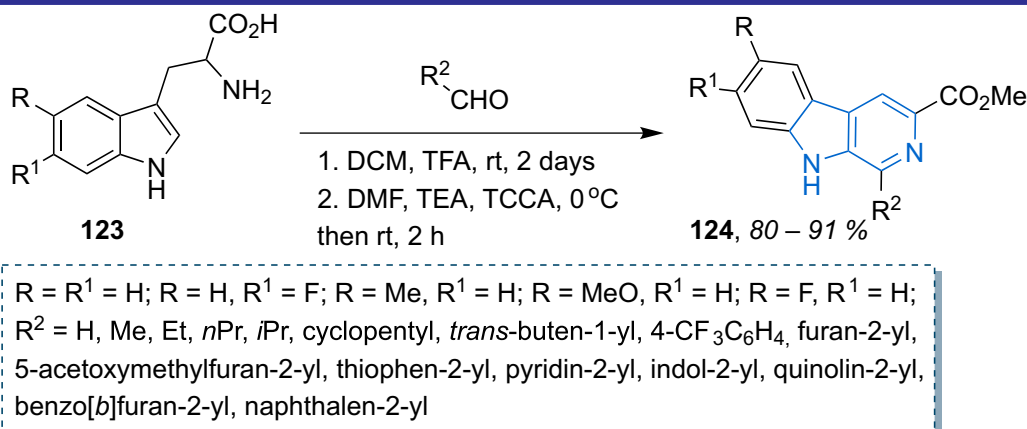
The oxidative cyclization mediated by tetrabutylammonium bromide (TBAB) proved to be an

effective method for obtaining β -carbolines **129** from readily available tryptophans **128** and aldehydes (Scheme 37) [65].

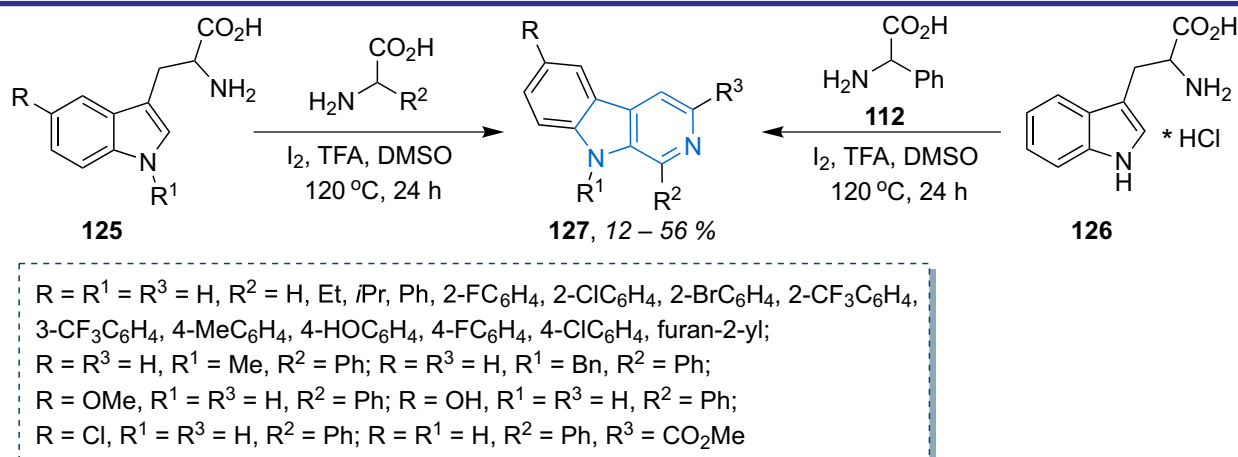
An efficient approach to the synthesis of β -carbolines **132**, **134** was implemented under metal-free conditions starting from heteroaromatic aldehydes **130**, propargylamines **131**, or but-3-yn-2-amines **133** (Scheme 38) [43].

The authors of study [66] successfully used a cascade *aza*-alkylation/*Michael* addition reaction sequence, exemplified by the interaction of functionalized enones **135** with α -bromoketones **136** to obtain diketoindoles **137**, which upon treatment with NH_4OAc in acetic acid yielded 1,3-disubstituted β -carbolines **138** (Scheme 39).

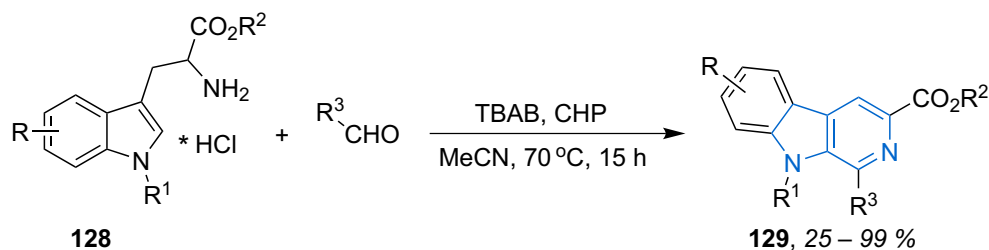
The conditions of the cascade reaction proved to be effective for the synthesis of ethyl 9*H*-pyrido[3,4-*b*]indole-3-carboxylate **143** as well. The required enone **141**, which was generated by the *Wittig* olefination of aldehyde **139** with phosphorane **140** in the subsequent one-pot process with 2-bromo-1-phenylethanone **142**, gave the target carboxylate **143** with the yield of 63 % (Scheme 40) [66].



Scheme 35. Another one-step method for synthesizing β -carboline derivatives



Scheme 36. The biomimetic approach to the synthesis of β -carbolines



R = R¹ = H, R² = Me, R³ = H, *n*Pr, Cy, Ph, 2-MeC₆H₄, 2-HOC₆H₄, 2-ClC₆H₄, 3-MeC₆H₄, 3-BrC₆H₄, 3-NCC₆H₄, 4-MeC₆H₄, 4-*i*PrC₆H₄, 4-MeOC₆H₄, 4-BnOC₆H₄, 4-FC₆H₄, 4-ClC₆H₄, 4-BrC₆H₄, 4-MeSC₆H₄, 4-MeSOC₆H₄, 4-NO₂C₆H₄, 4-HO₂CC₆H₄, 4-CF₃C₆H₄, 2,4-*di*-ClC₆H₃, 2-HO-6-BrC₆H₃, naphthalen-2-yl, thiophen-2-yl, quinol-2-yl;

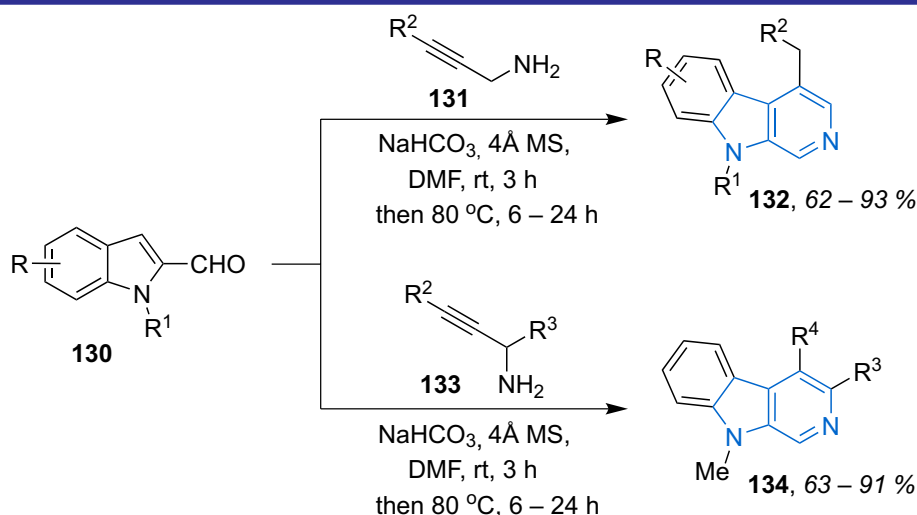
R = R¹ = H, R² = Et, R³ = Ph, 3-NCC₆H₄; R = R¹ = H, R² = OBn, R³ = Ph;

R = 6-Me, R¹ = H, R² = Me, R³ = Ph; R = 6-Br, R¹ = H, R² = OMe, R³ = Ph, 4-NO₂C₆H₄;

R = 6-CN, R¹ = H, R² = Me, R³ = 2-NO₂C₆H₄; R = 7-Cl, R¹ = H, R² = OMe, R³ = Ph, 4-NO₂C₆H₄;

R = H, R¹ = Me, R² = Me, R³ = Ph; R = H, R¹ = Me, R² = NH₂, R³ = Ph

Scheme 37. The synthesis of β -carbolines from readily available tryptophans and aldehydes



130: R = H, 5-MeO, 6-Me, 6-Br, 8-Me; R¹ = H, Me, Bn, Boc, Ph, Ts;

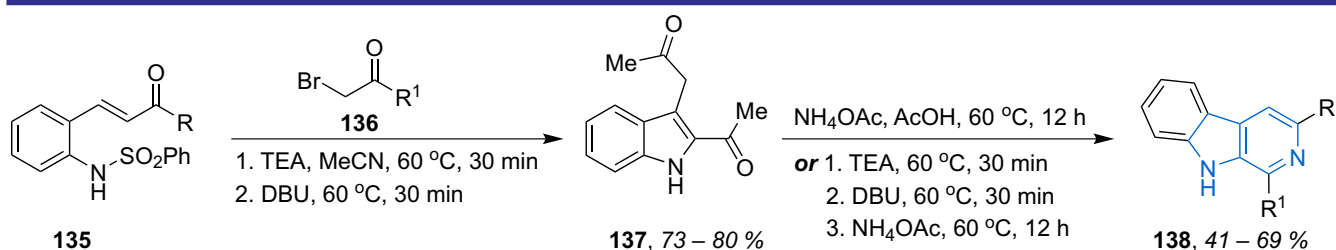
131: R² = H, Ph, 4-MeOC₆H₄, 4-NCC₆H₄, 4-NO₂C₆H₄, 4-AcC₆H₄,

4-CF₃C₆H₄, naphthalen-1-yl, thiophen-2-yl

130: R = H, R¹ = Me; **133**: R² = H, Ph, R³ = Me \rightarrow **134**: R³ = Me, R⁴ = Me

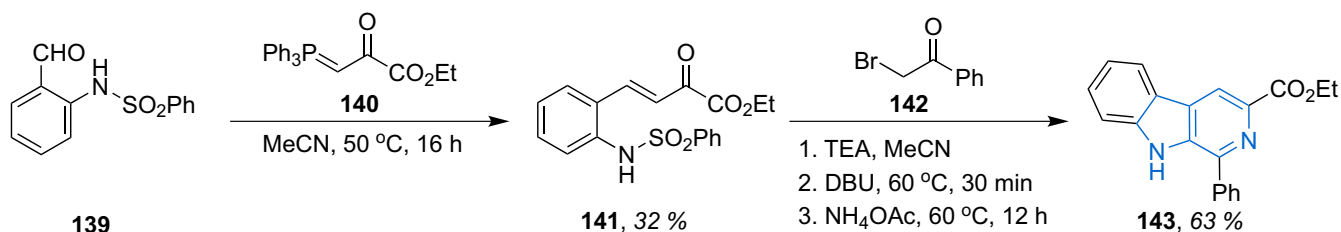
130: R = H, R¹ = Me; **133**: R² = CH₂Cl, R³ = H \rightarrow **134**: R³ = H, R⁴ = vinyl

Scheme 38. The synthesis of β -carbolines under metal-free conditions



R = Me, Et, Ph; R¹ = Me, Et, Ph

Scheme 39. The use of a cascade *aza*-alkylation/*Michael* addition reaction



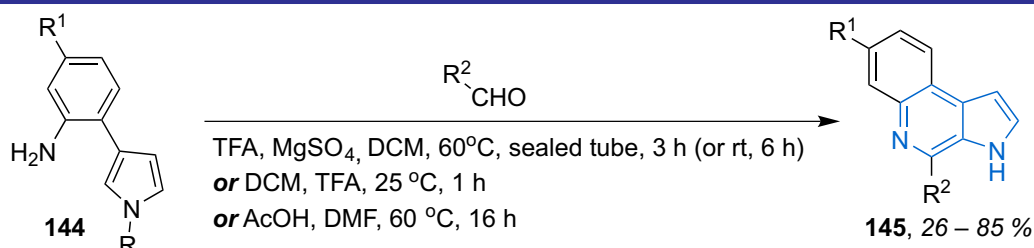
Scheme 40. The synthesis of ethyl 9H-pyrido[3,4-b]indole-3-carboxylate

The *Pictet-Spengler* reaction also serves as a general approach to the synthesis of marinoquinolines **145**. The interaction of substituted 2-(1*H*-pyrrole-3-yl)anilines **144** with a range of aliphatic, aromatic, and heteroaromatic aldehydes resulted in a library of 3*H*-pyrrolo[2,3-*c*]quinolines **145** (**Scheme 41**) [67–69].

2-(1*H*-Pyrrole-3-yl)anilines **146** have proven to be convenient substrates in the synthesis of pyrroloquinolines **149** through electrocyclization reactions. The interaction of the initial anilines with the pyrrol-3-yl fragment **146** with isocyanates in the DCM solution at room temperature yielded urea derivatives **147**. The treatment of these compounds with CBr_4 , PPh_3 , and TEA led to the formation of carbodiimides **148**. The subsequent deprotection of carbodiimides **148** with

tetrabutylammonium fluoride (TBAF) was accompanied by the electrocyclization reaction and the *in situ* formation of the desired marinoquinolines **149** (**Scheme 42**) [70].

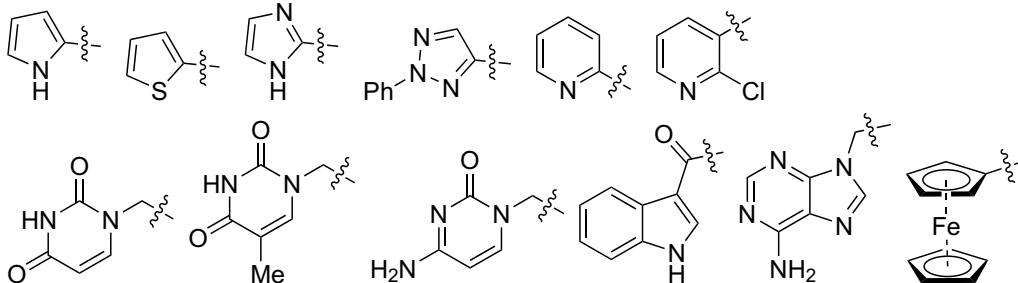
The authors of work [71] developed a Pd-catalyzed cyclization of imines **150** to create the 3*H*-pyrrolo[2,3-*c*]quinoline system **151**. It is a part of the natural antimalarial marine products apidopsamine A and marinoquinoline A. The base-induced deprotection of the phenylsulfonyl fragment from pyrroloquinoline **151** led to the formation of marinoquinoline A **152** with the yield of 96 %. For the synthesis of apidopsamine A **154**, the benzoyl peroxide (BPO) catalyzed bromination of pyrroloquinoline **151** was carried out using NBS to obtain bromide **153**. The reaction of the latter with 6-chloropurine in the DMF solution



R = H, TIPS

R¹ = H

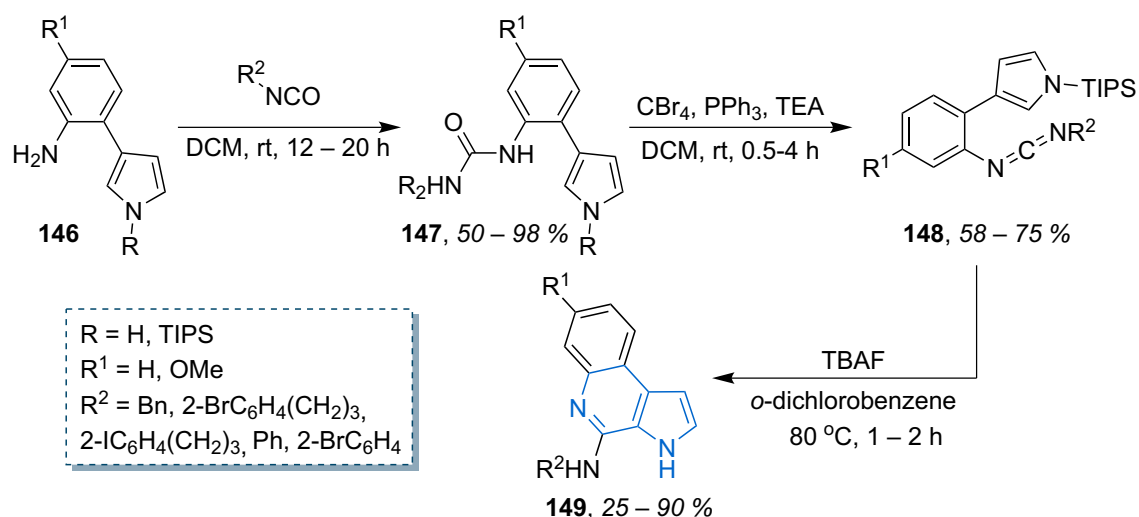
R² = Me, Et, *i*Bu, Bn, Ph, 4- $\text{H}_2\text{NC}_6\text{H}_4$, 4- $\text{Me}_2\text{NC}_6\text{H}_4$, 4- MeOC_6H_4 , 4- ClC_6H_4 , 4- BrC_6H_4 , 4- $\text{NO}_2\text{C}_6\text{H}_4$, 4- $\text{HO}_2\text{CC}_6\text{H}_4$, 4- $\text{MeO}_2\text{CC}_6\text{H}_4$, 4- $\text{F}_3\text{CC}_6\text{H}_4$, 3,5-*di*- MeOC_6H_3 , 3,4,5-*tri*- MeOC_6H_2 , indol-2-yl, indol-3-yl, 5-Br-indol-3-yl, 6-Br-indol-3-yl



R¹ = OMe, R² = Me, Et, *i*Bu, Bn, Ph, 4- $\text{NH}_2\text{C}_6\text{H}_4$, 4- $\text{NMe}_2\text{C}_6\text{H}_4$, 4- ClC_6H_4 , 4- $\text{NO}_2\text{C}_6\text{H}_4$, 4- $\text{HO}_2\text{CC}_6\text{H}_4$, 4- $\text{MeO}_2\text{CC}_6\text{H}_4$, 4- $\text{MeC(O)NHC}_6\text{H}_4$, 4-*t*BuCO₂NHC₆H₄, 3,5-*di*- MeOC_6H_3 , 3,4,5-*tri*- MeOC_6H_2 , indol-3-yl

R¹ = Br, R² = indol-3-yl

Scheme 41. The synthesis of marinoquinolines via the *Pictet-Spengler* reaction



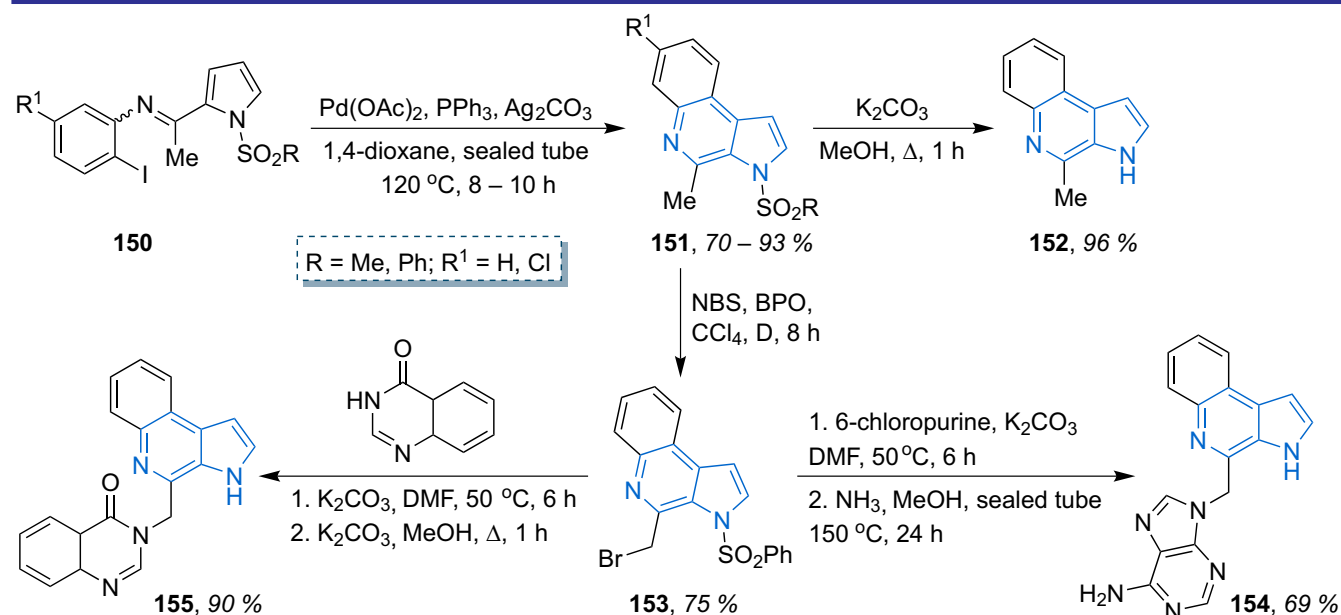
Scheme 42. Marinoquinolines from 2-(1H-pyrrol-3-yl)anilines

and the treatment of the intermediate with the saturated methanolic ammonia solution led to the formation of aplidopsamine A **154** with the yield of 69 %. Additionally, bromide **153** was used in the synthesis of the hybrid natural product analog NCLite-M1 **155** by the alkylation of quinoxalinone with bromomethylpyrroloquinoline **153** followed by the deprotection allowed for the production of NCLite-M1 **155** with the yield of 90 % (Scheme 43).

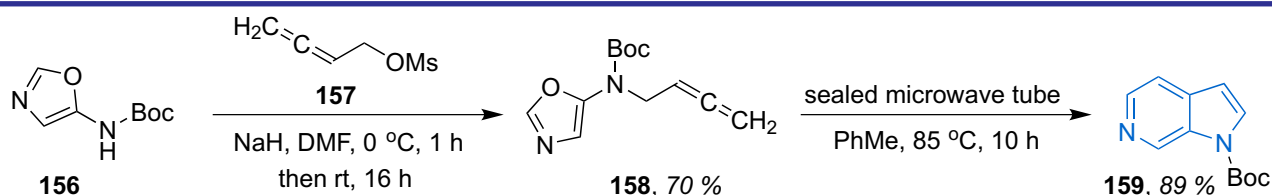
3. The synthesis of the 6-azaindole system with a single-step formation of pyrrole and pyridine rings

A new variant of constructing the 6-azaindole core **159** has been developed based on the intramolecular *Diels-Alder* cycloaddition of oxazole **156** obtained from the reaction of oxazole **156** with diene **157** (Scheme 44) [72].

The reaction of alkyne-allene isomerization of esters **162** *in situ* proved to be convenient for



Scheme 43. The Pd-catalyzed cyclization of imines for the synthesis of 3H-pyrrolo[2,3-c]quinolines

Scheme 44. The *Diels-Alder* reaction in the synthesis of the 6-azaindole core

the synthesis of ethyl pyrrolo[2,3-*c*]pyridine-4-carboxylates **163**. The Cu(I)-catalyzed interaction of alkyne **160** with ethyl diazoacetate **161** yielded the internal alkyne **162**; its further heating in the presence of TEA was accompanied by isomerization into an allene and a spontaneous formation of 6-azaindole-4-carboxylate **163** (Scheme 45) [72].

A one-pot synthesis of polycyclic systems containing the 6-azaindole fragment was carried out by the Pd-catalyzed *Sonogashira* coupling/intramolecular [2+2+2] cyclization. The reaction of *N*-alkynyl sulfonamide **164** with alkynyl nitriles **165** under cross-coupling conditions yielded di-*enyl* nitriles **166**, from which terminal alkynes **167** were obtained by removing the trimethylsilyl group. The Rh(I)-catalyzed cyclization of the latter led to the formation of the target pyrido[3,4-*b*]indoles **168** (Scheme 46) [73–75].

4. 6-Azaindoles of high MedChem importance

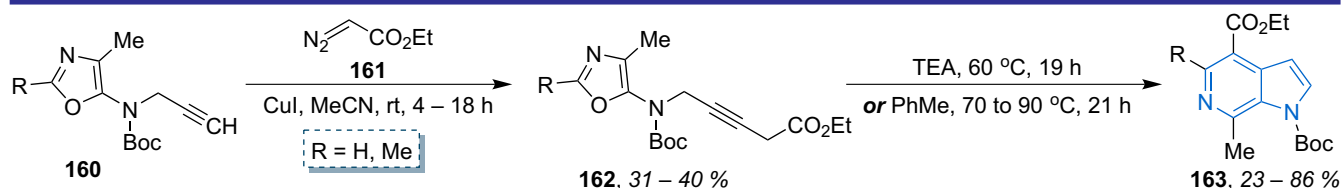
Pyrrolo[2,3-*c*]pyridines represent a significant class of heterocyclic compounds that exhibit a wide range of biological activities. Due to their structural similarity to natural alkaloids and their

ability to interact with various biological targets, these compounds have attracted considerable interest in medicinal chemistry and drug development. The key areas of the biological activity for pyrrolo[2,3-*c*]pyridines include the anticancer activity, antiviral properties, neuroprotective effects, anti-inflammatory and analgesic activities, anti-malarial activity, modulation of ion channels and receptors activity, etc.

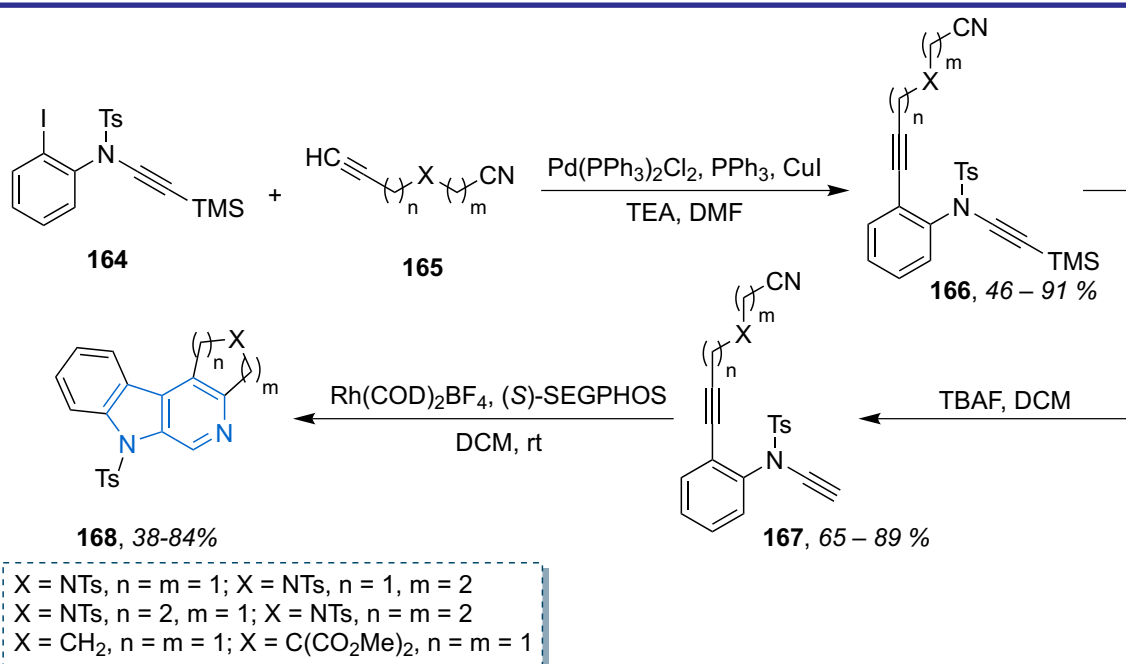
The 6-azaindole core is incorporated into the approved antiretroviral drug Fostemsavir **169** (Rukobia™) [76] and its prodrug Temsavir **170** (BMS-626529) [77] (Figure 1). They inhibit the attachment of the viral gp120 and prevent HIV entry. Both structures are widely used in the treatment of patients who have intolerance or resistance to other HIV/AIDS medications.

6-Azaindolyldmaleimide **171** (Figure 2) synthesized by the authors of [4] exhibits a high kinase selectivity toward oncogenesis-associated protein kinases VEGFR, FLT-3, and GSK-3β, demonstrating a potent inhibition of angiogenesis and cell proliferation.

Among the functionalized 6-methyl-1*H*-pyrrolo[2,3-*c*]pyridin-7(6*H*)-ones, bromodomain and



Scheme 45. The alkyne-allene isomerization and cyclization of esters **150**



Scheme 46. The preparation of 6-azaindoles through the Pd-catalyzed *Sonogashira* coupling/intramolecular [2+2+2] cyclization

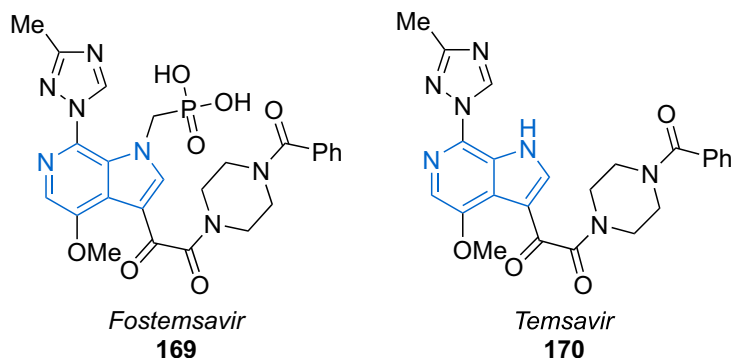
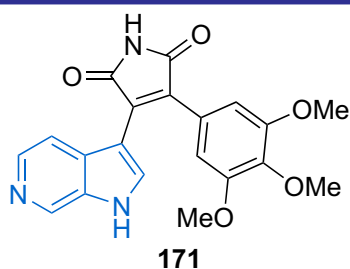


Figure 1. Antiretroviral drugs Fostemsavir and Temsavir



VEGFR-2: $IC_{50} = 48 \pm 3$ nM
FLT-3: $IC_{50} = 18 \pm 5$ nM
GSK-3b: $IC_{50} = 9 \pm 1$ nM

Figure 2. 6-Azaindolylmaleimide as a potential inhibitor of angiogenesis and cell proliferation

an extra-terminal domain (BET) inhibitor **172** (ABBV-075/mivebresib) were found. The latter is characterized by excellent pharmacokinetic properties and is currently undergoing phase I clinical trials [12]. Meanwhile, compound **173**

showed an excellent antiproliferative activity against the BxPC3 cell line, strongly induced the degradation of bromodomain-containing protein 4 (BRD4), and inhibited BRD4 BD1 [24] (**Figure 3**).

3-(2-Fluorophenyl)-*N*-phenyl-1*H*-pyrrolo[2,3-*c*]pyridine-7-amine **174** exhibited a high cytotoxic activity against prostate (PC-3) and colon (HCT116) cancer cell lines, and was found to be non-toxic to normal human fibroblast cells (WI-38) [10] (**Figure 4**).

Also, pyrrolo[2,3-*c*]pyridine core is a part of such β -carboline alkaloids as norharmane, harmane, eudistomin [78], trigonelline [79], aplidiopsamine A [80], and marinoquinolines [81]. The β -carboline structure is present in such synthetic drugs as Lefetamine **175**, which has antibiotic properties and antiproliferative action [82], and the anxiolytic drug Abecarnil **176** [83] (**Figure 5**).

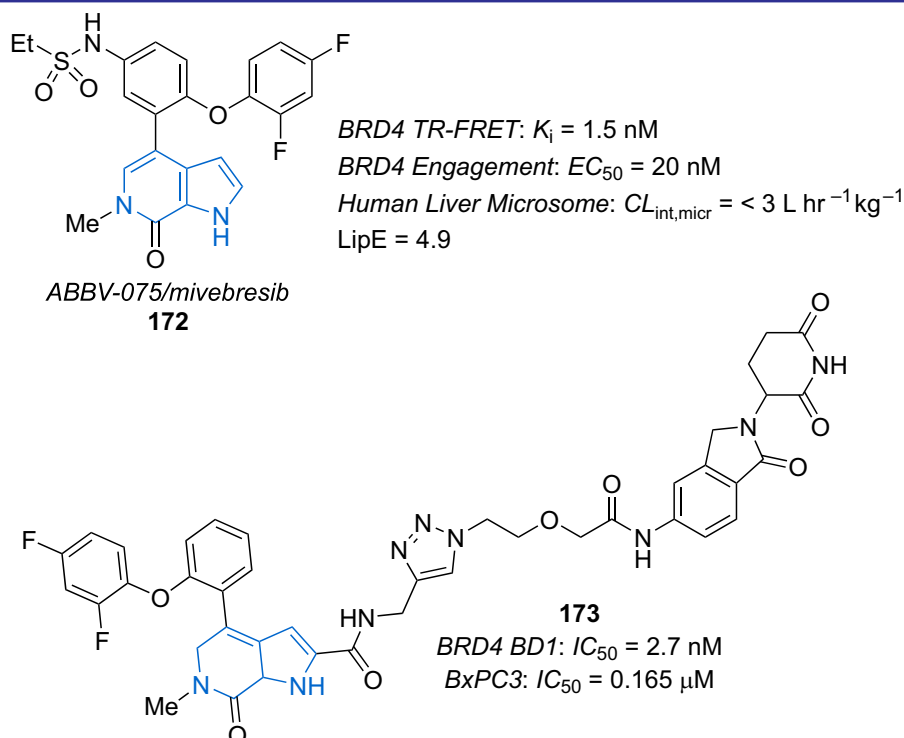


Figure 3. The 6-Azaindole core in BRD4 BD1 and BET inhibitors

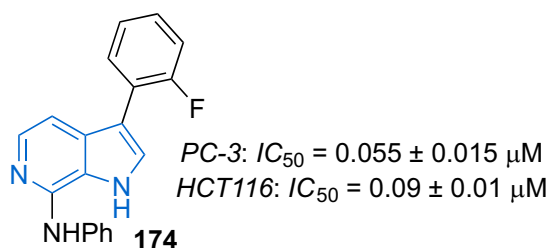


Figure 4. 3-(2-Fluorophenyl)-*N*-phenyl-1*H*-pyrrolo[2,3-*c*]pyridine-7-amine as a potential inhibitor of prostate (PC-3) and colon (HCT116) cancer cell lines

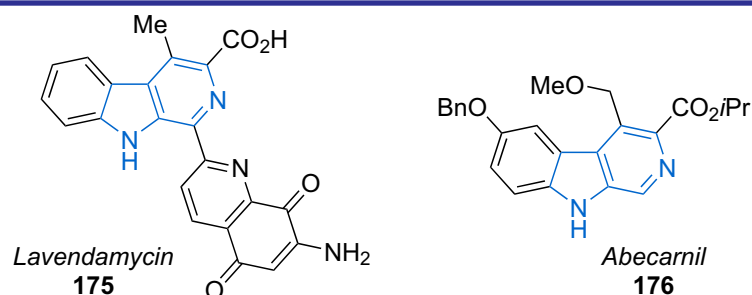


Figure 5. Lefetamine and the anxiolytic drug Abecarnil

1-Substituted β -carbolines have shown a significant fungi activity. Compound **177** is characterized by the high antifungal activity against *G. graminis*, while derivatives **178–180** are active against *B. cinerea* and *F. graminearum* [51] (**Figure 6**).

Tetrahydro- β -carbolines **169** and **170** demonstrated a good selectivity for inhibiting butyrylcholinesterase (BuChE), disaggregation of $A_{\beta 1-42}$, and an excellent neuroprotective activity by

alleviating damage induced by H_2O_2 , okadaic acid, and $A_{\beta 1-42}$, without cytotoxicity in SH-SY5Y cells. Thus, compounds **169** and **170** are potent multifunctional agents against Alzheimer's disease and can serve as promising lead candidates for further development [84] (**Figure 7**).

Compound **183** proved to be a potent, selective, and metabolically stable antagonist of the transient receptor potential melastatin 8 (TRPM8) ion channel (**Figure 8**). *In vivo*, **183** demonstrated

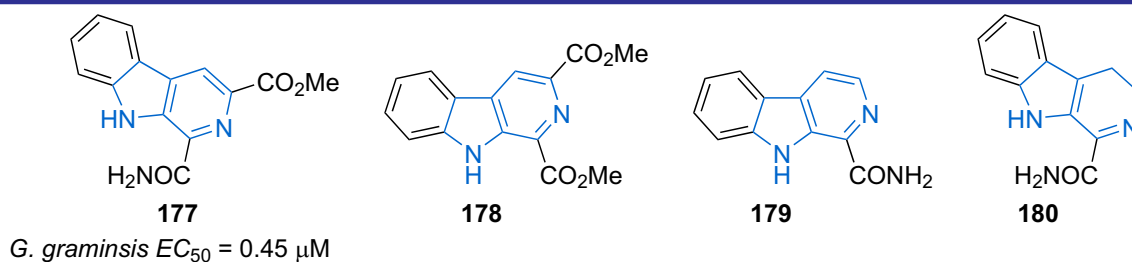


Figure 6. β -Carbolines with the fungicidal activity

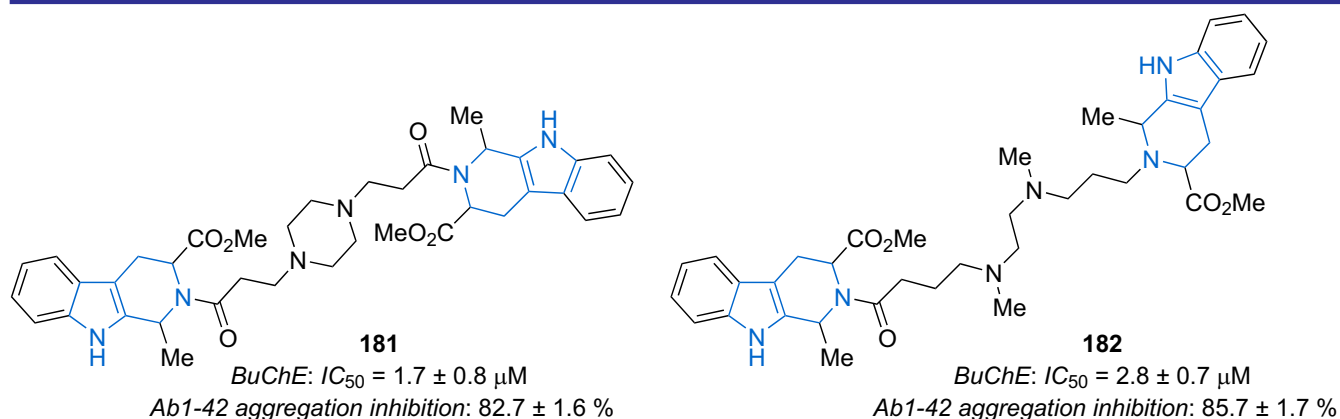


Figure 7. A promising lead candidate among 6-azaindoles against Alzheimer's diseases

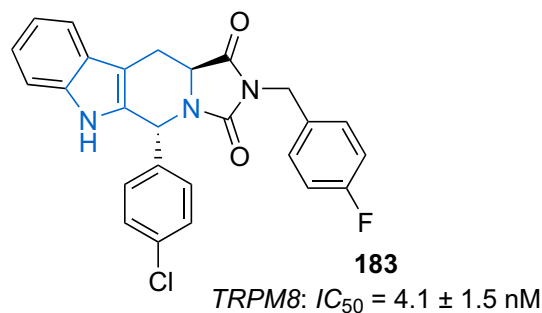


Figure 8. A metabolically stable antagonist of the TRPM8 ion channel

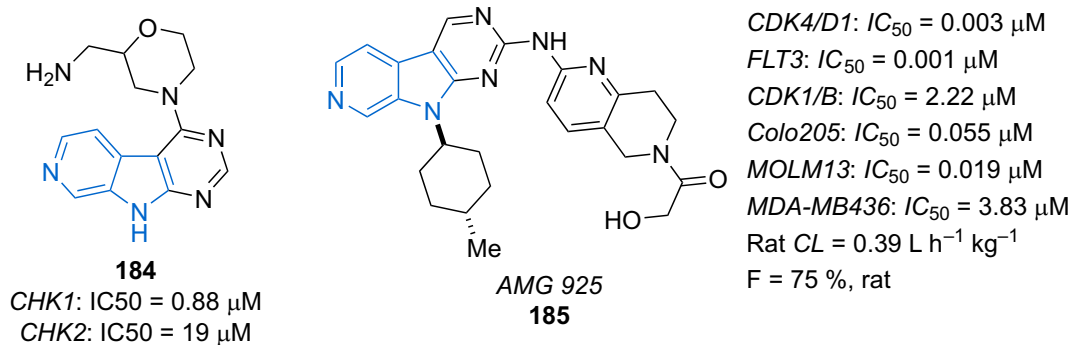


Figure 9. Pyrido[4',3':4,5]pyrrolo[2,3-d]pyrimidines and their pharmacokinetic profiles

a significant target coverage in murine models of icilin-induced wet dog shakes (WDS), cold allodynia induced by oxaliplatin, and thermal hyperalgesia induced by the chronic constriction injury (CCI). These results confirm the tryptophan moiety as a solid pharmacophore matrix for the development of high-potency modulators of the TRPM8-mediated activity [49].

A derivative of pyrido[4',3':4,5]pyrrolo[2,3-d]pyrimidine **184** was identified as an effective inhibitor of checkpoint kinases 1 and 2 (CHK1, CHK2) belonging to serine/threonine kinases and playing a central role in the mechanisms of the cellular regulation and DNA repair [41]. It is noteworthy that among compounds of this class of heterocycles, a potent and orally bioavailable dual inhibitor **185** (AMG 925) of cyclin-dependent kinase (CDK4) and tyrosine kinase (FLT3) was found. The derivative **185** inhibits the proliferation of a range of human tumor cell lines, including Colo205 (Rb+) and U937 (FLT3WT), induces cell death in MOLM13 (FLT3ITD), and even in MOLM13 (FLT3ITD, D835Y), which shows resistance to several FLT3 inhibitors. In well-tolerated doses, compound **185** leads to the significant inhibition of the growth of MOLM13 xenografts in mice, and the activity correlates with the inhibition of STAT5 and Rb phosphorylation [41] (**Figure 9**).

■ Conclusions

Thus, the analysis of the literature sources for the last 15 years has shown that the construction of the 6-azaindole core and its structural modification remains a topical issue in the organic synthesis and medicinal chemistry. Biologically, pyrrolo[2,3-c]pyridines have emerged as a significant class of compounds with a potent activity across the spectrum of targets. The elucidation of their mechanisms of action and the optimization of their pharmacokinetic profiles are still crucial for drug development. The identification of derivatives with activity against challenging targets, such as protein kinases and viral proteins underscores the potential of pyrrolo[2,3-c]pyridines in addressing unmet medical needs.

In this sense, the future of pyrrolo[2,3-c]pyridine study is promising, and we anticipate new discoveries that will further enrich our pharmacological arsenal and contribute to the advancement of medicinal chemistry. In particular, among the vast array of pharmacophores attached to the pyrrolo[2,3-c]pyridine framework, the promising trifluoromethyl group has been understudied, and we expect the results in the field will appear in the near future.

References

- Vitaku, E.; Smith, D. T.; Njardarson, J. T. Analysis of the Structural Diversity, Substitution Patterns, and Frequency of Nitrogen Heterocycles among U.S. FDA Approved Pharmaceuticals. *J. Med. Chem.* **2014**, *57* (22), 10257–10274. <https://doi.org/10.1021/jm501100b>.
- Popowycz, F.; Méroux, J.-Y.; Joseph, B. Synthesis and Reactivity of 4-, 5- and 6-azaindoles. *Tetrahedron* **2007**, *63* (36), 8689–8707. <https://doi.org/10.1016/j.tet.2007.05.078>.
- Blaazer, A. R.; Lange, J. H. M.; van der Neut, M. A. W.; Mulder, A.; den Boon, F. S.; Werkman, T. R.; Kruse, C. G.; Wadman, W. J. Novel Indole and Azaindole (Pyrrolopyridine) Cannabinoid (CB) Receptor Agonists: Design, Synthesis, Structure-Activity Relationships, Physicochemical Properties and Biological Activity. *Eur. J. Med. Chem.* **2011**, *46* (10), 5086–5098. <https://doi.org/10.1016/j.ejmech.2011.08.021>.
- Ganser, C.; Laueremann, E.; Maderer, A.; Stauder, T.; Kramb, J.-P.; Plutzki, S.; Kindler, T.; Moehler, M.; Dannhardt, G. Novel 3-Azaindoly-4-arylmaleimides Exhibiting Potent Antiangiogenic Efficacy, Protein Kinase Inhibition, and Antiproliferative Activity. *J. Med. Chem.* **2012**, *55* (22), 9531–9540. <https://doi.org/10.1021/jm301217c>.
- Lee, H.-Y.; Tsai, A.-C.; Chen, M.-C.; Shen, P.-J.; Cheng, Y.-C.; Kuo, C.-C.; Pan, S.-L.; Liu, Y.-M.; Liu, J.-F.; Yeh, T.-K.; Wang, J.-C.; Chang, C.-Y.; Chang, J.-Y.; Liou, J.-P. Azaindoly-sulfonamides, with a More Selective Inhibitory Effect on Histone Deacetylase 6 Activity, Exhibit Antitumor Activity in Colorectal Cancer HCT116 Cells. *J. Med. Chem.* **2014**, *57* (10), 4009–4022. <https://doi.org/10.1021/jm401899x>.
- Meuser, M. E.; Rashad, A. A.; Ozorowski, G.; Dick, A.; Ward, A. B.; Cocklin, S. Field-Based Affinity Optimization of a Novel Azabicyclohexane Scaffold HIV-1 Entry Inhibitor. *Molecules* **2019**, *24* (8), 1581. <https://doi.org/10.3390/molecules24081581>.
- Carbone, A.; Parrino, B.; Di Vita, G.; Attanzio, A.; Spanò, V.; Montalbano, A.; Barraja, P.; Tesoriere, L.; Livrea, M. A.; Diana, P.; Cirrincione, G. Synthesis and Antiproliferative Activity of Thiazolyl-bis-pyrrolo[2,3-b]pyridines and Indolyl-thiazolyl-pyrrolo[2,3-c]pyridines, Nortopsentin Analogues. *Mar. Drugs* **2015**, *13*(1), 460–492. <https://doi.org/10.3390/md13010460>.
- Plewe, M. B.; Butler, S. L.; Dress, K. R.; Hu, Q.; Johnson, T. W.; Kuehler, J. E.; Kuki, A.; Lam, H.; Liu, W.; Nowlin, D.; Peng, Q.; Rahavendran, S. V.; Tanis, S. P.; Tran, K. T.; Wang, H.; Yang, A.; Zhang, J. Azaindole Hydroxamic Acids are Potent HIV-1 Integrase Inhibitors. *J. Med. Chem.* **2009**, *52* (22), 7211–7219. <https://doi.org/10.1021/jm900862n>.
- Crawford, T. D.; Tsui, V.; Flynn, E. M.; Wang, S.; Taylor, A. M.; Côté, A.; Audia, J. E.; Beresini, M. H.; Burdick, D. J.; Cummings, R. T.; Dakin, L. A.; Duplessis, M.; Good, A. C.; Hewitt, M. C.; Huang, H.-R.; Jayaram, H.; Kiefer, J. R.; Jiang, Y.; Murray, J. M.; Nasveschuk, C. G.; Pardo, E.; Poy, F.; Romero, F. A.; Tang, Y.; Wang, J.; Xu, Z.; Zawadzke, L. E.; Zhu, X.; Albrecht, B. K.; Magnuson, S. R.; Bellon, S. F.; Cochran, A. G. Diving into the Water: Inducible Binding Conformations for BRD4, TAF1(2), BRD9, and CECR2 Bromodomains. *J. Med. Chem.* **2016**, *59* (11), 5391–5402. <https://doi.org/10.1021/acs.jmedchem.6b00264>.
- Dimitrakis, S.; Gavriil, E.-S.; Pousias, A.; Lougiakis, N.; Marakos, P.; Pouli, N.; Gioti, K.; Tenta, R. Novel Substituted Purine Isosteres: Synthesis, Structure-Activity Relationships and Cytotoxic Activity Evaluation. *Molecules* **2022**, *27* (1), 247. <https://doi.org/10.3390/molecules27010247>.
- Lougiakis, N.; Sakalis, N.; Georgiou, M.; Marakos, P.; Pouli, N.; Skaltsounis, A.-L.; Mavrogonatou, E.; Pratsinis, H.; Kletsas, D. Synthesis, cytotoxic activity evaluation and mechanistic investigation of novel 3,7-diarylsubstituted 6-azaindoles. *Eur. J. Med. Chem.* **2023**, *261*, 115804. <https://doi.org/10.1016/j.ejmech.2023.115804>.
- McDaniel, K. F.; Wang, L.; Soltwedel, T.; Fidanze, S. D.; Hasvold, L. A.; Liu, D.; Mantei, R. A.; Pratt, J. K.; Sheppard, G. S.; Bui, M. H.; Faivre, E. J.; Huang, X.; Li, L.; Lin, X.; Wang, R.; Warder, S. E.; Wilcox, D.; Albert, D. H.; Magoc, T. J.; Rajaraman, G.; Park, C. H.; Hutchins, C. W.; Shen, J. W.; Edalji, R. P.; Sun, C. C.; Martin, R.; Gao, W.; Wong, S.; Fang, G.; Elmore, S. W.; Shen, Y.; Kati, W. M. Discovery of N-(4-(2,4-Difluorophenoxy)-3-(6-methyl-7-oxo-6,7-dihydro-1H-pyrrolo[2,3-c]pyridin-4-yl)phenyl)ethanesulfonamide (ABBV-075/Mivebresib), a Potent and Orally Available Bromodomain and Extraterminal Domain (BET) Family Bromodomain Inhibitor. *J. Med. Chem.* **2017**, *60* (20), 8369–8384. <https://doi.org/10.1021/acs.jmedchem.7b00746>.
- Linz, S.; Müller, H.; Hübner, H.; Gmeiner, P.; Troschütz, R. Design, synthesis and dopamine D4 receptor binding activities of new N-heteroaromatic 5/6-ring Mannich bases. *Bioorg. Med. Chem.* **2009**, *17* (13), 4448–4458. <https://doi.org/10.1016/j.bmc.2009.05.015>.
- Arikawa, Y.; Hasuoka, A.; Hirase, K.; Inatomi, N.; Sato, F.; Hori, Y.; Takagi, T.; Tarui, N.; Kawamoto, M.; Kajino, M. Molecular Modeling, Design, Synthesis, and Biological Activity of 1H-Pyrrolo[2,3-c]pyridine-7-amine Derivatives as Potassium-Competitive Acid Blockers. *Chem. Pharm. Bull.* **2014**, *62* (4), 336–342. <https://doi.org/10.1248/cpb.c13-00878>.
- McDonald, I. M.; Mate, R.; Ng, A.; Park, H.; Olson, R. E. Novel Tricyclic Diamines 2. Synthesis of 1,7-Diazaisoadamantane, 1,5-Diazaisoadamantane and 1,6-Diazahomobrendane. *Tetrahedron Lett.* **2018**, *59*, 751–754. <https://doi.org/10.1016/j.tetlet.2018.01.028>.
- Song, J. J.; Tan, Z.; Gallou, F.; Xu, J.; Yee, N. K.; Senanayake, C. H. A Novel One-Step Synthesis of 2-Substituted 6-Azaindoles from 3-Amino-4-Picoline and Carboxylic Esters. *J. Org. Chem.* **2005**, *70* (16), 6512–6514. <https://doi.org/10.1021/jo0506480>.
- Fang, Y.-Q.; Yuen, J.; Lautens, M. A General Modular Method of Azaindole and Thienopyrrole Synthesis Via Pd-Catalyzed Tandem Couplings of gem-Dichloroolefins. *J. Org. Chem.* **2007**, *72* (14), 5152–5160. <https://doi.org/10.1021/jo070460b>.
- Gorugantula, S. P.; Carrero-Martínez, G. M.; Dantale, S. W.; Söderberg, B. C. G. Palladium-Catalyzed Reductive N-Heterocyclization of Alkenyl-Substituted Nitroarenes as a Viable Method for the Preparation of Bicyclic Pyrrolo-Fused Heteroaromatic Compounds. *Tetrahedron* **2010**, *66* (10), 1800–1805. <https://doi.org/10.1016/j.tet.2010.01.029>.
- Formenti, D.; Ferretti, F.; Ragaini, F. Synthesis of N-Heterocycles by Reductive Cyclization of Nitro Compounds Using Formate Esters as CO Surrogates. *ChemCatChem* **2018**, *10* (1), 148–152. <https://doi.org/10.1002/cctc.201701214>.
- Son, N. T.; Nguyen, T. A.; Blanco, M.; Ehlers, P.; Thuan, N. T.; Dang, T. T.; Langer, P. Synthesis of 5- and 6-Azaindoles by Sequential Site-Selective Palladium-Catalyzed C–C and C–N Coupling Reactions. *Synlett* **2020**, *31* (13), 1308–1312. <https://doi.org/10.1055/s-0040-1707853>.
- Xu, Z.; Hu, W.; Zhang, F.; Li, Q.; Lü, Z.; Zhang, L.; Jia, Y. Palladium-Catalyzed Indole and Azaindole Synthesis by Direct Annulation of Electron-Poor o-Chloroanilines and o-Chloroaminopyridines with Aldehydes. *Synthesis* **2008**, *24*, 3981–3987. <https://doi.org/10.1055/s-0028-1083225>.
- Jeanty, M.; Blu, J.; Suzenet, F.; Guillaumet, G. Synthesis of 4- and 6-Azaindoles via the Fischer Reaction. *Org. Lett.* **2009**, *11* (22), 5142–5145. <https://doi.org/10.1021/ol902139r>.
- Parrino, B.; Spanò, V.; Carbone, A.; Barraja, P.; Diana, P.; Cirrincione, G.; Montalbano, A. Synthesis of the New Ring System Bispyrido[4',3':4,5]pyrrolo[1,2-a:1',2'-d]pyrazine and Its Deaza Analogue. *Molecules* **2014**, *19* (9), 13342–13357. <https://doi.org/10.3390/molecules190913342>.
- Zhang, J.; Chen, P.; Zhu, P.; Zheng, P.; Wang, T.; Wang, L.; Xu, C.; Zhou, J.; Zhang, H. Development of Small-Molecule BRD4 Degraders Based on Pyrrolopyridone Derivative. *Bioorg. Chem.* **2020**, *99*, 103817. <https://doi.org/10.1016/j.bioorg.2020.103817>.
- Sheppard, G. S.; Wang, L.; Fidanze, S. D.; Hasvold, L. A.; Liu, D.; Pratt, J. K.; Park, C. H.; Longenecker, K.; Qiu, W.; Torrent, M.; Kovar, P. J.; Bui, M.; Faivre, E.; Huang, X.; Lin, X.; Wilcox, D.; Zhang, L.; Shen, Y.; Albert, D. H.; Magoc, T. J.; Rajaraman, G.; Kati, W. M.; McDaniel, K. F. Discovery of N-Ethyl-4-[2-(4-fluoro-2,6-dimethyl-phenoxy)-5-(1-hydroxy-1-methyl-ethyl)phenyl]-6-methyl-7-oxo-1H-pyrrolo[2,3-c]pyridine-2-carboxamide (ABBV-744), a BET Bromodomain Inhibitor with Selectivity for the Second Bromodomain. *J. Med. Chem.* **2020**, *63* (10), 5585–5623. <https://doi.org/10.1021/acs.jmedchem.0c00628>.

26. Tzvetkov, N. T.; Müller, C. E. Facile Synthesis of 5-Amino- and 7-Amino-6-Azaoxindole Derivatives. *Tetrahedron Lett.* **2012**, *53* (42), 5597–5601. <https://doi.org/10.1016/j.tetlet.2012.07.140>.
27. Tzvetkov, N. T.; Müller, C. E. A Simple Approach to Multifunctionalized N1-Alkylated 7-Amino-6-azaoxindole Derivatives Using Their in Situ Stabilized Tautomer Form. *Tetrahedron* **2016**, *72* (41), 6455–6466. <https://doi.org/10.1016/j.tet.2016.08.055>.
28. Veselovská, L.; Kudlová, N.; Gurská, S.; Lišková, B.; Medvedíková, M.; Hodek, O.; Tloušťová, E.; Milisavljevic, N.; Tichý, M.; Perlíková, P.; Mertlíková-Kaiserová, H.; Trylčová, J.; Pohl, R.; Klepetářová, B.; Džubák, P.; Hajdúch, M.; Hocek, M. Synthesis and Cytotoxic and Antiviral Activity Profiling of All-Four Isomeric Series of Pyrido-Fused 7-Deazapurine Ribonucleosides. *Chem. – Eur. J.* **2020**, *26* (57), 13002–13015. <https://doi.org/10.1002/chem.202001124>.
29. Reader, J. C.; Matthews, T. P.; Klair, S.; Cheung, K.-M.; Scanlon, J.; Proisy, N.; Addison, G.; Ellard, J.; Piton, N.; Taylor, S.; Cherry, M.; Fisher, M.; Boxall, K.; Burns, S.; Walton, M. I.; Westwood, I. M.; Hayes, A.; Eve, P.; Valenti, M.; de Haven Brandon, A.; Box, G.; van Montfort, R. L. M.; Williams, D. H.; Aherne, G. W.; Raynaud, F. I.; Eccles, S. A.; Garrett, M. D.; Collins, I. Structure-Guided Evolution of Potent and Selective CHK1 Inhibitors through Scaffold Morphing. *J. Med. Chem.* **2011**, *54* (24), 8328–8342. <https://doi.org/10.1021/jm2007326>.
30. Söderberg, B. C. G.; Banini, S. R.; Turner, M. R.; Minter, A. R.; Arrington, A. K. Palladium-Catalyzed Synthesis of 3-Indolecarboxylic Acid Derivatives. *Synthesis* **2008**, *6*, 903–912. <https://doi.org/10.1055/s-2008-1032208>.
31. Walewska-Królikiewicz, M.; Wilk, B.; Kwast, A.; Wróbel, Z. Two-step, regioselective, multigram-scale synthesis of 2-(trifluoromethyl)indoles from 2-nitrotoluenes. *Tetrahedron Lett.* **2021**, *86*, 153515. <https://doi.org/10.1016/j.tetlet.2021.153515>.
32. Ivonin, S. P.; Yurchenko, A. A.; Voloshchuk, V. V.; Yurchenko, S. A.; Rusanov, E. B.; Pirozhenko, V. V.; Volochnyuk, D. M.; Kostyuk, A. N. A convenient approach to 3-trifluoromethyl-6-azaindoles. *J. Fluorine Chem.* **2020**, *233*, 109509. <https://doi.org/10.1016/j.jfluchem.2020.109509>.
33. Ivonin, S.; Voloshchuk, V.; Stepanova, D.; Ryabukhin, S.; Volochnyuk, D. Synthesis of 3-Formyl-6-Azaindoles via Vilsmeier-Haack Formylation of 3-Amino-4-Methyl Pyridines. *ChemRxiv* **2024**. <https://doi.org/10.26434/chemrxiv-2024-4ps8d>.
34. Ivonin, S. P.; Voloshchuk, V. V.; Rusanov, E. B.; Suikov, S.; Ryabukhin, S. V.; Volochnyuk, D. M. Synthesis of 6-azaindoles via formal electrophilic [4+1]-cyclization of 3-amino-4-methyl pyridines: new frontiers of diversity. *Organic Chemistry Frontiers* **2024**, *11* (7), 2088–2094. <https://doi.org/10.1039/D3Q001937C>.
35. Luo, D.-Y.; Hu, X.-M.; Huang, R.; Cui, S.-S.; Yan, S.-J. Base-Promoted Relay Reaction of Heterocyclic Ketene Aminals with o-Difluorobenzene Derivatives for the Highly Site-Selective Synthesis of Functionalized Indoles. *Tetrahedron* **2021**, *92*, 132275. <https://doi.org/10.1016/j.tet.2021.132275>.
36. Beveridge, R. E.; Gerstenberger, B. S. A Direct Copper-Catalyzed Route to Pyrrolo-Fused Heterocycles from Boronic Acids. *Tetrahedron Lett.* **2012**, *53* (5), 564–569. <https://doi.org/10.1016/j.tetlet.2011.11.091>.
37. Sathiyalingam, S.; Roesner, S. Synthesis of α - and β -Carbolines by a Metalation/Negishi Cross-Coupling/SNAr Reaction Sequence. *Adv. Synth. Catal.* **2022**, *364* (10), 1769–1774. <https://doi.org/10.1002/adsc.202200127>.
38. Van Phuc, B.; Do, H. N.; Quan, N. M.; Tuan, N. N.; An, N. Q.; Van Tuyen, N.; Anh, H. L. T.; Hung, T. Q.; Dang, T. T.; Langer, P. Copper-Catalyzed Synthesis of β - and δ -Carbolines by Double N-Arylation of Primary Amines. *Synlett* **2021**, *32* (10), 1004–1008. <https://doi.org/10.1055/s-0040-1720461>.
39. Hung, T. Q.; Hieu, D. T.; Tinh, D. V.; Do, H. N.; Nguyen Tien, T. A.; Do, D. V.; Son, L. T.; Tran, N. H.; Tuyen, N. V.; Tan, V. M.; Ehlers, P.; Dang, T. T.; Langer, P. Efficient Access to β - and γ -Carbolines from a Common Starting Material by Sequential Site-Selective Pd-Catalyzed C–C, C–N Coupling Reactions. *Tetrahedron* **2019**, *75* (40), 130569. <https://doi.org/10.1016/j.tet.2019.130569>.
40. Ye, S.; Guo, R.; Wang, Y.; Duan, Y.; Wang, L. Exploiting Novel Electron-Deficient Moiety 2,5-Diazarcarbazole to Functionally Construct DPA-Containing Electron Transporting Materials for Highly Efficient Sky-Blue Fluorescent OLEDs. *Dyes Pigm.* **2021**, *185*, 108935. <https://doi.org/10.1016/j.dyepig.2020.108935>.
41. Li, Z.; Wang, X.; Eksterowicz, J.; Gribble, M. W., Jr.; Alba, G. Q.; Ayres, M.; Carlson, T. J.; Chen, A.; Chen, X.; Cho, R.; Connors, R. V.; DeGraffenreid, M.; Deignan, J. T.; Duquette, J.; Fan, P.; Fisher, B.; Fu, J.; Huard, J. N.; Kaizerman, J.; Keegan, K. S.; Li, C.; Li, K.; Li, Y.; Liang, L.; Liu, W.; Lively, S. E.; Lo, M.-C.; Ma, J.; McMinn, D. L.; Mihalic, J. T.; Modi, K.; Ngo, R.; Pattabiraman, K.; Piper, D. E.; Queva, C.; Ragains, M. L.; Suchomel, J.; Thibault, S.; Walker, N.; Wang, X.; Wang, Z.; Wanska, M.; Weidner, M. F.; Zhang, A. J.; Zhao, X.; Kamb, A.; Wickramasinghe, D.; Dai, K.; McGee, L. R.; Medina, J. C. Discovery of AMG 925, a FLT3 and CDK4 Dual Kinase Inhibitor with Preferential Affinity for the Activated State of FLT3. *J. Med. Chem.* **2014**, *57* (8), 3430–3449. <https://doi.org/10.1021/jm500118j>.
42. Şendil, K.; Keskin, S.; Balci, M. Concise Design and Synthesis of Pyridine-Fused Heterocycles via 6π -Azaelectrocyclization Process of Iminoalkyne Derivatives. *Tetrahedron* **2019**, *75* (46), 130660. <https://doi.org/10.1016/j.tet.2019.130660>.
43. Uredi, D.; Motati, D. R.; Watkins, E. B. A Unified Strategy for the Synthesis of β -Carbolines, γ -Carbolines, and Other Fused Azaheteroaromatics under Mild, Metal-Free Conditions. *Org. Lett.* **2018**, *20* (20), 6336–6339. <https://doi.org/10.1021/acs.orglett.8b02441>.
44. Fischer, D.; Tomeba, H.; Pahadi, N. K.; Patil, N. T.; Huo, Z.; Yamamoto, Y. Iodine-Mediated Electrophilic Cyclization of 2-Alkynyl-1-methylene Azide Aromatics Leading to Highly Substituted Isoquinolines and Its Application to the Synthesis of Norchelerythrine. *J. Am. Chem. Soc.* **2008**, *130* (46), 15720–15725. <https://doi.org/10.1021/ja805326f>.
45. Johnson, T. W.; Tanis, S. P.; Butler, S. L.; Dalvie, D.; DeLisle, D. M.; Dress, K. R.; Flahive, E. J.; Hu, Q.; Kuehler, J. E.; Kuki, A.; Liu, W.; McClellan, G. A.; Peng, Q.; Plewe, M. B.; Richardson, P. F.; Smith, G. L.; Solowiej, J.; Tran, K. T.; Wang, H.; Yu, X.; Zhang, J.; Zhu, H. Design and Synthesis of Novel N-Hydroxy-Dihydronaphthyridinones as Potent and Orally Bioavailable HIV-1 Integrase Inhibitors. *J. Med. Chem.* **2011**, *54* (9), 3393–3417. <https://doi.org/10.1021/jm200208d>.
46. Phatake, R. S.; Patel, P.; Ramana, C. V. Ir(III)-Catalyzed Synthesis of Isoquinoline N-Oxides from Aryloxime and α -Diazocarbonyl Compounds. *Org. Lett.* **2016**, *18* (2), 292–295. <https://doi.org/10.1021/acs.orglett.5b03462>.
47. Abdelwaly, A.; Salama, I.; Gomaa, M. S.; Helal, M. A. Discovery of Tetrahydro- β -Carboline Derivatives as a New Class of Phosphodiesterase 4 Inhibitors. *Med. Chem. Res.* **2017**, *26* (12), 3173–3187. <https://doi.org/10.1007/s00044-017-2011-x>.
48. Buaban, K.; Phutdhawong, W.; Taechowisan, T.; Phutdhawong, W. S. Synthesis and Investigation of Tetrahydro- β -carboline Derivatives as Inhibitors of Plant Pathogenic Fungi. *Molecules* **2021**, *26* (1), 207. <https://doi.org/10.3390/molecules26010207>.
49. Bertamino, A.; Ostacolo, C.; Medina, A.; Di Sarno, V.; Lauro, G.; Ciaglia, T.; Vestuto, V.; Pepe, G.; Basilicata, M. G.; Musella, S.; Smaldone, G.; Cristiano, C.; Gonzalez-Rodriguez, S.; Fernandez-Carvajal, A.; Bifulco, G.; Campiglia, P.; Gomez-Monterrey, I.; Russo, R. Exploration of TRPM8 Binding Sites by β -Carboline-Based Antagonists and Their In Vitro Characterization and In Vivo Analgesic Activities. *J. Med. Chem.* **2020**, *63* (17), 9672–9694. <https://doi.org/10.1021/acs.jmedchem.0c00816>.
50. Xin, B.; Tang, W.; Wang, Y.; Lin, G.; Liu, H.; Jiao, Y.; Zhu, Y.; Yuan, H.; Chen, Y.; Lu, T. Design, Synthesis, and Biological Evaluation of β -Carboline Derivatives as Novel Inhibitors Targeting B-Raf Kinase. *Bioorg. Med. Chem. Lett.* **2012**, *22* (14), 4783–4786. <https://doi.org/10.1016/j.bmcl.2012.05.053>.

51. Sheng, T.; Kong, M.; Wang, Y.; Wu, H.; Gu, Q.; Chuang, A. S.; Li, S.; Gao, X. Discovery and Preliminary Mechanism of 1-Carbamoyl β -Carbolines as New Antifungal Candidates. *Eur. J. Med. Chem.* **2021**, *222*, 113563. <https://doi.org/10.1016/j.ejmech.2021.113563>.
52. Szabó, T.; Hazai, V.; Volk, B.; Simig, G.; Milen, M. First Total Synthesis of the β -Carboline Alkaloids Trigonostemine A, Trigonostemine B and a New Synthesis of Pityriacitrin and Hyrtiosulawesine. *Tetrahedron Lett.* **2019**, *60* (22), 1471–1475. <https://doi.org/10.1016/j.tetlet.2019.04.044>.
53. Zhao, Z.; Sun, Y.; Wang, L.; Chen, X.; Sun, Y.; Lin, L.; Tang, Y.; Li, F.; Chen, D. Organic Base-Promoted Efficient Dehydrogenative/Decarboxylative Aromatization of Tetrahydro- β -Carbolines into β -Carbolines Under Air. *Tetrahedron Lett.* **2019**, *60* (11), 800–804. <https://doi.org/10.1016/j.tetlet.2019.02.020>.
54. Ikeda, R.; Iwaki, T.; Iida, T.; Okabayashi, T.; Nishi, E.; Kurosawa, M.; Sakai, N.; Konakahara, T. 3-Benzylamino- β -carboline Derivatives Induce Apoptosis through G2/M Arrest in Human Carcinoma Cells HeLa S-3. *Eur. J. Med. Chem.* **2011**, *46* (2), 636–646. <https://doi.org/10.1016/j.ejmech.2010.11.044>.
55. Ikeda, R.; Kimura, T.; Tsutsumi, T.; Tamura, S.; Sakai, N.; Konakahara, T. Structure–Activity Relationship in the Antitumor Activity of 6-, 8- or 6,8-Substituted 3-Benzylamino- β -Carboline Derivatives. *Bioorg. Med. Chem. Lett.* **2012**, *22* (14), 3506–3515. <https://doi.org/10.1016/j.bmcl.2012.03.077>.
56. Xu, W.; Zhao, M.; Wang, Y.; Zhu, H.; Wang, Y.; Zhao, S.; Wu, J.; Peng, S. Design, Synthesis, In Vivo Evaluations of Benzyl Nw-nitro-N α -(9H-pyrido[3,4-b]indole-3-carbonyl)-L-argininate as Apoptosis Inducer Capable of Decreasing Serum Concentration of P-selectin. *Med. Chem. Commun.* **2016**, *7* (9), 1730–1737. <https://doi.org/10.1039/C6MD00215C>.
57. Ling, Y.; Gao, W.-J.; Ling, C.; Liu, J.; Meng, C.; Qian, J.; Liu, S.; Gan, H.; Wu, H.; Tao, J.; Dai, H.; Zhang, Y. β -Carboline and N-hydroxycinnamide hybrids as anticancer agents for drug-resistant hepatocellular carcinoma. *Eur. J. Med. Chem.* **2019**, *168*, 515–526. <https://doi.org/10.1016/j.ejmech.2019.02.054>.
58. Gu, H.; Li, N.; Dai, J.; Xi, Y.; Wang, S.; Wang, J. Synthesis and In Vitro Antitumor Activity of Novel Bivalent β -Carboline-3-carboxylic Acid Derivatives with DNA as a Potential Target. *Int. J. Mol. Sci.* **2018**, *19* (10), 3179. <https://doi.org/10.3390/ijms19103179>.
59. Lan, J.-S.; Xie, S.-S.; Li, S.-Y.; Pan, L.-F.; Wang, X.-B.; Kong, L.-Y. Design, Synthesis and Evaluation of Novel Tacrine-(β -carboline) Hybrids as Multifunctional Agents for the Treatment of Alzheimer's Disease. *Bioorg. Med. Chem.* **2014**, *22* (21), 6089–6104. <https://doi.org/10.1016/j.bmc.2014.08.035>.
60. Misra, S.; Ghatak, S.; Patil, N.; Dandawate, P.; Ambike, V.; Adsule, S.; Unni, D.; Venkateswara Swamy, K.; Padhye, S. Novel dual cyclooxygenase and lipoxygenase inhibitors targeting hyaluronan–CD44v6 pathway and inducing cytotoxicity in colon cancer cells. *Bioorg. Med. Chem.* **2013**, *21* (9), 2551–2559. <https://doi.org/10.1016/j.bmc.2013.02.033>.
61. Lu, X.; Liu, Y.-C.; Orvig, C.; Liang, H.; Chen, Z.-F. Discovery of β -carboline copper(II) complexes as Mcl-1 inhibitor and *in vitro* and *in vivo* activity in cancer models. *Eur. J. Med. Chem.* **2019**, *181*, 111567. <https://doi.org/10.1016/j.ejmech.2019.111567>.
62. Skrott, Z.; Mistrik, M.; Andersen, K. K.; Friis, S.; Majera, D.; Gursky, J.; Ozdian, T.; Bartkova, J.; Turi, Z.; Moudry, P.; Kraus, M.; Michalova, M.; Vaclavkova, J.; Dzubak, P.; Vrobel, I.; Pouckova, P.; Sedlacek, J.; Miklovicova, A.; Kutt, A.; Li, J.; Mattova, J.; Driessen, C.; Dou, Q. P.; Olsen, J.; Hajdich, M.; Cvek, B.; Deshaies, R. J.; Bartek, J. Alcohol-abuse drug disulfiram targets cancer via p97 segregase adaptor NPL4. *Nature* **2017**, *552* (7684), 194–199. <https://doi.org/10.1038/nature25016>.
63. Tang, J.-G.; Liu, H.; Zhou, Z.-Y.; Liu, J.-K. Facile and Efficient One-Pot Synthesis of β -Carbolines. *Synth. Commun.* **2010**, *40* (10), 1411–1417. <https://doi.org/10.1080/00397910903097245>.
64. Wang, Z.-X.; Xiang, J.-C.; Cheng, Y.; Ma, J.-T.; Wu, Y.-D.; Wu, A.-X. Direct Biomimetic Synthesis of β -Carboline Alkaloids from Two Amino Acids. *J. Org. Chem.* **2018**, *83* (19), 12247–12254. <https://doi.org/10.1021/acs.joc.8b01668>.
65. Wang, Z.; Yu, Z.; Yao, Y.; Zhang, Y.; Xiao, X.; Wang, B. A practical synthesis of β -carbolines by tetra-n-butylammonium bromide (TBAB)-mediated cycloaromatization reaction of aldehydes with tryptophan derivatives. *Chin. Chem. Lett.* **2019**, *30* (8), 1541–1544. <https://doi.org/10.1016/j.ccllet.2019.07.001>.
66. Pichette Drapeau, M.; Tlili, A. Modern synthesis of carbamoyl fluorides. *Tetrahedron Lett.* **2020**, *61* (47), 152539. <https://doi.org/10.1016/j.tetlet.2020.152539>.
67. Schwalm, C. S.; Correia, C. R. D. Divergent total synthesis of the natural antimalarial marinoquinolines A, B, C, E and unnatural analogues. *Tetrahedron Lett.* **2012**, *53* (36), 4836–4840. <https://doi.org/10.1016/j.tetlet.2012.06.115>.
68. Aguiar, A. C. C.; Panciera, M.; Simão dos Santos, E. F.; Singh, M. K.; Garcia, M. L.; de Souza, G. E.; Nakabashi, M.; Costa, J. L.; Garcia, C. R. S.; Oliva, G.; Correia, C. R. D.; Guido, R. V. C. Discovery of Marinoquinolines as Potent and Fast-Acting Plasmodium falciparum Inhibitors with *in vivo* Activity. *J. Med. Chem.* **2018**, *61* (13), 5547–5568. <https://doi.org/10.1021/acs.jmedchem.8b00143>.
69. Akula, M.; Sridevi, J. P.; Yogeewari, P.; Sriram, D.; Bhattacharya, A. New Class of Antitubercular Compounds: Synthesis and Anti-Tubercular Activity of 4-Substituted Pyrrolo[2,3-c]quinolines. *Monatsh. Chem.* **2014**, *145* (5), 811–819. <https://doi.org/10.1007/s00706-013-1141-1>.
70. Nishiyama, T.; Hamada, E.; Ishii, D.; Kihara, Y.; Choshi, N.; Nakanishi, N.; Murakami, M.; Taninaka, K.; Hatae, N.; Choshi, T. Total Synthesis of Pyrrolo[2,3-c]quinoline Alkaloid: Trigonoinine B. *Beilstein J. Org. Chem.* **2021**, *17*, 730–736. <https://doi.org/10.3762/bjoc.17.62>.
71. Mahajan, J. P.; Suryawanshi, Y. R.; Mhaske, S. B. Pd-Catalyzed Imine Cyclization: Synthesis of Antimalarial Natural Products Aplidiopsamine A, Marinoquinoline A, and Their Potential Hybrid NCLite-M1. *Org. Lett.* **2012**, *14* (22), 5804–5807. <https://doi.org/10.1021/ol302676v>.
72. Osano, M.; Jhaveri, D. P.; Wipf, P. Formation of 6-Azaindoles by Intramolecular Diels–Alder Reaction of Oxazoles and Total Synthesis of Marinoquinoline A. *Org. Lett.* **2020**, *22* (6), 2215–2219. <https://doi.org/10.1021/acs.orglett.0c00417>.
73. Mulcahy, S. P.; Varelas, J. G. Three-step synthesis of an annulated β -carboline via palladium catalysis. *Tetrahedron Lett.* **2013**, *54* (48), 6599–6601. <https://doi.org/10.1016/j.tetlet.2013.09.108>.
74. Varelas, J. G.; Khanal, S.; O'Donnell, M. A.; Mulcahy, S. P. Concise Synthesis of Annulated Pyrrolo[3,4-b]indoles via Rh(II)-Catalyzed Cyclization. *Org. Lett.* **2015**, *17* (21), 5512–5514. <https://doi.org/10.1021/acs.orglett.5b02807>.
75. Saliba, B. M.; Khanal, S.; O'Donnell, M. A.; Queenan, K. E.; Song, J.; Gentile, M. R.; Mulcahy, S. P. Parallel Strategies for the Synthesis of Annulated Pyrrolo[3,4-b]indoles via Rh(II)- and Pd(0)-catalyzed Cyclotrimerization. *Tetrahedron Lett.* **2018**, *59* (49), 4311–4314. <https://doi.org/10.1016/j.tetlet.2018.10.050>.
76. Wang, T.; Ueda, Y.; Zhang, Z.; Yin, Z.; Matiske, J.; Pearce, B. C.; Yang, Z.; Zheng, M.; Parker, D. D.; Yamanaka, G. A.; Gong, Y.-F.; Ho, H.-T.; Colonno, R. J.; Langley, D. R.; Lin, P.-F.; Meanwell, N. A.; Kadow, J. F. Discovery of the Human Immunodeficiency Virus Type 1 (HIV-1) Attachment Inhibitor Temsavir and Its Phosphonoxyethyl Prodrug Fostemsavir. *J. Med. Chem.* **2018**, *61* (13), 6308–6327. <https://doi.org/10.1021/acs.jmedchem.8b00759>.
77. Boutin, M.; Vézina, D.; Ding, S.; Prévost, J.; Laumaea, A.; Marchitto, L.; Anand, S. P.; Medjahed, H.; Gendron-Lepage, G.; Bourassa, C.; Goyette, G.; Clark, A.; Richard, J.; Finzi, A. Temsavir Treatment of HIV-1-Infected Cells Decreases Envelope Glycoprotein Recognition by Broadly Neutralizing Antibodies. *mBio* **2022**, *13* (3), e00577-22. <https://doi.org/10.1128/mbio.00577-22>.

78. Kamal, A.; Tangella, Y.; Kesari, M. L.; Manda, S.; Srinivasulu, V.; Jadala, C.; Alarifi, A. PhI(OAc)₂-Mediated one-pot oxidative decarboxylation and aromatization of tetrahydro- β -carbolines: synthesis of norharmine, harmine, eudistomin U, and eudistomin I. *Org. Biomol. Chem.* **2015**, *13* (32), 8652–8662. <https://doi.org/10.1039/C5OB00871A>.
79. Li, S.-F.; Di, Y.-T.; He, H.-P.; Zhang, Y.; Wang, Y.-H.; Yin, J.-L.; Tan, C.-J.; Lin, S.-L.; Hao, X.-J. Trigonines A and B, Two Novel Alkaloids from the Leaves of *Trigonostemon liliifolius*. *Tetrahedron Lett.* **2011**, *52* (22), 3186–3188. <https://doi.org/10.1016/j.tetlet.2011.03.015>.
80. Carroll, A. R.; Duffy, S.; Avery, V. M. Aplidiopsamine A, an Antiplasmodial Alkaloid from the Temperate Australian Ascidian, *Aplidiopsis confluata*. *J. Org. Chem.* **2010**, *75* (23), 8291–8294. <https://doi.org/10.1021/jo101695v>.
81. Sangnoi, Y.; Sakulkeo, O.; Yuenyongsawad, S.; Kanjana-opas, A.; Ingkaninan, K.; Plubrukarn, A.; Suwanborirux, K. Acetylcholinesterase-Inhibiting Activity of Pyrrole Derivatives from a Novel Marine Gliding Bacterium, *Rapidithrix thailandica*. *Marine Drugs* **2008**, *6* (4), 578–586. <https://doi.org/10.3390/md6040578>.
82. England, D. B.; Padwa, A. Gold-Catalyzed Cycloisomerization of N-Propargylindole-2-carboxamides: Application toward the Synthesis of Lavendamycin Analogues. *Org. Lett.* **2008**, *10* (16), 3631–3634. <https://doi.org/10.1021/ol801385h>.
83. Stephens, D. N.; Schneider, H. H.; Kehr, W.; Andrews, J. S.; Rettig, K. J.; Turski, L.; Schmiechen, R.; Turner, J. D.; Jensen, L. H.; Petersen, E. N. Abecarnil, a metabolically stable, anxiolytic beta-carboline acting at benzodiazepine receptors. *J. Pharmacol. Exp. Ther.* **1990**, *253* (1), 334–343.
84. Zhao, Y.; Ye, F.; Xu, J.; Liao, Q.; Chen, L.; Zhang, W.; Sun, H.; Liu, W.; Feng, F.; Qu, W. Design, Synthesis, and Evaluation of Novel Bivalent β -Carboline Derivatives as Multifunctional Agents for the Treatment of Alzheimer's Disease. *Bioorg. Med. Chem.* **2018**, *26* (13), 3812–3824. <https://doi.org/10.1016/j.bmc.2018.06.018>.

Information about the authors:

Volodymyr V. Voloshchuk (*corresponding author*), Ph.D. Student of the Institute of Organic Chemistry of the National Academy of Sciences of Ukraine; Head of the Organic Chemistry Laboratory, Enamine Ltd.; <https://orcid.org/0009-0001-9403-0176>; e-mail for correspondence: v.v.voloshchuk@gmail.com.

Sergey P. Ivonin, Dr.Sci. in Chemistry, Senior Researcher of the Medicinal Chemistry Department, Institute of Organic Chemistry of the National Academy of Sciences of Ukraine; e-mail for correspondence: s.p.ivonin@gmail.com.

UDC 577.15:5615.2:547.2333.4

M. Ye. Blazheyevskiy, O. V. Kovalska

National University of Pharmacy of the Ministry of Health of Ukraine,
53 Hryhorii Skovoroda str., 61002 Kharkiv, Ukraine

The Quantitative Determination of Etonium by the Enzymatic Kinetic-Spectrophotometric Method

Abstract

The use of the cholinesterase enzyme as a component of the analytical system has made it possible to develop a new kinetic-spectrophotometric method, which is alternative to the pharmacopoeial method, for determining the quaternary ammonium salt – etonium in the substance and a dosage form. This method is characterized by high sensitivity and specificity, and is relatively cheap. The relative standard deviation of the procedure does not exceed 2.7%, and the limit of quantification is 17 ng mL⁻¹.

Keywords: surfactant; etonium; cholinesterase; acetylcholine

М. Є. Блажеєвський, О. В. Ковальська

Національний фармацевтичний університет Міністерства охорони здоров'я України,
вул. Григорія Сковороди, 53, м. Харків, 61002, Україна

Кількісне визначення етонію ферментативним кінетико-спектрофотометричним методом

Анотація

Використання ферменту холінестерази як компонента аналітичної системи дозволило розробити нову, альтернативну фармакопейній, кінетико-спектрофотометричну методику визначення четвертинної амонійної солі етонію в субстанції та лікарському засобі. Методика характеризується високою чутливістю і специфічністю та є відносно дешевою. Відносно стандартне відхилення методики не перевищувало 2,7%, а межа визначення становила 17 нг мл⁻¹.

Ключові слова: поверхнево-активні речовини; етоній; холінестераза; ацетилхолін

Citation: Blazheyevskiy, M. Ye.; Kovalska, O. V. The Quantitative Determination of Etonium by the Enzymatic Kinetic-Spectrophotometric Method. *Journal of Organic and Pharmaceutical Chemistry* 2024, 22 (1), 57–62.

<https://doi.org/10.24959/ophcj.24.304120>

Received: 10 January 2024; **Revised:** 5 May 2024; **Accepted:** 11 May 2024

Copyright © 2024, M. Ye. Blazheyevskiy, O. V. Kovalska. This is an open access article under the CC BY license (<http://creativecommons.org/licenses/by/4.0>).

Funding: The authors received no specific funding for this work.

Conflict of interests: The authors have no conflict of interests to declare.

■ Introduction

Etonium (1,2-ethylene-*bis*-(N-dimethylcarboxymethyl)ammonium dichloride, **Figure 1**) is a *bis*-quaternary ammonium salt. It exhibits several valuable biomedical properties, e.g. displays the bacteriostatic and bactericidal activity against streptococci, staphylococci, and other microorganisms, acts as an antitoxic agent against the staphylococcal toxin, has a local anesthetic effect, stimulates wound healing, etc. [1].

According to the features described, etonium has found application as an antimicrobial,

analgesic, and regenerative agent in treating various diseases of the skin and mucous membranes, such as bedsores, cracked nipples, vaginitis, burns, trophic ulcers, radiation lesions, etc. [2].

It is manufactured as a substance and is included as an active ingredient in various medicinal formulations, for instance, 1% ointment and 1% or 0.5% gel for external application; 0.02–1% solutions for the treatment of wounds, ulcers, keratitis, and other eye lesions; the etonium paste for the use in dental practice [3].

The etonium content control in any substance or preparations can be achieved by several

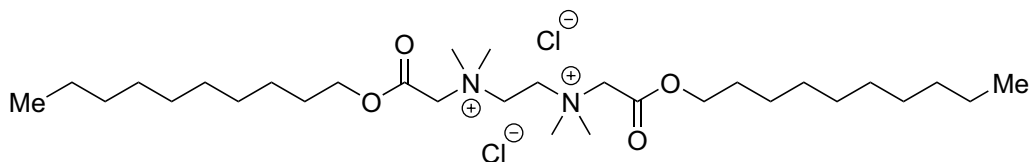


Figure 1. The structural formula of ethonium

analytical methods, including titration with perchloric acid in a non-aqueous medium [4], bichromatometry and mercurimetry [5, 6], the photometric and extraction-photometric determination in the form of associates with inorganic or organic dyes [7–11], gas-liquid chromatography [12, 13], and ionometry [14]. Although the methods mentioned are relatively simple, their general drawback is the low selectivity (except for the ionometry method). Thus, in the analysis of ethonium by bichromatometric or mercurimetric methods, the determination is carried out with respect to the chloride anion, and not to the organic cation. The method of ionometry involves the preliminary manufacturing of an indicator electrode, which is very inconvenient. Therefore, despite a number of existing methods for the quantitative determination of ethonium, the development of simple, accessible, and selective methods is still an open question.

Previously, a new enzymatic kinetic-spectrophotometric method for determining the quaternary ammonium salts was developed in our laboratory. This allows to use the ability of salts to inhibit the catalytic activity of cholinesterase [15]. The degree of inhibition was determined using two conjugated reactions of the acetylcholine perhydrolysis followed by the oxidation of *p*-phenetidine with the peroxyacetic acid formed. Adhering to the research direction in this work, we present the results of the quantitative determination of ethonium in a medicinal product by the enzymatic kinetic-spectrophotometric method.

Materials and methods

Reagents and equipment

ETONIY® (Aethonium) powder (substance, 99.9%) was produced by OJSC Farmak, Kyiv, Ukraine, CAS 21954-74-5, MW 585.736 g mol⁻¹.

Ethonium gel, 0.5%, 50 mL, batch No. 74 (Apr 2023) was manufactured by APTEKA PAVLOVA Ltd (Odesa, Ukraine). Its composition is ethonium (active pharmaceutical ingredient) – 0.5 g; glycerin – 20.0 g; propylene glycol – 20.0 g; PEG 400 – 50.0 g; PEG 1500 – 10.0 g; purified water – 10.0 mL. The quantitative content of the active substance according to the certificate was 4.4525% (*w/w*).

p-Phenetidine, 98% (Sigma-Aldrich, batch A0281408); *p*-Phenetidine hydrochloride was prepared by dissolution of *p*-phenetidine in chloroform followed by precipitation of the salt by gaseous hydrogen chloride.

Disodium hydrogen phosphate dodecahydrate (Na₂HPO₄·12H₂O), puriss. p.a. (“ReaChem”, Kharkiv, Ukraine) was used.

Stabilized hydrogen peroxide, 30–40% solution, puriss. p.a., (LLC Inter-Synthes, Boryslav, Ukraine) was used; the content of hydrogen peroxide was determined permanganometrically according to the State Pharmacopoeia of Ukraine [16].

Acetylcholine chloride (Pharm Grade), 0.2 g per amp/5 mL, was produced by “Vector” – State Science Center of Virology and Biotechnology (Russia).

A dry cholinesterase (EC 3.1.1.8) powder from horse serum (SMU “Biomed”, Russia), 80 mg in an ampoule (VI class, activity 28 AU mg⁻¹) was used in the study. The catalytic activity of 1 activity unit (AU) is manifested in such an amount of this enzyme preparation that converts 1 μmol of the substrate in 1 min under specified reaction conditions.

High-purity double distilled water was used throughout the experiment.

The pH measurements were performed with a combined glass electrode (SP20B) together with an EAL-1M3.1 reference standard silver chloride electrode.

The absorbance measurements were performed on an SF-26 spectrophotometer ($\lambda = 358$ nm, $l = 10$ mm).

Preparation of solutions

Solution of 0.2 M phosphate buffer (pH 8.35)

Disodium hydrogen phosphate dodecahydrate (35.75 g) was dissolved in a 500 mL flask using double-distilled water. Then 0.1 M solution of hydrochloric acid (19 mL) was added. The pH of the final solution was controlled potentiometrically.

0.5% p-Phenetidine hydrochloride (p-Ph) solution

p-Phenetidine hydrochloride (0.50 g) was dissolved in double-distilled water (80 mL) in a 100 mL volumetric flask and diluted to the volume with the same solvent.

Solution of 10% Hydrogen peroxide

The solution was prepared from a 30–40% solution of hydrogen peroxide by dilution with the required amount of double distilled water. The content of hydrogen peroxide in a 10% working solution was determined permanganatometrically.

Solution of cholinesterase (ChE)

An accurately weighed content of an ampoule containing the cholinesterase powder (80 mg) was dissolved in double-distilled water (20.0 mL) under gentle heating on a water heater. The shelf life of the solution is 1 day.

Solution of acetylcholine chloride (ACh)

The solution with the initial concentration of $5.4 \cdot 10^{-3} \text{ mol L}^{-1}$ was prepared by dissolving the ampoule content (0.2 g of acetylcholine) in 200 mL of double-distilled water. For this purpose, the ampoule was opened, 4.0 mL of water was pipetted and added to the ampoule, and then shaken until acetylcholine was completely dissolved. Then the solution was transferred into a 200 mL volumetric flask and diluted to the volume with double-distilled water.

Stock Solution of Ethonium (ET) ($1 \times 10^{-4} \text{ mol L}^{-1}$)

An accurately weighed powder of the ethonium substance containing 0.058574 g of the main ingredient was dissolved in 500 mL of double-distilled water in a 1000 mL volumetric flask. The solution was diluted to the volume with the same solvent at +20 °C and mixed thoroughly.

Work Standard (WS) Solution of Ethonium $1 \times 10^{-6} \text{ mol L}^{-1}$

A 10 mL aliquot of Stock Solution of the drug ($1 \times 10^{-4} \text{ mol L}^{-1}$) was transferred into a 1000 mL volumetric flask and diluted to the volume with double-distilled water at +20 °C.

The procedure for constructing the kinetic curves

Part 1 – working experiments “ACh + (ChE + ET)”

The buffer solution (10.00 mL, pH 8.35) is added to each of the four 20 mL graduated test tubes with a ground joint stopper. Then 0.50, 1.00, 2.00, and 3.00 mL of the ethonium WS solution was added to the test tubes followed by 2.00, 1.50, 0.50, and 0.00 mL of double-distilled water, respectively. After that 0.50 mL of the ChE solution was added to the test tubes, the content was thoroughly shaken, and the test tubes were kept in a thermostat at +38 °C for 10 min. Shortly thereafter, the ACh solution (1.00 mL) was added to each test tube, the mixture was shaken thoroughly and thermostated for 10 min at +38 °C again. Then a 10% hydrogen peroxide solution (1.60 mL)

was added to each test tube and incubated for 10 min at +38 °C. Further, the *p*-phenetidine hydrochloride solution (1.00 mL) was added, and the solution was diluted to the volume with double-distilled water, shaken thoroughly, and scanned photometrically on a spectrophotometer at a wavelength of 358 nm in a 1 cm cuvette every minute over 15 min. The phosphate buffer was used as a reference solution. The relative rate of the reaction $[(\text{ChE} + \text{ET}) + \text{ACh}] + \text{H}_2\text{O}_2 + p\text{-Ph}$ ($t_{ga} \text{ (Inh)}$, min^{-1}) was determined as the slope of a linear section of the “optical density (*A*) vs time (*t*, min)” kinetic curve.

Part 2 – control experiment #1 “ACh”

The control experiment was carried out in the absence of ChE and the inhibitor. The buffer solution (10.00 mL), 3.00 mL of double-distilled water, 1.00 mL of the ACh solution, 1.60 mL of the hydrogen peroxide solution were successively added to a 20 mL graduated test tube with a ground joint stopper. The test tube was thoroughly shaken, and then thermostated for 10 min at +38 °C. After that the *p*-Ph solution (1.00 mL) was added, the solution was diluted to the volume with double-distilled water, and the mixture was thoroughly shaken. Then the solution was scanned photometrically on a spectrophotometer at a wavelength of 358 nm in a 1 cm cuvette every minute over 15 min. The phosphate buffer was used as a reference solution. According to the plotted kinetic curve “optical density (*A*) vs time (*t*, min)”, the relative rate of the reaction $[(\text{ACh} + \text{H}_2\text{O}_2) + p\text{-Ph}]$ was determined as a slope of a linear section of the curve ($t_{ga} \text{ (ACh)}$, min^{-1}).

Part 3 – control experiment #2 “ACh + ChE”

The buffer solution (10.00 mL), 2.50 mL of double-distilled water, 0.50 mL of the ChE solution, and 1.00 mL of the ACh solution were successively added to a 20 mL graduated test tube with a ground joint stopper. The content was thoroughly shaken and kept at +38 °C within 10 min. Next, the hydrogen peroxide solution (1.60 mL) was added, and the mixture was thoroughly shaken and thermostated for 10 min at +38 °C. After that, the *p*-Ph solution (1.00 mL) was added, and the solution was diluted to the volume with double-distilled water. Then the solution was scanned photometrically on a spectrophotometer at a wavelength of 358 nm in a 1 cm cuvette every minute over 15 min. The phosphate buffer was used as a reference solution. According to the plotted kinetic curve “optical density (*A*) vs time (*t*, min)”, the relative rate of the reaction $[(\text{ChE} + \text{ACh}) + \text{H}_2\text{O}_2 + p\text{-Ph}]$ was

determined as a slope of a linear section of the curve (tga (ACh + ChE), min^{-1}).

The relative rates of the reactions determined (expressed as tangents of the slope angles) were used to calculate the inhibition degree of the enzymatic hydrolysis of ACh (U , %), in the presence of ethonium according to the following equation:

$$U (\%) = \frac{[tga (\text{Inh}) - tga (\text{ACh} + \text{ChE})]}{[tga (\text{ACh}) - tga (\text{ACh} + \text{ChE})]} \times 100 \%$$

where $tga (\text{Inh})$ (min^{-1}) – is the relative reaction rate of the p -Ph oxidation by peroxyacetic acid formed during the perhydrolysis of unreacted ACh in the working experiment at various concentrations of the inhibitor (ET);

$tga (\text{ACh})$ (min^{-1}) – is the relative reaction rate of the p -Ph oxidation by peroxyacetic acid formed in the reaction of the ACh perhydrolysis in the absence of the inhibitor and ChE (control experiment #1);

$tga (\text{ACh} + \text{ChE})$ (min^{-1}) – is the relative reaction rate of the p -Ph oxidation by peroxyacetic acid formed in the reaction of the perhydrolysis of unreacted ACh in the presence of ChE and the absence of the inhibitor (ET) (control experiment #2).

The calculated values of U (%) were used to plot the calibration graph “inhibition degree (U , %) vs ethonium concentration (c , ng mL^{-1})”.

Results and Discussion

Previously, a study was conducted to analyze the parameters that might affect the performance of the approach proposed [17]. This allowed us to determine the optimal working conditions and concentrations of reagents used in the present research.

Kinetic curves constructed were based on the experimental data on the dependence of optical density on time. They are given in **Figure 2**.

The calibration graph (**Figure 3**) was constructed in the coordinates of the inhibition degree (U , %) vs the concentration (c , ng mL^{-1}). One can see that within the inhibition interval of 20–80% the dependence on the ethonium concentration is linear. This corresponds to the concentrations of the inhibitor from 17 ng mL^{-1} to 120 ng mL^{-1} . The limit of quantitation (LOQ) was defined as the concentration corresponding to 20% of the inhibition degree, and it was 17 ng mL^{-1} .

This method was further applied to determine the content of ethonium in a 0.5% gel formulation and a 0.1% solution. The results of these experiments are presented below.

The method for the quantitative determination of ethonium in a 0.5% gel formulation

0.1 g (accurate weight) of the ethonium gel was dissolved in 1000 mL of double-distilled water. Then, 10.0 mL of the phosphate buffer solution,

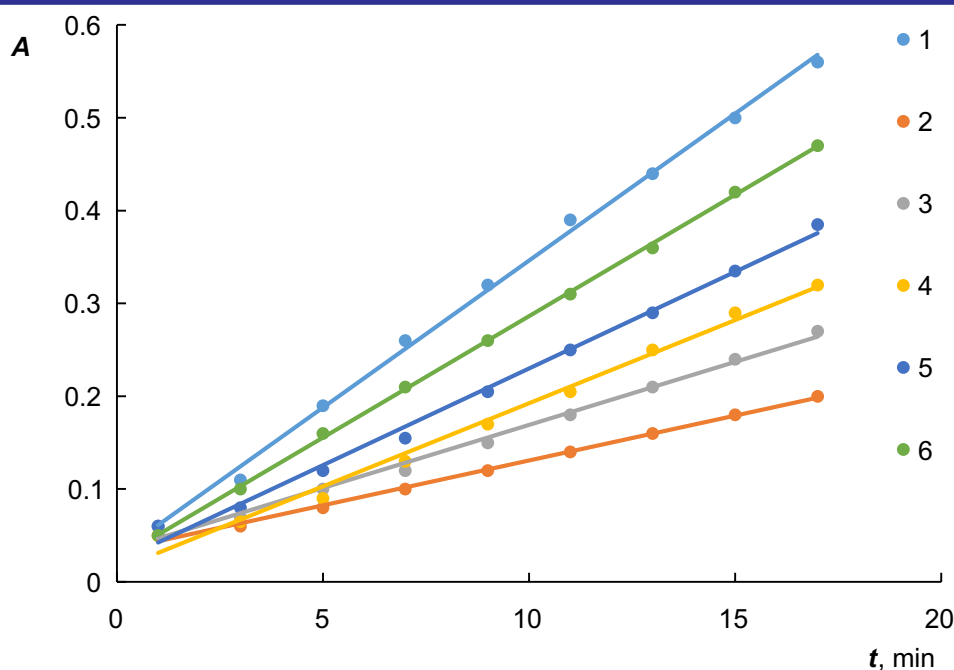


Figure 2. Kinetic curves of the conjugated oxidation of p -Phenetidine with hydrogen peroxide in the presence of: ACh (1), mixtures ACh + ChE (2) and ACh + ChE + Inh (3–6). c (ACh) = $3.3 \times 10^{-4} \text{ mol L}^{-1}$; w (H_2O_2) = 1%; w (AChE) = 0.24 mg mL^{-1} . w (ET): 17 ng mL^{-1} (3); 34 ng mL^{-1} (4); 68 ng mL^{-1} (5); 102 ng mL^{-1} (6); w (p -Ph) = 0.3%

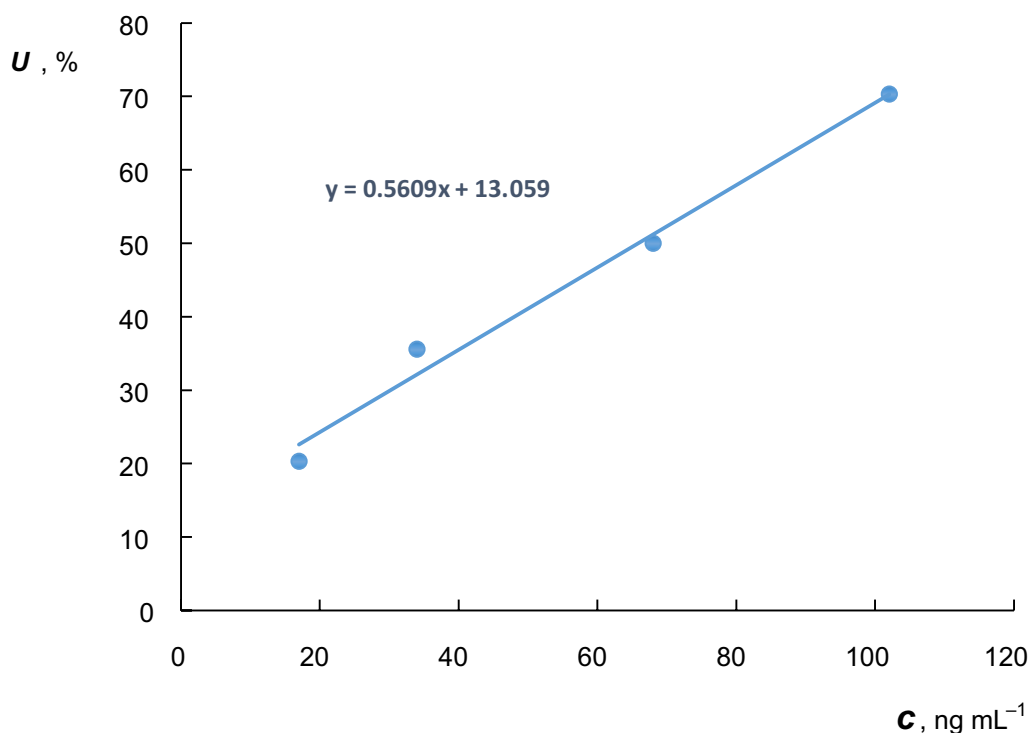


Figure 3. The calibration graph of the dependence of the inhibition degree on the concentration of ethonium in the mixture analyzed [ACh + (ChE + ET)] determined by the indicator reaction of *p*-Ph oxidation by hydrogen peroxide in the presence of residual ACh

2.5 mL of the gel solution, and 0.5 mL of the ChE solution were successively added to a 20 mL graduated test tube, the mixture was thoroughly shaken and incubated at +38 °C for 10 min. After that, 1.0 mL of the ACh solution was added, and the content was thoroughly shaken and incubated for another 10 min at +38 °C. Further, 1.6 mL of the hydrogen peroxide solution was added, and the test tube was incubated again at +38 °C for 10 min. After that, 1.0 mL of the *p*-Ph solution was added, diluted to the volume with double-distilled water, and the optical density of the solution was measured at 358 nm in a 1 cm cuvette with the aid of a spectrophotometer for 15 min. According to the plot of the dependence of optical density on time (kinetic curve), the tangent of the slope angle for the linear section $tga(\text{Inh})$ was found, in min^{-1} .

In parallel, two more experiments were carried out. One of them involved acetylcholine and cholinesterase without the inhibitor and another was performed without the use of cholinesterase

enzyme. Both of the experiments were guided by the procedure for constructing the kinetic curves described in the previous section. As a result, the other two tangents $tga(\text{ACh} + \text{ChE})$ and $tga(\text{ACh})$, respectively, were determined.

The content of ethonium in the gel formulation ($w, \%$) was calculated by the formula:

$$w(\%, w/w) = \frac{0.00059574[tga(\text{Inh}) - tga(\text{ACh} + \text{ChE})] \times 100\%}{g \times [tga(\text{ACh}) - tga(\text{ACh} + \text{ChE})]}$$

where 0.00059574 – is the mass of ethonium contained in a 10.00 mL aliquot of the *Stock Solution* of the drug, g;

g – is the mass of the ethonium gel sample taken for the analysis, g;

$tga(\text{Inh})$ – is the relative reaction rate in the working experiment with the sample solution of the drug studied, min^{-1} ;

$tga(\text{ACh} + \text{ChE})$ – is the relative reaction rate in the absence of the inhibitor, min^{-1} ;

Table. The results of the analysis of a 0.5% ethonium gel and a 0.1% ethonium solution according to the procedure proposed by the kinetic-spectrophotometric enzyme method

The substance analyzed	ET found ($\bar{x} \pm \Delta x$), % ^a	RSD, %	The quality certificate data, %	Accuracy (δ , %) ^b
Ethonium gel 0.5% (APTEKA PAVLOVA Ltd, Odesa, Ukraine)	0.446 ± 0.015	2.7	0.445	+ 0.23
Ethonium solution 0.1% (prepared <i>ex tempore</i>)	0.101 ± 0.003	2.5	0.100	+1.00

Notes: ^a Mean of 5 measurements ($P = 0.95$); ^b $\delta = (\bar{x} - \mu) \times 100\% \times \mu^{-1}$; μ is the actual content of ET according to the Certificate

t_{ga} (ACh) – is the relative reaction rate (the tangent of the slope angle of the kinetic curve), in the working experiment without the use of the inhibitor and cholinesterase, min^{-1} ;

For the quantitative determination of the inhibitor in a 0.1% ethonium solution, 1.0 g (accurate weight) of the ethonium substance was dissolved in 1000 mL of double-distilled water. Next, the analysis was performed similarly to the procedure for the 0.5% gel formulation.

The results of the quantitative determination of ethonium in a 0.5% ethonium gel and a 0.1% solution according to the kinetic-spectrophotometric enzyme method proposed are presented in **Table**. They indicate that the relative

standard deviation (RSD) $\leq 2.7\%$, with the correctness (δ) = +0.23 – 1.00%, $\delta < RSD$.

■ Conclusions

Thus, a new enzymatic kinetic-spectrophotometric method for determining the quaternary ammonium surface-active substance – ethonium in a gel preparation has been developed. The approach is based on the inhibition of the cholinesterase enzyme activity assessed by the residual acetylcholine substrate using the indicator reaction of *p*-phenetidine oxidation. The relative standard deviation of the procedure does not exceed 2.7%. The limit of quantitation is 17 ng mL^{-1} .

■ References

1. Compendium – likarski preparaty. Aktyvni rechovyny, Etonii (Aethonium). [Compendium – medicines. Active ingredients, Ethonium (Aethonium), in *Ukrainian*]. <https://compendium.com.ua/uk/akt/65/237/aethonium/> (accessed March 12, 2024).
2. Ivantsyk, L. B.; Drogozov, S. M.; Gerbina, N. A.; K. A, K.; Shtroblia, V. V. Advantages of the composition and activity of a new combined ointment with ethony for treatment of the wound process. *Likars'ka sprava* **2019**, 1–2. [https://doi.org/10.31640/JVD.1-2.2019\(19\)](https://doi.org/10.31640/JVD.1-2.2019(19)).
3. Shestakov, P. K. Primenenie pasty etoniiia pri lechenii glubokolo a riesa zubov [The use of ethonium paste in the treatment of deep dental caries, in *Russian*]. *Stomatologiya* **1971**, 50 (2), 79–80. PMID: 5291203.
4. Maksyutina, N. P.; Kagan, F. B.; Kirichenko, L. A.; Mitchenko, F. A. *Metody analiza lekarstv* [Drug analysis methods, in *Russian*]; Zdorovia: Kyiv, 1984; pp 20–24.
5. Pogodina, L. I. Bihromatometricheskoe opredelenie etoniya v lekarstvennykh formakh [Bichromatometric determination of ethonium in drug forms, in *Russian*]. *Farmatsiya* **1979**, 28 (5), 50–51. PMID: 488403.
6. Lipkovska, N. O.; Barvinchenko, V. M. Supramolekuliarni vzaiemodii pryrodnykh flavonoidiv z kationnoi PAR etoniem v rozchynakh i na poverkhni nanokremnezemu [Supramolecular interactions of natural flavonoids with cationic surfactant ethonium in solutions and on silica surface, in *Ukrainian*]. *Chemistry, Physics and Technology of Surface* **2018**, 9 (1), 92–103. <https://doi.org/10.15407/hftp09.01.092>.
7. Zhebentchev, A. I.; Mchedlov-Petrosyan, N. O. Vzaimodeystvie biologicheskii aktivnykh chetvertichnykh amoniievnykh soley s eozinovyimi krasitelnyami [Interaction of biologically active quaternary ammonium salts with eosin dyes, in *Russian*]. *Zhurnal analiticheskoy himii* **1987**, 42 (3), 518–524.
8. Kalashnikov, V. P.; Dolotova, T. M. Quantitative determination of ethonium in solutions of extemporaneous production [Kilksne viznachennya etoniya v rozchynakh ekstemporalnogo vigotovlennya, in *Ukrainian*]. *Farm. Zh.* **1988**, 6, 68–70.
9. Gladyshevskaya, V.; Pisko, G. T. Chutlyvist' klebsiella do etoniiu v doslidakh *in vitro* ta *in vivo* [Sensitivity of Klebsiella to ethonium in experiments *in vitro* and *in vivo*, in *Ukrainian*]. *Mikrobiolohichniy zhurnal* **1970**, 32 (5), 649–650. PMID: 5517684.
10. Sukhodub, L. F.; Kosevich, M. V.; Shelkovskii, V. S.; Boriak, O. A.; Volianskii Iu. L.; Moleva, V. I.; Chumachenko, T. A. Identifikatsiya bischetvertichnykh ammoniievnykh soedinenii s pomoshch'iu miagkoionizatsionnoi mass-spektrometrii [Identification of bis-quaternary ammonium compounds using mild ionization mass spectrometry, in *Russian*]. *Antibiot. Khimioter.* **1990**, 35 (2), 10–12. PMID: 2337368.
11. Nguyen, R.; Seguin, R. P.; Ross, D. H.; Chen, P.; Richardson, S.; Liem, J.; Lin, Y. S.; Xu, L. Development and Application of a Multidimensional Database for the Detection of Quaternary Ammonium Compounds and Their Phase I Hepatic Metabolites in Humans. *Environ. Sci. Technol.* **2024**, 58 (14), 6236–6249. <https://doi.org/10.1021/acs.est.3c10845>.
12. Thalhamer, B.; Guntner, A. S.; Buchberger, W. Simultaneous analysis of quaternary ammonium cations and corresponding halide counterions by pyrolysis gas chromatography / mass spectrometry. *J. Anal. Appl. Pyrolysis* **2022**, 162, 105447. <https://doi.org/10.1016/j.jaap.2022.105447>.
13. Fernández, P.; Alder, A. C.; Suter, M. J. F.; Giger, W. Determination of the Quaternary Ammonium Surfactant Ditallowdimethylammonium in Digested Sludges and Marine Sediments by Supercritical Fluid Extraction and Liquid Chromatography with Postcolumn Ion-Pair Formation. *Anal. Chem.* **1996**, 68 (5), 921–929. <https://doi.org/10.1021/ac9505482>.
14. Pohrebennyk, V. D.; Romaniuk, A. V. Eksperymentalni doslidzhennia potentsialiv ionoselektyvnykh elektrodov [Experimental studies of the potentials of ion-selective electrodes, in *Ukrainian*]. *Visnyk Natsionalnoho universytetu «Lvivska politekhnika»* **2008**, 608, 69–73.
15. Blazheevskiy, M. Ye.; Koval'ska, O. V. Application of the enzymatic method for the quantitative determination of dequalinium chloride in lozenges. *Journal of Organic and Pharmaceutical Chemistry* **2022**, 20 (1), 21–27. <https://doi.org/10.24959/ophcj.22.252499>.
16. *Derzhavna farmakopeia Ukrainy: v 3 tomakh*, 2 vydannia [The State Pharmacopoeia of Ukraine: in 3 volumes, 2nd ed., in *Ukrainian*]; State Enterprise "Ukrainian Scientific Pharmacopoeial Center for Quality of Medicines": Kharkiv, 2015; Vol. 1.
17. Blazheevskiy, M. E.; Koval'ska, O. V.; Dyadchenko, V. V. (National University of Pharmacy, Kharkiv, Ukraine). Sposib vyznachennia aktyvnosti kholinesterazy krovi [Method for determining blood cholinesterase activity, in *Ukrainian*]. Ukraine Patent 117474, 26.06.2017.

Information about the authors:

Olena V. Koval'ska (corresponding author), Ph.D. in Pharmacy, Associate Professor of the General Chemistry Department, National University of Pharmacy of the Ministry of Health of Ukraine; <https://orcid.org/0000-0003-0113-7060>; e-mail for correspondence: lena05021985@ukr.net; tel. +380 97 0710498.

Mykola Ye. Blazheevskiy, D.Sci. in Chemistry, Professor of the General Chemistry Department, National University of Pharmacy of the Ministry of Health of Ukraine; <https://orcid.org/0000-0002-8032-347X>.

ЗМІСТ / CONTENTS

Original Research

- M. M. Suleiman, A. P. Semenets, N. P. Kobzar, L. O. Perekhoda
 THE THEORETICAL SUBSTANTIATION OF THE TARGETED SEARCH FOR NEW
 DPP4 INHIBITORS. COMPUTATIONAL STUDIES OF POTENTIAL CANDIDATES 3

М. М. Сулейман, А. П. Семенець, Н. П. Кобзар, Л. О. Перехода / Теоретичне обґрунтування
 цілеспрямованого пошуку нових інгібіторів DPP4. Обчислювальні дослідження потенційних
 кандидатів

MiniReview

- O. F. Piminov, R. V. Sahaidak-Nikitiuk, A. I. Kvitchata, S. M. Rolik-Attia
 IMMUNOTHERAPY OF DISEASES AND NANOTECHNOLOGY: CURRENT STATE
 AND PROSPECTS 13

О. Ф. Пімінов, Р. В. Сагайдак-Нікітюк, А. І. Квітчата, С. М. Ролік-Аттія /
 Імуноterapia захворювань та нанотехнології: сучасний стан та перспективи

Original Research

- T. M. Sokolenko, Yu. L. Yagupolskii
 5-TRIFLUOROMETHOXY-SUBSTITUTED NICOTINIC ACID, NICOTINAMIDE
 AND RELATED COMPOUNDS 22

Т. М. Соколенко, Ю. Л. Ягупольський / 5-Трифлуорометоксизаміщена ніотинова кислота,
 нікотинамід і споріднені сполуки

Review Article

- V. V. Voloshchuk, S. P. Ivonin
 RECENT ADVANCES IN THE SYNTHESIS AND BIOLOGICAL ACTIVITY
 OF PYRROLO[2,3-*c*]PYRIDINES 31

В. В. Волощук, С. П. Івонін / Останні досягнення в синтезі та біологічній активності
 піроло[2,3-*c*]піридинів

Original Research

- M. Ye. Blazheyevskiy, O. V. Kovalska
 THE QUANTITATIVE DETERMINATION OF ETONIUM BY THE ENZYMATIC
 KINETIC-SPECTROPHOTOMETRIC METHOD 57

М. Є. Блажеевський, О. В. Ковальська / Кількісне визначення етонію ферментативним
 кінетико-спектрофотометричним методом